

10294
NACA TN 3956

NATIONAL ADVISORY COMMITTEE FOR AERONAUTICS

TECHNICAL NOTE 3956

LOAN COPY: RE
AFWL TECHNICAL
KIRTLAND AFB

TECH LIBRARY KAFB, NM
00672118

LIFT AND MOMENT RESPONSES TO PENETRATION OF SHARP-EDGED
TRAVELING GUSTS, WITH APPLICATION TO
PENETRATION OF WEAK BLAST WAVES

By Joseph A. Drischler and Franklin W. Diederich

Langley Aeronautical Laboratory
Langley Field, Va.



Washington
May 1957

AFM LC
TECHNICAL LIBRARY
APR 28 11



NATIONAL ADVISORY COMMITTEE FOR AERONAUTICS

TECHNICAL NOTE 3956

LIFT AND MOMENT RESPONSES TO PENETRATION OF SHARP-EDGED
TRAVELING GUSTS, WITH APPLICATION TO
PENETRATION OF WEAK BLAST WAVES

By Joseph A. Drischler and Franklin W. Diederich

SUMMARY

The lift and moment responses to penetration of sharp-edged traveling gusts are calculated for wings in incompressible and supersonic two-dimensional flow, for wide delta and rectangular wings in supersonic flow, and for very narrow delta wings. By using the two-dimensional indicial-lift functions, some calculations of normal-acceleration response are made for two mass ratios.

The results of these calculations indicate that the forward speed of the gusts has a large effect on the lift- and moment-response functions. For incompressible flow, peaks exist in the early portion of the lift response, which may be much larger than the steady-state value. Some peaks also occur in the lift-response functions for supersonic speeds but are much less pronounced and exceed the steady-state value in only a few instances.

Calculations have also been made of the normal-acceleration response to sharp-edged traveling gusts and indicate that this response tends to follow the lift response very closely in the first few instants of penetration; thus, the large peaks which exist in the lift response at subsonic speeds are duplicated in the acceleration response.

The relation between gusts traveling at supersonic speeds and blast waves is indicated, and the manner in which the calculated lift and moment responses can be used in a linearized approach to the blast-load problem is outlined.

INTRODUCTION

The growth of the lift and moment on a wing entering a stationary sharp-edged gust has been the subject of numerous investigations since it was first calculated for incompressible two-dimensional flow in

references 1 and 2. However, very little work appears to have been done on the subject of lift and moment response to traveling sharp-edged gusts, the only published results being those presented for incompressible two-dimensional flow in reference 3.

The reason for this shortage of information is probably due to the fact that gusts (in the literal sense) traveling at high speeds are not likely to be encountered in practice. However, the lifts and moments due to penetration of traveling gusts can be used to calculate the loads and motions of an airplane or missile dropped from another airplane, of an airplane crossing the wake of or flying past another airplane, of a helicopter blade traversing the wake produced by itself and the other blades of the rotor (a problem which furnished the motivation for ref. 3), of an airplane flying through a sonic "boom," and of an airplane encountering or being overtaken by a blast wave.

In the first section of this paper the unsteady lift and moment pursuant to penetration of a traveling sharp-edged gust are calculated by linear theory for incompressible two-dimensional flow (by a method different from the one employed in ref. 3), for two-dimensional supersonic flow, for delta wings with supersonic leading edges, for rectangular wings in supersonic flow, and for very narrow delta wings in incompressible and compressible flow. The unsteady-lift functions presented here may be considered to be generalized unsteady-lift functions in the sense that they include as special cases the two previously calculated unsteady-lift functions: namely, the gust-penetration (Küssner) function, which corresponds to zero gust speed, and the unsteady-lift function due to airplane motion (the Wagner function, first calculated in ref. 4), which corresponds to infinite gust speed.

By using the unsteady-lift functions calculated for two-dimensional incompressible and supersonic compressible flow, the normal-acceleration response is calculated in the second section of this paper for airplanes with two different mass ratios and for various values of the speed of gust propagation in order to indicate the effect of this speed on the accelerations.

The relation between traveling gusts and blast waves is indicated in the third section of this paper. The results presented herein for supersonic speeds are thus pertinent to the penetration of blast waves, although the results calculated by linear theory are usable only if the blast waves are weak, and although for blasts the unsteady-lift functions calculated in this manner represent only the effects of the change in flow direction induced at the wing. The effects of the finite pressure jump, which are of first order, are not taken into account entirely and may require separate treatment; and neither are the effects of the discontinuities in density and temperature taken into account. However, these effects are of higher order and, hence, negligible for a weak blast wave.

General relations between the lift or moment responses to sharp-edged gusts (traveling or stationary) and the responses to indicial flap deflections are given in the appendix. These relations have been used to calculate the unsteady-lift and unsteady-moment functions given herein for incompressible two-dimensional flow and to check the results obtained for some other conditions.

SYMBOLS

A	aspect ratio
a	speed of sound of undisturbed stream
$b(x')$	local span
$C(k)$	Theodorsen function
C_L	lift coefficient
C_{L_α}	slope of lift curve
C_m	pitching-moment coefficient (steady-state value)
$C_m(s)$	instantaneous value of pitching-moment coefficient
C_p	pressure coefficient
c	chord, root chord in case of delta wing
c_l	section lift coefficient
c_{l_α}	section slope of lift curve
c_m	section pitching-moment coefficient
d	distance behind wave front
\dot{h}	local effective sinking speed of wing
K	alleviation factor for sharp-edged gust
k	reduced frequency, $\frac{\omega}{2V/c}$

$k(s)$	unsteady-lift function for penetration of traveling sharp-edged gusts
$k_{\delta}(s, \xi)$	unsteady-lift function for indicial flap deflection
$k_1(s)$	unsteady-lift function for indicial change of angle of attack
$k_2(s)$	unsteady-lift function for penetration of stationary gust
$l(x')$	lift per unit length along chord
M	Mach number, V/a
M_e	equivalent Mach number, $M + M_g$
M_g	Mach number corresponding to gust propagation speed
m	slope of leading edge, $b(x')/2x'$
m_a	mass of airplane
Δp	differences in pressures on upper and lower wing surface at a given point
p_b	overpressure in blast
q	dynamic pressure, $\frac{1}{2} \rho V^2$
S	wing area
s	distance traveled, semichords or root semichords (unless specified otherwise)
t	transformed time (distance traveled by sound wave), at'
t'	physical time
V	forward velocity of wing
V_g	propagation velocity of gust, positive when moving in direction opposite to that of wing
W	vertical velocity of gust

- x transformed ordinate corresponding to x' , $(x' - Vt')$
- x' ordinate along flight path, measured rearward from leading edge or apex of wing
- \ddot{z} acceleration of airfoil due to traveling sharp-edged gust
- \ddot{z}_s static acceleration, $\frac{qSc_{L\alpha}}{m_a} \frac{W}{V}$
- α_0 angle of attack of wing prior to gust entry, radians

$$\beta = \sqrt{|1 - M^2|}$$

$\delta(s)$ unit impulse function or Dirac delta function

λ speed ratio, $\frac{V}{V + V_g}$

μ mass ratio, $\frac{4m_a}{\rho Sc c_{L\alpha}}$

ρ air density

ϕ perturbation velocity potential

ω circular frequency

$\int(s)$ unit jump function

Subscripts:

b blast

t time

Dots indicate differentiation with respect to time.

CALCULATION OF UNSTEADY-LIFT AND UNSTEADY-MOMENT FUNCTIONS
 FOR TRAVELING SHARP-EDGED GUSTS

The unsteady-lift and unsteady-moment functions for indicial angle-of-attack change and for penetration of a sharp-edged stationary gust have been calculated for a large variety of conditions. (See refs. 1 to 11, for instance.) This information is not sufficient in itself to calculate the unsteady-lift and unsteady-moment functions for traveling sharp-edged gusts. Therefore, in this section most of the functions are calculated directly by solving the given boundary-value problem by use of the techniques employed previously to solve the other problems.

The desired functions can be calculated if additional information is available for the indicial-response functions, such as the indicial responses to flap deflections. This approach is outlined in the appendix and will be used in this section to calculate the desired responses for incompressible two-dimensional flow.

The Boundary-Value Problem

The linearized partial differential equation for the velocity potential of a wing traveling at a constant speed V in a compressible inviscid medium is the wave equation and can be written in coordinates fixed in the wing surface as

$$(1 - M^2)\phi_{x'x'} + \phi_{y'y'} + \phi_{z'z'} = \frac{1}{a^2}(2V\phi_{x't'} + \phi_{t't'}) \quad (1)$$

and for the lifting case the pressure difference Δp between the upper and lower surface is given in terms of the potential on the surface by

$$\frac{\Delta p}{q} = \frac{4}{V^2}(V\phi_{x'} + \phi_{t'}) \quad (2)$$

For the sharp-edged gust-penetration problem the primary boundary condition is that the downwash ϕ_z be zero on the part of the wing which has not yet been reached by the gust front, and be equal to W on that part of the wing which has been passed over by the gust front; that is, on the wing surface,

$$\left. \begin{aligned} \phi_{z'} &= 0 & (x' > (V + V_g)t') \\ \phi_{z'} &= W & (x' < (V + V_g)t') \end{aligned} \right\} \quad (3)$$

Other boundary conditions are that the pressures on the plane of the wing be zero (except on the wing) and that the pressure difference at subsonic trailing edges be zero.

For supersonic flow the following coordinate transformation often facilitates the solution of the problem:

$$\left. \begin{aligned} x &= x' - Vt' \\ y &= y' \\ z &= z' \\ t &= at' \end{aligned} \right\} \quad (4)$$

Under this transformation, equation (1) becomes the normalized wave equation in stationary coordinates

$$\phi_{xx} + \phi_{yy} + \phi_{zz} = \phi_{tt} \quad (5)$$

equation (2) becomes

$$\frac{\Delta p}{q} = \frac{4}{VM} \phi_t \quad (6)$$

and equation (3) becomes, for the transformed wing surface,

$$\left. \begin{aligned} \phi_z &= 0 & (x > M_g t) \\ \phi_z &= W & (x < M_g t) \end{aligned} \right\} \quad (7a)$$

for gusts traversing the wing from the leading edge to the trailing edge. Similarly,

$$\left. \begin{aligned} \phi_z &= 0 & (x < c + M_g t) \\ \phi_z &= W & (x > c + M_g t) \end{aligned} \right\} \quad (7b)$$

for gusts overtaking the wing.

Definitions of Unsteady-Lift and Unsteady-Moment Functions

The section lift and moment coefficients can be obtained by integration of the pressure distribution along a chord, namely,

$$\left. \begin{aligned} c_l &= \frac{1}{c} \int_0^c \frac{\Delta p}{q} dx' \\ c_m &= \frac{1}{c^2} \int_0^c \frac{\Delta p}{q} x' dx' \end{aligned} \right\} \quad (8)$$

On a wing of finite section the loading on a spanwise strip can be obtained by integrating over y , namely,

$$\frac{l(x')}{q} = \int_{-b(x')/2}^{b(x')/2} \frac{\Delta p}{q} dy' \quad (9)$$

and, hence, the lift and moment coefficients can be obtained from

$$\left. \begin{aligned} c_L &= \frac{1}{S} \int_0^c \frac{l(x')}{q} dx' \\ c_m &= \frac{1}{Sc} \int_0^c \frac{l(x')}{q} x' dx' \end{aligned} \right\} \quad (10)$$

The unsteady-lift functions for penetration of traveling sharp-edged gusts will be normalized to their steady-state values and, hence, be defined for two-dimensional flow as

$$k(s) \equiv \frac{c_l(s)}{c_{l\alpha} \frac{W}{V}}$$

and for three-dimensional flow as

$$k(s) \equiv \frac{C_L(s)}{C_{L\alpha} \frac{W}{V}}$$

where both $c_l(s)$ and $C_L(s)$ pertain to vertical gusts of intensity W , and s is the distance traveled in semichords (for two-dimensional and rectangular wings) or root semichords (for delta wings).

For the unsteady-moment functions no common designation exists. Therefore, unsteady-moment coefficients will be presented directly for unit W/V and will not be normalized with respect to the steady-state values.

When the gust propagation speed is zero, the function $k(s)$ reduces to the commonly used gust-penetration function, which is usually designated by $k_2(s)$ and referred to as the Küssner function. Thus,

$$k(s) \Big|_{V_g=0} = k_2(s)$$

Similarly, when the gust propagation speed is infinite, the angle of attack over the entire wing is changed instantaneously; therefore, the unsteady-lift function becomes that for indicial change of angle of attack, which is usually designated by $k_1(s)$ and is referred to as the Wagner function. Thus,

$$k(s) \Big|_{V_g=\infty} = k_1(s)$$

Between these extremes, when the gust propagation speed is positive, the gust approaches the wing; when it is negative but less in magnitude than

the speed of the wing, the wing overtakes the gust. When the gust speed is negative but greater in magnitude than that of the wing, the gust overtakes the wing; that is, it approaches the wing from the rear. All these possibilities will be considered in this paper.

Incompressible Two-Dimensional Flow

For incompressible two-dimensional flow, equation (1) becomes the two-dimensional Laplace equation, and its direct solution for the unsteady boundary condition represented by equation (3) constitutes a difficult problem. This problem has been solved in reference 3 by an indirect approach, which consists in using the known results for the lift response due to an infinite train of traveling sinusoidal gusts and in obtaining the response for sharp-edged gusts by means of the well-known superposition integral given in reference 5. However, in order to effect this transformation, the results for sinusoidal gusts have to be expanded in a series; thus, the results for the sharp-edged traveling gust contain a certain degree of approximation.

The same function had been obtained by an altogether different method in connection with the present paper before reference 3 became available. This method is based on the approach outlined in the appendix and consists in relating the lift or moment response to penetration of a stationary or traveling sharp-edged gust to indicial lifts and moments due to flap deflection by means of superposition integrals. Its application to the case of incompressible two-dimensional flow is outlined in the following paragraphs. Although this approach also contains an approximation, a comparison of its results with those of reference 3 should furnish an indication of the validity of the two approximations.

Equations (A1) and (A2) of the appendix serve to express the desired unsteady-lift function $k(s)$ for traveling gusts in terms of the unsteady-lift function for indicial flap deflection $k_g(s, \xi)$ for the wing with the given plan form and Mach number; for incompressible two-dimensional flow this function k_g is given by equation (A8). Thus, upon substituting this function into equation (A1), the following expression is obtained for traveling gusts which pass over the wing from the leading edge toward the trailing edge:

$$k(s) = - \int_0^{\min(2, \frac{s}{\lambda})} \left[\frac{1}{\pi} k_{1,c}(s-\lambda\sigma) \frac{1}{\pi} \left(\frac{dT_{10}}{d\xi} \right)_{\xi=\sigma} + \frac{1}{2\pi} \delta(s-\lambda\sigma) \left(\frac{dT_{14}}{d\xi} \right)_{\xi=\sigma} \right] d\sigma \quad (11)$$

where $k_{1,c}(s)$ is the continuous part of the indicial-lift function $k_1(s)$, that is, the part of $k_1(s)$ excluding the delta function for this case. (The notation in the upper limit of the integral specifies that the upper limit is the smaller of the two quantities 2 and s/λ .) The functions T_{14} and T_{10} are (see eq. (A6))

$$\left. \begin{aligned} T_{14} &= (\xi - 1) \sqrt{2\xi - \xi^2} - \cos^{-1}(\xi - 1) \\ T_{10} &= \sqrt{2\xi - \xi^2} + \cos^{-1}(\xi - 1) \end{aligned} \right\} \quad (12)$$

Similarly, for gusts overtaking the wing (passing over the wing from the trailing edge toward the leading edge), equations (A2) and (A8) yield

$$k(s) = \int_0^{\min(2, \frac{s}{\lambda})} \left[\frac{1}{\pi} k_{1,c}(s - |\lambda|\sigma) \left(\frac{-dT_{10}}{d\xi} \right)_{\xi=2-\sigma} - \frac{1}{2\pi} \delta(s - |\lambda|\sigma) \left(\frac{-dT_{14}}{d\xi} \right)_{\xi=2-\sigma} \right] d\sigma \quad (13)$$

Hence, for gusts approaching the wing or receding from it at a speed below that of the wing, equations (11) and (12) yield

$$\left. \begin{aligned} k(s) &= \frac{1}{\pi} \int_0^{s/\lambda} k_1(s - \lambda s_1) \sqrt{\frac{s_1}{2 - s_1}} ds_1 + \frac{1}{\pi\lambda^2} \sqrt{s(2\lambda - s)} \quad (s \leq 2\lambda) \\ k(s) &= \frac{1}{\pi} \int_0^2 k_1(s - \lambda s_1) \sqrt{\frac{s_1}{2 - s_1}} ds_1 \quad (s \geq 2\lambda) \end{aligned} \right\} \quad (14)$$

and, similarly, for gusts overtaking the wing, equations (12) and (13) yield

$$\left. \begin{aligned}
 k(s) &= \frac{1}{\pi} \int_0^{s/|\lambda|} k_1(s-|\lambda|s_1) \sqrt{\frac{2-s_1}{s_1}} ds_1 + \\
 &\quad \frac{1}{\pi\lambda^2} \sqrt{s(2|\lambda|-s)} \quad (s \leq 2|\lambda|) \\
 k(s) &= \frac{1}{\pi} \int_0^2 k_1(s-|\lambda|s_1) \sqrt{\frac{2-s_1}{s_1}} ds_1 \quad (s > 2|\lambda|)
 \end{aligned} \right\} \quad (15)$$

In the same manner, expressions for the unsteady-moment function $c_m(s)$ for traveling gusts can be obtained from equations (A1) and (A2) by using the moment function for indicial flap deflection given in equation (A11) and the function T_8 defined in equation (A9).

The expressions for the lift due to penetration of traveling gusts cannot be evaluated exactly because no explicit expression for $k_{1,c}(s)$ is known. However, the following simple function was shown in reference 5 to be a good approximation to the Wagner function:

$$k_{1,c}(s) \approx 1 - \frac{2}{4+s} \quad (16)$$

With this expression the unsteady-lift functions $k(s)$ can be evaluated readily. The results are given in table 1 and are plotted in figure 1 for several values of λ . (In fig. 1 the abscissa is interrupted at $s \approx 5$ and different scales are used in order to exhibit the behavior of the response functions at both small and large values of s .) For $\lambda = 0$ ($V_g = \pm \infty$), the functions $k(s)$ given by equations (14) and (15), respectively, reduce to the approximate Wagner function given in equation (16); and for $\lambda = 1$ ($V_g = 0$), the expression for gusts approaching the wing reduces to an equivalent approximation to the Küssner function.

The analytic expressions given here for $k(s)$ can be compared directly with those given in reference 3 only for small and very large values of s , in which range the agreement is very good. In the intermediate range of s the numerical results presented in figure 1 agree with those estimated in reference 3 to within the width of the lines.

Therefore, in view of the entirely different nature of the approximations made in the two methods, the excellent agreement of the results is gratifying.

An examination of figure 1(a) indicates that, as the propagation speed of the gust increases from 0 to ∞ (λ decreases from 1 to 0), the continuous part of the lift-response function $k(s)$, which represents the circulatory contribution, increases gradually for all finite values of s from the Küssner function to the Wagner function. At the same time the noncirculatory contribution increases also and more rapidly, giving rise to a hump in the response function with a maximum at approximately the value of s which corresponds to the time it takes the gust to traverse one-half of the wing chord. This hump, which exists neither in the Küssner nor the Wagner function (as usually defined), may be very large, much larger than the steady-state value, in fact. As the forward speed of the gust approaches infinity, this hump approaches the function $\frac{1}{2} \delta(s)$, which represents the noncirculatory contribution associated with the singular part of the Wagner function.

When the gust recedes from the wing at speeds less than that of the wing ($\lambda > 1$), both the circulatory and the noncirculatory part of the response tend to decrease until, when the gust travels almost as fast as the wing, the response increases very slowly and thus takes a very long time to attain its steady-state value of unity.

The lift-response functions for gusts overtaking the wing, that is, for $V_g < -V$ and, hence, for negative values of λ , are shown in figure 1(b). For very large gust speeds the response function again approaches the Wagner function. For smaller speeds both the circulatory and the noncirculatory part of the lift gradually decrease, until, when the gust overtakes the wing with a speed barely higher than that of the wing, the lift increases very slowly toward its steady-state value. As in the case of gusts approaching the wing, the noncirculatory contribution again leads to a hump which may be very large.

The circulatory part of the lift tends to be greater for gusts overtaking the wing than for gusts approaching the wing or receding from it, for the same reason that trailing-edge flaps are more effective in producing lift than leading-edge flaps, although the noncirculatory part is the same (for a given value of $|\lambda|$). Thus, for a gust overtaking a wing the lift response is larger at all finite values of s than for a gust being overtaken by the wing at the same relative speed, namely, $|V + V_g|$.

The unsteady-moment functions $c_m(s)$ which were calculated in a similar manner are given in table 2 and are shown in figure 2. As may be

seen from equations (A10) and (A11) by the absence of terms proportional to $C(k)$ and $k_{1,c}(s)$, the moment about the quarter-chord points contains no contribution due to circulatory effects. Hence, no approximation of the type indicated in equation (16) needs to be made for the moment function. The behavior of the functions $c_m(s)$ shown in figure 2 is thus similar to the variation of the humps in $k(s)$ discussed previously.

As the forward propagation speed of the gust approaches infinity, the moment function approaches the function $-\pi\delta(s)$, which indicates that the lift represented by the contribution $\frac{1}{2}\delta(s)$ to $k(s)$ for that case acts at the midchord. As the forward speed of the gust decreases, the initial center of pressure moves forward until it reaches the quarter-chord point of the wing when the forward speed of the gust is zero. As the gust recedes from the wing at velocities $0 > V_g > -V$, the initial center-of-pressure location is forward of the quarter chord, thus resulting in positive initial pitching moments.

Supersonic Two-Dimensional Flow

For supersonic two-dimensional flow the functions $k_1(s)$ and $k_2(s)$ have been calculated in references 6 and 7. The function $k(s)$ and $c_m(s)$ can be obtained in the same manner. For this purpose equations (5), (6), and (7) are convenient, because they serve to identify the actual boundary-value problem (in the transformed coordinates) with the boundary-value problem of a three-dimensional wing with supersonic edges in steady flow parallel to the t -axis with a Mach number of $\sqrt{2}$. The potential and pressure for this wing are then also the ones for the problem of interest here.

The fictitious three-dimensional wings are shown in figure 3. The leading and trailing edges are indicated, and the leading edge also includes the part of the t -axis between 0 and c . The boundary conditions are that in the shaded region $\phi_z = \frac{W}{V}$, elsewhere on the wing $\phi_z = 0$, and ahead of the wing $\phi = 0$. For these boundary conditions the pressure coefficient can be obtained readily by a superposition of sources or by conical-flow methods, and these are given in table 3. The lift and moment coefficients as a function of time can be obtained from equation (8), and the lift function can be reduced to $k(s)$ by dividing by $\frac{W}{V} \frac{4}{\sqrt{M^2 - 1}}$. The results for $k(s)$ and $c_m(s)$ are given in tables 4 and 5 and are shown for $M = 2$ in figures 4 and 5 for several values of M_g . For $M_g = 0$ and $M_g = \infty$ the function $k(s)$ reduces to the functions $k_1(s)$ and $k_2(s)$ given in reference 7, as may be expected.

As may be seen from figure 4(a), as the forward speed of the gusts increases, the rate of lift growth at small values of s increases and tends to approach infinity as the gust speed approaches infinity. For low gust speeds the increase is steady, but for high gust speeds ($M_g \geq 1$ for $M = 2$) the lift increases to the initial value of the k_1 function and dips down before it increases again toward the steady-state value of unity. The large peaks associated with the noncirculatory contribution in incompressible (and presumably subsonic) flow are not present for supersonic flow.

For gusts receding from the wing the gust-response function increases steadily, and the rate of increase decreases with gust speed until, for gusts receding at almost the speed of the wing, the function increases very slowly.

Similarly, as may be seen from figure 4(b), for gusts overtaking the wing, the lift response increases linearly (at a rate which increases with the speed of the gust) until it reaches a value intermediate between the initial value of the Wagner function and the steady-state value of unity, and then continues increasing at a much lower rate.

Similar observations may be made for the moment functions shown in figure 5.

Delta Wings With Supersonic Leading Edges

For delta wings with supersonic leading edges, that is, for delta wings with an aspect ratio A larger than $4/\sqrt{M^2 - 1}$ or a slope m of the leading edge (tangent of the apex half-angle) larger than $1/\sqrt{M^2 - 1}$, the functions $k_1(s)$ and $k_2(s)$ have been given in references 8 and 9. Again, the functions $k(s)$ and $C_m(s)$ can be obtained in a similar manner.

The detailed solution of this three-dimensional-flow problem is much more difficult than that of the two-dimensional-flow problem discussed in the preceding section. However, if attention is confined to the chordwise load-distribution function $l(x)$ and the total lift and pitching moment, the problem can be reduced to a two-dimensional one similar to the problem considered in the preceding section. This reduction can be effected (see ref. 8) by considering the integral of ϕ over the local span, that is,

$$\Phi = \int_{-\infty}^{\infty} \phi \, dy'$$

for which, in the coordinates x, z, t , the partial differential equation is equation (5), with the y derivatives deleted. The loading function $l(x)$ is then given by the equivalent of equation (6), namely,

$$\frac{l(x)}{q} = \frac{4}{VM} \phi_t$$

and the boundary condition is the equivalent of equation (7), namely, for the fictitious wing surface in transformed coordinates,

$$\phi_z \equiv \int_{-m(x+Mt)}^{m(x+Mt)} \phi_z \, dy$$

Thus,

$$\phi_z = 0 \quad (x > M_g t)$$

$$\phi_z = 2Wm(x + Mt) \quad (x < M_g t)$$

or

$$\phi_z = 0 \quad (x < c + M_g t)$$

$$\phi_z = 2Wm(x + Mt) \quad (x > c + M_g t)$$

depending on whether M_g is greater than or less than $-M$.

The geometric characteristics of the fictitious wing are again those indicated in figure 3 (where c now refers to the root chord) and the boundary condition on ϕ is again specified on the shaded part of the wing and is zero elsewhere; but it is not constant as it was before. The solution of the problem cannot, therefore, be obtained readily by conical-flow methods; but the source-superposition method can still be used conveniently, that is,

$$\phi(x, 0, t) = -\frac{1}{\pi} \int \int_{\text{Mach forecone}} \frac{\phi_z(x_1, t_1) dx_1 dt_1}{\sqrt{(t - t_1)^2 - (x - x_1)^2}}$$

The resulting expressions for the loading function are given in table 3, and the corresponding values of $k(s)$ and $C_m(s)$ are given in

L

tables 4 and 5 and are shown in figures 6 and 7 for $M = 2$ and several values of M_g . Again, the function $k(s)$ reduces to the known functions $k_1(s)$ and $k_2(s)$ (see ref. 9, for instance) for $M_g = \infty$ and $M_g = 0$, respectively. The behavior of these functions may be seen to be similar to that of the functions for supersonic two-dimensional flow. (See figs. 4 and 5.)

Rectangular Wings in Supersonic Flow

The pressure distribution in the region of a rectangular wing ahead of the Mach cones emanating from the wing tips is identical to that of a two-dimensional wing. Although the pressure distribution within the Mach cones cannot be calculated readily, the chordwise loading and the total lift and moment contributed by these regions can be determined readily by a technique similar to that used in the preceding section provided the Mach cone emanating from one wing tip does not cross the opposite side edge, that is, provided A is larger than $1/\sqrt{M^2 - 1}$. For such wings which will be referred to as wide rectangular wings, the functions $k_1(s)$ and $k_2(s)$ have been given in reference 10 and elsewhere.

In reference 10 the unsteady-lift coefficient for a wide rectangular wing with a downwash distribution of the form

$$\phi_z'(x', y', 0, t') = V f(x') \underline{\int}(t' - t'_0)$$

(where $\underline{\int}$ represents the unit jump function and t'_0 may depend on x') is expressed as

$$C_L(t') = C_{L,0}(t') - \Delta C_L(t') \tag{17}$$

where $C_{L,0}(t')$ is the indicial-lift coefficient for a two-dimensional wing with the same downwash condition.

The correction term which must be added to the two-dimensional value can be expressed as an integral of a chordwise-loading function $\gamma(x', t')$ and is, for a wing of unit chord,

$$\Delta C_L(t') = \frac{4}{A(M^2 - 1)} \int_0^1 \gamma(x', t') dx' \tag{18a}$$

An analogous correction for the moment coefficient is

$$\Delta C_m(t') = \frac{4}{A(M^2 - 1)} \int_0^1 \gamma(x', t') x' dx' \quad (18b)$$

where

$$\gamma(x', t') = \int_0^{x'} a_1 \left[\frac{x' - \xi}{V(t' - t'_0)} \right] f(\xi) d\xi \quad (19)$$

where, in turn, the indicial-response function $a_1(\tau)$ is given by

$$\begin{aligned} a_1(\tau) &= 0 & (\tau < 0) \\ &= 1 & (0 \leq \tau \leq m_1) \\ &= \frac{m_1}{2} & (m_1 \leq \tau \leq n_1) \\ &= 0 & (\tau \geq n_1) \end{aligned}$$

and

$$\begin{aligned} m_1 &= \frac{M - 1}{M} \\ n_1 &= \frac{M + 1}{M} \end{aligned}$$

Now, for a wide rectangular wing penetrating a traveling sharp-edged gust of intensity W and speed V_g ,

$$f(\xi) = \frac{W}{V} \quad (20)$$

$$t_0(\xi) = \frac{\xi}{aM_e} \quad (M_g > -M) \quad (21a)$$

and

$$t_0(\xi) = \frac{1 - \xi}{a|M_e|} \quad (M_g < -M) \quad (21b)$$

where

$$M_e = M + M_g$$

Substitution of equations (20) and (21a) into equation (19) yields

$$\gamma(x', t) = \frac{W}{V} \int_0^{x'} a_1 \left[\frac{x' - \xi}{\frac{M}{M_e} (M_e t - \xi)} \right] d\xi$$

or, changing the variable of integration to

$$\tau \equiv \frac{M_e}{M} \frac{x' - \xi}{M_e t - \xi}$$

gives

$$\gamma(x', t) = \frac{-W}{V} \frac{M_e}{M} (x' - M_e t) \int_0^{\frac{x'}{M t}} \frac{a_1(\tau)}{\left(\tau - \frac{M_e}{M}\right)^2} d\tau \quad (M_g \geq -M) \quad (22)$$

and, similarly,

$$\gamma(x', t) = \frac{-W}{V} \frac{M_e}{M} (x' - l - M_e t) \int_0^{\frac{M_e x'}{M(M_e t + 1)}} \frac{a_1(\tau)}{\left(\tau - \frac{M_e}{M}\right)^2} d\tau \quad (M_g < -M) \quad (23)$$

The geometric characteristics of this problem are indicated in figure 8. The integrations required in equations (22) and (23) take place along lines $Mt = \text{Constant}$ from $\xi = x'$ (where $\tau = 0$) to $\xi = 0$ (where $\tau = \frac{x'}{Mt}$ or $\tau = \frac{M_e x'}{M(M_e t + 1)}$, depending on whether $M_g \geq -M$). The

resulting expressions for γ are given in table 6. These expressions have been integrated to obtain the correction for the lift and moment coefficients. (See eqs. (18).) The results are given in tables 4 and 5. The unsteady-lift function $k(s)$, which is obtained by normalizing the corrected value of the two-dimensional unsteady-lift function (see

eq. (17)), is shown in figures 9 to 12 for $M = 2$ and several values of M_g and A . Similarly, the unsteady-moment coefficients are given in figures 13 to 16 for several values of M_g and A . Again, the unsteady-lift function $k(s)$ reduces to the known functions $k_1(s)$ and $k_2(s)$ for this case, which are given in reference 10.

The behavior of the lift-response and moment-response functions is similar to that for supersonic two-dimensional flow, except for the slight differences associated with the fact that for finite aspect ratios the initial value of the k_1 function can be greater than the steady-state value.

Very Narrow Delta Wings

For very narrow delta wings and bodies, derivatives with respect to x' or x tend to be small compared with the others in the equations of motion (eqs. (1) and (5)). For incompressible flow, equation (1) therefore becomes the two-dimensional Laplace equation in the $Y'Z'$ -plane and can be solved readily for both steady and unsteady boundary conditions. If only the chordwise-loading function and the total lift and moment are of interest, the solution of the boundary-value problem can be avoided, because the chordwise loading can be obtained directly from apparent-mass considerations. This approach was used in reference 11 to calculate the functions $k_1(s)$ and $k_2(s)$.

For compressible flow, equation (5) becomes the two-dimensional-wave equation with boundary conditions in the case of interest here which can be construed as pertaining to a three-dimensional wing in steady supersonic flow, as was done for the functions $k_1(s)$ and $k_2(s)$ in reference 12.

Incompressible flow.- The expression for the chordwise loading given in reference 11 is

$$z(x') = \left(\frac{\partial}{\partial t'} + V \frac{\partial}{\partial x'} \right) \left[\pi \rho \frac{b^2(x')}{4} \dot{h}(x', t') \right]$$

where $b(x)/2$ is, for a delta wing, equal to mx' , m being the tangent of the semiapex angle of the wing. For a wing flying at speed V and penetrating a traveling sharp-edged gust approaching from the leading edge with speed V_g , the effective sinking speed \dot{h} is given by

$$\dot{h}(x', t') = \dot{w} \int \left(t' - \frac{x'}{V_e} \right) \quad (24)$$

where $V_e \equiv V + V_g$ and \int designates the unit jump function, as before. The total indicial lift and moment about the two-thirds root-chord point of the wing are thus

$$k(s) = \frac{s^2}{4\lambda^3} [1 - \int (s-2\lambda)] + \int (s-2\lambda)$$

$$\frac{C_m(s)}{C_L(\infty)} = \left[\frac{s^3}{24\lambda^4} (3 - \lambda) - \frac{s^2}{6\lambda^3} \right] [1 - \int (s-2\lambda)]$$

When λ is zero or infinite, the following two limiting cases are obtained:

$$\begin{aligned} k(s)|_{\lambda=1} &= \frac{s^2}{4} & (s \leq 2) \\ &= 1 & (s > 2) \end{aligned}$$

and

$$k(s)|_{\lambda=0} = \frac{2}{3} \delta(s) + \int (s)$$

where $\delta(s)$ is the Dirac delta function. These results are identical with the functions $k_1(s)$ and $k_2(s)$ presented in reference 11 for this case.

Similarly, for gusts overtaking the wing,

$$h(x', t') = W \int \left(t' + \frac{c - x'}{V_e} \right)$$

Thus, the lift and moment functions become

$$\begin{aligned} k(s) &= \frac{1}{|\lambda|} \left(1 - \frac{s}{2|\lambda|} \right)^2 [1 - \int (s-2|\lambda|)] + 1 \\ \frac{C_m(s)}{C_L(\infty)} &= \frac{1}{3\lambda} \left(1 + \frac{s}{2\lambda} \right)^2 \left[2 - \left(1 + \frac{s}{2\lambda} \right) (3 - \lambda) \right] [1 - \int (s-2|\lambda|)] \end{aligned}$$

where $\frac{C_m(s)}{C_L(\infty)}$ is again referred to the two-thirds root-chord point. For the special case for which V_g is infinite, this function $k(s)$ reduces to the function $k_1(s)$ given in reference 11. When $V_g = -V$ (the case of a gust traveling just behind the trailing edge), $k(s) = 0$; however, if $V_g = -\lim_{\epsilon \rightarrow 0} (V_0 + \epsilon)$ (the case of a gust traveling at the same velocity as the airfoil and with its leading edge just ahead of the trailing edge of the wing), then

$$k(s) = \int(s) _$$

The functions $k(s)$ and $C_m(s)$ for gusts approaching the wing from either direction are shown in figures 17 and 18 for several values of λ .

The behavior of the response functions is similar to that of the functions for incompressible two-dimensional flow. Again, large peaks associated with the noncirculatory contribution to the lift exist at low values of s for gusts approaching the wing or overtaking the wing; and, again, the value of the response function at all finite values of s tends to be much larger for gusts overtaking the wing than for gusts approaching it or receding from it at the same relative speed.

Compressible flow.- For compressible flow the lift and moment responses can be obtained by the method used in reference 12. The resulting expressions are given in tables 7 and 8. They involve a function $f(\eta)$ which is defined and tabulated in reference 8. Inasmuch as no simple explicit expressions for $f(\eta)$ are available, the integrations required to obtain the functions of interest here would have to be performed numerically. No such calculations have been made. However, the unsteady-lift functions given here can be shown to reduce to the functions $k_1(s)$ and $k_2(s)$ given in reference 12.

NORMAL-ACCELERATION RESPONSE OF AN AIRPLANE TO TRAVELLING GUSTS

The purpose of this section is to indicate the effect that changes in the response function which result from changes in the gust speed may have on the acceleration response of an airplane to sharp-edged gusts. For this purpose the airplane will be assumed to be free to move in only one degree of freedom, vertical translation. Ignoring the pitching degree of freedom implies that not only pitching motions and their effect on the normal acceleration but also the unsteady moment which results from the fact that the gust strikes the wing and tail at different

instants of time are disregarded. Nonetheless, this assumption is made very often in gust-load studies, particularly in primarily qualitative studies, and will be used here for that purpose. For airplanes with a high mass ratio, with a relatively high pitching moment of inertia, or with a well-damped short-period mode, or for literally sharp-edged gusts (such as those represented by a blast), this approach is even capable of yielding useful quantitative information.

In terms of the unsteady-lift functions $k(s)$ and $k_1(s)$ due to traveling-gust penetration and plunging, respectively, the equation of motion for this case can be written in dimensionless form as

$$K(s) \equiv \frac{\ddot{z}(s)}{\ddot{z}_s} = k(s) - \frac{1}{\mu} \int_0^s k_1(s-s_1)K(s_1)ds_1 \quad (25)$$

where $K(s)$ is an alleviation factor referred to the reference "static" acceleration

$$\ddot{z}_s \equiv \frac{qSc_{L\alpha} W}{m_a V}$$

which is the initial acceleration response if unsteady-lift effects are ignored, and μ is a mass parameter defined by

$$\mu = \frac{4m_a}{\rho Sc c_{L\alpha}}$$

An examination of equation (25) indicates that for large values of the mass parameter the alleviation factor K is substantially equal to the lift-response function $k(s)$. Thus, any changes in $k(s)$ are then directly reflected in similar changes in the normal-acceleration response.

For smaller values of the mass parameter the integral equation has to be solved for $K(s)$ by using operational methods (if $k(s)$ and $k_1(s)$ are, or can approximately be, expressed by simple functions), by iteration, or by numerical methods. Numerical calculations have been made for $\mu = 50$ and 200 by using the two-dimensional unsteady-lift functions for incompressible and supersonic flow. The value of $\mu = 50$ represents a transport airplane flying at low or moderately high altitudes; the other value represents a fighter or bomber airplane at low altitudes, or the transport airplane at high altitudes. The results are shown in figures 19 to 22.

In using response functions for two-dimensional flow to represent those for an actual tapered wing, basically two approximations are made, inasmuch as both the steady-state lift and the manner in which it is approached as a function of time differ for a wing of finite and infinite span. The differences in steady-state values can be removed by using the unsteady-lift functions $k(s)$ which are normalized with the steady-state lift; the differences in the manner in which this value is approached can be minimized by referring s to a more representative chord than the root chord, such as the mean aerodynamic chord. If s is redefined in this manner for the purpose of using the two-dimensional response function to better advantage, the mass parameter μ must also be referred to that chord rather than to c . The values of μ and s used in figures 19 to 22 should, therefore, be considered to be defined in this modified manner.

Comparison of the results presented in these figures with those for the unsteady-lift functions themselves indicates that, as expected, the acceleration response follows the lift response not only for large values of μ (around 200) but also during the first few instants of travel (in which time the peak in the lift response due to noncirculatory flow effects occurs in subsonic flow) for smaller mass ratios (around 50); however, thereafter the acceleration response does depend on the mass parameter. These statements are true for gusts both approaching the wing and overtaking it. For supersonic speeds calculations have been made only for a mass ratio μ of 50, because even for this value the acceleration responses follow substantially the lift-response characteristics; they can be expected to do so to an even greater extent for larger values of the mass ratio. The conclusion can, therefore, be drawn from these curves that the acceleration response depends to a large extent on the magnitude and direction of the gust speed.

In the preceding paragraphs only sharp-edged gusts have been considered. For traveling gusts, the intensity of which is a function of the distance behind the wave front d , the acceleration response can be determined by superposition from the sharp-edged gust response obtained by solving equation (25). Inasmuch as

$$d = \frac{cs}{2\lambda}$$

the gust intensity can also be expressed as a function of s , namely, $W(s)$. In terms of this function and the acceleration-response function $K(s)$, the normal acceleration for a time-dependent gust can be written as

$$\ddot{z}(s) = \frac{qSC_{L\alpha}}{m_a V} \left[W(0)K(s) + \int_0^s K(s-s_1) \frac{dW(s_1)}{ds_1} ds_1 \right] \quad (26)$$

The convolution process indicated in this equation may tend to obscure some of the minor effects resulting from changes in gust speed, but the major conclusions reached concerning the effect of such changes on the acceleration response to sharp-edged gusts are likely to be valid for the acceleration response to other types of gusts as well.

RELATION BETWEEN BLAST WAVES AND TRAVELING GUSTS

When a blast wave strikes a stationary object, the instantaneous pressures on the surface of the object are proportional to the peak overpressure of the blast, the constant of proportionality being a reflection factor which depends on the geometric characteristics of the object and, for strong shocks, on the shock strength as well. (See ref. 13.) This overpressure is due not only to the fact that the object is initially exposed to the shock but also to the fact that it arrests the propagation of that shock or deflects it. The manner in which the problem of calculating this overpressure (the diffraction problem) can be solved is indicated in reference 14, where the results of several such calculations are also given.

When the object is a wing flying initially through still air, its response to the overpressure of the shock is similar, but in addition to this effect it also responds to the velocity behind the shock. The effects of overpressure and velocity overlap and cannot be divorced from each other readily. For instance, for a weak shock, which propagates substantially at the speed of sound, the overpressure p_b and the velocity W_b are related by the limiting form, for small overpressures, of the Rankine-Hugoniot equation, namely,

$$p_b = \rho a W_b$$

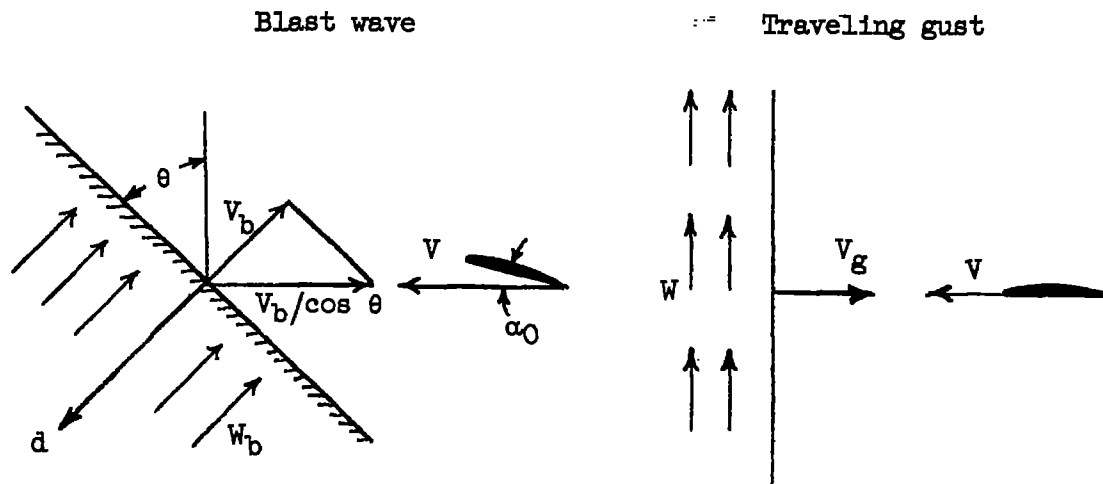
If this shock strikes a plate parallel to its front, the initial pressure on its exposed surface is $2p_b$, whether the plate is stationary or moving parallel to the shock front, and the initial pressure coefficient for the surface is

$$\frac{\Delta p}{q} = \frac{4}{M} \frac{W_b}{V}$$

However, this initial pressure coefficient is also precisely the one associated with instantaneous entry into a vertical gust of intensity W_b ; thus, consideration of either the overpressure or velocity yields a result for the initial response which includes the effects of the other in this case. On the other hand, after some time has elapsed, the overpressure equalizes around the plate and, hence, produces no pressure difference directly, although in subsonic flow it can still influence the lift through the vorticity shed while it was acting; thus, except for this induction effect in subsonic flow, the pressure difference is then due to the velocity effect alone.

In this section only the effects of the change in relative velocity occasioned by entry into a weak blast are considered. In view of the preceding argument, these effects include at least some of the effects of the overpressure associated with the given blast. Inasmuch as attention is confined to weak blasts, the effects of change in temperature (and hence speed of sound) and density across the blast wave, which produce only second-order effects on the lift of the wing, will be disregarded.

The relation between a blast wave and a traveling gust is indicated in the following sketches:



The equivalent vertical gust intensity is determined by a consideration of the conditions prior to and subsequent to gust and blast entry. Thus,

$$W = W_b \sin \theta$$

The other (horizontal) component of the blast velocity is parallel to the chord and is equivalent to a horizontal gust which, within the scope of a linearized treatment, produces the same lift as a vertical gust of intensity equal to $2\alpha_0$ times the intensity of the horizontal gust. Thus, if this effect is taken into account,

$$W = W_b(\sin \theta + 2\alpha_0 \cos \theta) \quad (27)$$

For blasts striking from almost straight ahead or behind, the second term may be more important than the first.

The equivalent speed of the traveling gust is determined by a consideration of the time required for the gust and the blast wave to traverse a given horizontal distance. Thus, the time required for the blast wave to pass over a given distance Δx along the flight path is $\Delta x \cos \theta / V_b$, and the time for the gust is $\Delta x / V_g$. Therefore, the equivalent gust speed is

$$\left. \begin{aligned} V_g &= \frac{V_b}{\cos \theta} \\ V_g &\approx \frac{a}{\cos \theta} \end{aligned} \right\} \quad (28)$$

inasmuch as for a weak blast wave, V_b is approximately the speed of sound a . The equivalent value of V_g associated with a blast must, therefore, always be supersonic.

With the equivalent relations given by equations (27) and (28), the gust-response functions for supersonic values of V_g and acceleration-response calculations presented here can thus be used for the blast-penetration problem. The variation of the blast velocity W_b behind the blast front can be taken into account by expressing this variation as a function of s by using the relation

$$d = \frac{cs}{2} \left(\cos \theta + \frac{V_b}{V} \right)$$

and then by using equation (26) to calculate the acceleration response.

DISCUSSION

The lift and moment responses have been calculated herein for two-dimensional wings in incompressible and supersonic flow, for wide delta and rectangular wings in supersonic flow, and for very narrow delta wings. The reason for selecting these cases was that for them the functions of interest could be readily calculated. For three-dimensional incompressible flow and for two-dimensional compressible flow the functions k_1 and k_2 have been calculated in previous investigations, but the methods used do not lend themselves to the calculation of the more general response functions of interest here; also no simple methods are available for calculating the desired responses of wings with subsonic leading edges in supersonic flow.

The results of calculations for very narrow delta wings have been included despite the fact that the results of linear theory for these wings are of limited practical utility, inasmuch as for even relatively low angles of attack the wake of these wings tends to curl up and introduce deviations from linearity in force and moment responses. The reasons for including these results is that they are obtained very easily for incompressible flow and serve as the only indication of aspect-ratio effects in subsonic flow available at present. In other words, their significance stems primarily from the fact that these wings serve as a theoretical limiting case. However, no numerical calculations have been made for these wings in compressible flow because such calculations would have required more effort than the results are considered to warrant.

In this paper only entry into traveling gusts and blasts is considered. However, the results also apply to the problem of exit from traveling gusts and blasts, inasmuch as exit from a gust of given intensity can be considered to represent an entry into a gust of equal and opposite intensity; thus, this problem need not be treated explicitly, and all statements made in this paper concerning responses due to entry into gusts and blasts are equally valid for exit from gusts and blasts.

A full discussion of the implications and limitations of linear theory are beyond the scope of this paper. It should be pointed out that, in order for the results of this theory to be valid, all disturbances must be small; therefore, the gust intensity and the magnitude of the resulting motion must not be too large. For most problems other than those related to blast loads, these conditions are likely to be satisfied, except possibly for very narrow delta wings. On the other hand, for blasts they may not be satisfied unless the airplane is fairly far away from the center of the blast. The limiting distance depends on the magnitude of the blast; the orientation relative to the airplane (blasts from almost directly ahead of or behind the airplane result in low induced

angles of attack); the speed of the airplane (the higher the speed the smaller the angle-of-attack change is caused by a given blast velocity; but for high subsonic, transonic, and high supersonic speeds, only small angles of attack can generally be tolerated within linear theory); and the plan form (the aerodynamic forces on low-aspect-ratio wings tend to be linear only in a small angle-of-attack range). Nonetheless, despite these limitations and despite the possible presence of the aforementioned pressure effects which have been ignored herein, the results presented herein which pertain to supersonic speeds of gust propagation should furnish a first step in the theoretical analysis of the blast-load problem.

CONCLUDING REMARKS

The lift and moment responses to penetration of sharp-edged traveling gusts have been calculated for wings in incompressible and supersonic two-dimensional flow, for wide delta and rectangular wings in supersonic flow, and for very narrow delta wings. By using the two-dimensional indicial-lift functions, some calculations of normal-acceleration response have been made for two mass ratios.

The results of these calculations indicate that the propagation speed of the gusts has a large effect on the lift- and moment-response functions. For incompressible flow (and presumably for compressible subsonic flow as well), peaks exist in the early portion of the lift response which may be much larger than the steady-state value. Some peaks also occur in the lift-response functions for supersonic speeds but are much less pronounced and exceed the steady-state value in only a few instances.

The normal-acceleration responses tend to follow the lift response very closely in the first few instants of penetration provided the mass of the airplane is not impractically small; thus, the large peaks which exist in the lift response at subsonic speeds are duplicated in the acceleration response. After the first few instants the acceleration response depends to a relatively larger extent on the mass of the airplane.

The relation between gusts traveling at supersonic speeds and blast waves has been indicated, and the manner in which the calculated lift and moment responses can be used in a linearized approach to the blast-load problem has been outlined.

Langley Aeronautical Laboratory,
National Advisory Committee for Aeronautics,
Langley Field, Va., January 16, 1957.

APPENDIX

RELATION BETWEEN UNSTEADY-LIFT FUNCTIONS FOR GUST PENETRATION
 AND FOR INDICIAL FLAP DEFLECTION

As pointed out in the text of this paper, the unsteady-lift or unsteady-moment functions for gust penetration cannot, in general, be obtained directly from the lift and moment functions for indicial angle-of-attack change. However, they can be obtained from the unsteady-lift and unsteady-moment functions for indicial flap deflection. This approach is similar to the one used by Klüssner in reference 1 for stationary gusts. However, in reference 1 consideration is given initially to sinusoidal gusts and flap deflections; whereas here the desired results are established by working with indicial responses directly.

As may be seen from equation (3), the boundary condition for gust penetration is, at any instant t' , the same as that for a wing with a leading-edge flap which extends to the point $x' = (V + V_g)t'$. Consequently, if the lift or moment due to indicial flap deflection is known, the lift due to gust penetration can be obtained by superposition. Thus, if the normalized unsteady-lift function for indicial deflection of a trailing-edge flap extending rearward from $\bar{x}' = \xi \frac{c}{2}$ is designated by $k_g(s, \xi)$, the unsteady-lift function for gust penetration can be obtained by considering segments of the wing to deflect indicially in a progressive fashion; thus,

$$k(s) \approx [k_g(s, 0) - k_g(s, \Delta\xi)] + [k_g(s - \Delta s, \Delta\xi) - k_g(s - \Delta s, 2\Delta\xi)] + \dots$$

$$\approx -\Delta\xi \frac{d}{d\xi} [k_g(s, 0) + k_g(s - \Delta s, \Delta\xi) + k_g(s - 2\Delta s, 2\Delta\xi) + \dots]$$

with

$$\Delta\xi = \frac{V + V_g}{V} \Delta s$$

$$= \frac{\Delta s}{\lambda}$$

Hence, in the limit as $\Delta\xi \rightarrow 0$,

$$k(s) = -\int_0^{\min(2, \frac{s}{\lambda})} \left[\frac{d}{d\xi} k_{\delta}(s-\lambda\sigma, \xi) \right]_{\xi=\sigma} d\sigma \quad (A1)$$

This relation pertains to stationary gusts ($\lambda = 1$) as well as for all gusts traversing the wing from the leading edge to the trailing edge ($\lambda > -1$). For gusts traversing the wing from the trailing edge to the leading edge ($\lambda < -1$), the following relation may be obtained in the same manner:

$$k(s) = \int_0^{\min(2, \frac{s}{|\lambda|})} \left[\frac{d}{d\xi} k_{\delta}(s-|\lambda|\sigma, 2-\xi) \right]_{\xi=\sigma} d\sigma \quad (A2)$$

Equations (A1) and (A2) represent the desired relations between the unsteady-lift functions for gust penetration and indicial flap deflection. Identical relations exist between the unsteady-moment functions.

The unsteady lift (or moment) due to an indicial flap deflecting, as used in the preceding relations, is the lift on a wing which has a flap deflected by a unit angle, is initially at rest, is accelerated instantaneously to speed V at time $t' = 0$, and then continues to fly at that speed with zero angle of attack. This lift is related to but not necessarily identical to the lift on a wing initially flying at speed V and experiencing an abrupt flap deflection at time $t' = 0$, because such a deflection involves transient effects, namely, those due to an impulsive rate of rotation (a condition which implies an impulsive vertical velocity proportional to the distance from the axis of rotation), which are spurious for the present purpose.

Similarly, the lift for a flap which is abruptly given a constant rate of vertical displacement at time $t' = 0$ contains other effects which are spurious for the present purpose, namely, those due to the chordwise discontinuity in displacement at the leading edge of the flap which must exist in this case.

The unsteady-lift (or moment) functions for abrupt flap displacements can be obtained from those due to oscillating displacements, which are often calculated for use in flutter studies, by means of the relation (see ref. 5)

$$k_{\delta}(s, \xi) = \int_0^{\infty} \frac{F_{\delta}(k, \xi)e^{-iks}}{ik} dk \quad (A3)$$

where F_{δ} is the real part of the normalized unsteady-lift function for sinusoidal flap displacements, and k is a reduced frequency equal to $\frac{\omega c}{2V}$. A similar relation exists between the moments.

The following two examples indicate the manner in which the required functions may be obtained.

For supersonic two-dimensional flow, a trailing-edge flap of chord c_f experiences the same lift and moment as if it were a wing with chord c_f ; and the rest of the wing contributes nothing to the lift and moment. Hence,

$$k_{\delta}(s, \xi) = \frac{c_f}{c} k_1\left(\frac{c}{c_f} s\right)$$

where $k_1(s)$ represents the unsteady-lift function for indicial angle-of-attack change, and inasmuch as $\xi = 2\left(1 - \frac{c_f}{c}\right)$,

$$k_{\delta}(s, \xi) = \frac{1}{2}(2 - \xi)k_1\left(\frac{2s}{2-\xi}\right) \quad (A4)$$

Similarly, if $C_{m,1}(s)$ is the unsteady-moment function for indicial angle-of-attack change and the moments are taken about the leading edge,

$$C_{m_{\delta}}(s, \xi) = \frac{1}{4}(2 - \xi)^2 C_{m,1}\left(\frac{2s}{2-\xi}\right) - \frac{\xi}{4}(2 - \xi) C_{L_{\alpha}} k_1\left(\frac{2s}{2-\xi}\right) \quad (A5)$$

where $C_{L_{\alpha}}$, the lift-curve slope, is the value with which $k_1(s)$ and $k(s)$ are normalized.

For incompressible two-dimensional flow the normalized complex lift function for a trailing-edge flap undergoing oscillatory displacements of amplitude $H_0 \frac{c}{2}$ with frequency ω can be obtained from those of the terms of equation (22) of reference 15 which contain the product $\beta l = H$. The following result is obtained in this manner:

$$C_L = - \left[2\sqrt{2\xi - \xi^2} \frac{c}{2} \frac{\dot{H}}{V} - \left(\frac{c}{2}\right)^2 T_4 \frac{\ddot{H}}{V^2} \right] - 2\pi C \left[\frac{T_{21}}{\pi} H + \frac{T_{10}}{\pi} \frac{c}{2} \frac{\dot{H}}{V} \right]$$

where C is a function of the reduced frequency k which is defined in reference 15, and generally is known as the Theodorsen function, and where

the functions T_4 , T_{10} , and T_{21} are defined in reference 15 in terms of a parameter c which in the notation of the present paper is $\xi - 1$; thus,

$$\left. \begin{aligned} T_4 &= (\xi - 1)\sqrt{2\xi - \xi^2} - \cos^{-1}(\xi - 1) \\ T_{10} &= \sqrt{2\xi - \xi^2} + \cos^{-1}(\xi - 1) \end{aligned} \right\} \quad (A6)$$

In the expression for C_L the terms in the first bracket are associated with noncirculatory flow, the others with circulatory flow. In each bracket the first term is due to the vertical displacement of the flap; therefore, it is not pertinent to the present purpose. (Only the contribution of the potential ϕ_H given in eq. (7) of ref. 15 is pertinent here; the potential ϕ_H given by eq. (6) of ref. 15 is not pertinent.) The desired normalized steady-lift function is, therefore, for unit downwash, that is, for $\frac{\dot{h}c}{2V} = -1$, where

$$C_B(k, \xi) = -\frac{ikT_4}{2\pi} + C(k) \frac{T_{10}}{\pi} \quad (A7)$$

Thus, equation (A3) yields

$$k_B(s, \xi) = \frac{T_{10}}{\pi} k_{1,c}(s) - \frac{T_4}{2\pi} \delta(s) \quad (A8)$$

where $\delta(s)$ is the unit impulse (Dirac delta) function and $k_{1,c}(s)$ is the continuous part of the indicial-lift-response function, which is the part obtained directly from the circulatory part of the lift due to sinusoidal vertical oscillations, namely, $C(k)$, by using equation (A3).

Similarly, the moment about the quarter-chord point can be obtained from equation (23) of reference 15 by setting $a = -\frac{1}{2}$ and retaining only the terms containing βl ; therefore,

$$C_m = -\frac{1}{2} \left[T_{22} \frac{\dot{h}}{V} + T_{23} \frac{c}{2} \frac{\dot{h}}{V} + T_{24} \left(\frac{c}{2} \right)^2 \frac{\dot{h}}{V} \right]$$

This moment is due entirely to potential effects. Again, the first term and part of the second are due to the chordwise discontinuity and are spurious. The other two terms can be expressed in terms of the functions T_4 and T_{10} used for the lift and a function T_8 defined by

$$T_8 = -\frac{1}{3}(2\xi - \xi^2)^{3/2} - (\xi - 1)T_4 \quad (A9)$$

Thus, again for $\frac{h_c}{2V} = -1$, this moment function becomes

$$C'_8(k, \xi) = -\frac{1}{2}(T_4 + T_{10}) + \frac{ik}{2} \left[T_8 + \left(\xi - \frac{1}{2} \right) T_4 \right] \quad (A10)$$

Hence, by using equation (A3), the following expression is obtained for $C_{m_8}(s, \xi)$:

$$C_{m_8}(s, \xi) = -\frac{1}{2}(T_4 + T_{10})I(s) + \frac{1}{2} \left[T_8 + \left(\xi - \frac{1}{2} \right) T_4 \right] \delta(s) \quad (A11)$$

The manner in which these functions can be used to calculate the lift and moment responses to traveling gusts by means of equations (A1) and (A2) is illustrated in the text of this paper for incompressible two-dimensional flow.

REFERENCES

1. Küssner, H. G.: Zusammenfassender Bericht über den instationären Auftrieb von Flügeln. Luftfahrtforschung, Bd. 13, Nr. 12, Dec. 20, 1936, pp. 410-424.
2. Von Kármán, Th., and Sears, W. R.: Airfoil Theory for Non-Uniform Motion. Jour. Aero. Sci., vol. 5, no. 10, Aug. 1938, pp. 379-390.
3. Miles, J. W.: The Aerodynamic Force on an Airfoil in a Moving Gust - A Generalization of the Two-Dimensional Gust Problem. Rep. No. SM-18598, Douglas Aircraft Co., Inc., Oct. 1954.
4. Wagner, Herbert: Über die Entstehung des dynamischen Auftriebes von Tragflügeln. Z.a.M.M., Bd. 5, Heft 1, Feb. 1925, pp. 17-35.
5. Garrick, I. E.: On Some Reciprocal Relations in the Theory of Non-stationary Flows. NACA Rep. 629, 1938.
6. Biot, M. A.: Loads on a Supersonic Wing Striking a Sharp-Edged Gust. Jour. Aero. Sci., vol. 16, no. 5, May 1949, pp. 296-300, 310.
7. Heaslet, Max. A., and Lomax, Harvard: Two-Dimensional Unsteady Lift Problems in Supersonic Flight. NACA Rep. 945, 1949. (Supersedes NACA TN 1621.)
8. Lomax, Harvard, Heaslet, Max. A., Fuller, Franklyn B., and Sluder, Loma: Two- and Three-Dimensional Unsteady Lift Problems in High-Speed Flight. NACA Rep. 1077, 1952. (Supersedes NACA TN 2403 by Lomax, Heaslet, Sluder and TN 2387 by Lomax, Heaslet, Fuller; contains material from TN 2256 by Lomax, Heaslet, Fuller.)
9. Miles, John W.: Transient Loading of Wide Delta Airfoils at Supersonic Speeds. Jour. Aero. Sci., vol. 18, no. 8, Aug. 1951, pp. 543-554.
10. Miles, John W.: Transient Loading of Supersonic Rectangular Airfoils. Jour. Aero. Sci., vol. 17, no. 10, Oct. 1950, pp. 647-652.
11. Drischler, Joseph A.: Approximate Indicial Lift Functions for Several Wings of Finite Span in Incompressible Flow As Obtained From Oscillatory Lift Coefficients. NACA TN 3639, 1956.
12. Drischler, Joseph A.: Calculation and Compilation of the Unsteady-Lift Functions for a Rigid Wing Subjected to Sinusoidal Gusts and to Sinusoidal Sinking Oscillations. NACA TN 3748, 1956.

13. Anon.: The Effects of Atomic Weapons. Los Alamos Scientific Lab. (Los Alamos, N. M.), June 1950, pp. 114-179.
14. Ludloff, H. F.: On Aerodynamics of Blasts. Vol. III of Advances in Applied Mechanics, Richard von Mises and Theodore von Kármán, eds., Academic Press, Inc. (New York), 1953, pp. 109-144.
15. Theodorsen, Theodore, and Garrick, I. E.: Nonstationary Flow About a Wing-Aileron-Tab Combination Including Aerodynamic Balance. NACA Rep. 736, 1942.

TABLE 1.- UNSTEADY-LIFT FUNCTION $k(s)$ FOR INCOMPRESSIBLE TWO-DIMENSIONAL FLOW

Gust condition	Range of s for -	
	$0 < s \leq 2 \lambda $ (a)	$s \geq 2 \lambda $
Gust approaching wing and gust receding from wing at speeds less than that of wing ($\lambda > 0$)	$\frac{1}{2} \left(1 + \frac{2}{\lambda}\right) \cos^{-1} \frac{\lambda - s}{\lambda} + \frac{1 - \lambda}{\pi \lambda^2} \sqrt{s(2\lambda - s)} -$ $\frac{2}{\pi \lambda} \sqrt{\frac{k + s}{ 2\lambda - k - s }} \cos^{-1} \frac{s(2\lambda - s) + k(\lambda - s)}{k\lambda}$	$1 + \frac{2}{\lambda} \left(1 - \sqrt{\frac{k + s}{k + s - 2\lambda}}\right)$
Gust overtaking wing ($\lambda < 0$)	$\frac{1}{2} \left(1 + \frac{2}{\lambda}\right) \cos^{-1} \frac{\lambda + s}{\lambda} + \frac{1 - \lambda}{\pi \lambda^2} \sqrt{ s(2\lambda + s) } -$ $\frac{2}{\pi \lambda} \sqrt{\frac{ s + k + 2\lambda }{k + s}} \cos^{-1} \frac{s(2\lambda + s) + k(\lambda + s)}{k\lambda}$	$1 + \frac{2}{\lambda} \left(1 - \sqrt{\frac{s + k + 2\lambda}{s + k}}\right)$

^aIn the last term the function \cos^{-1} is replaced by \cosh^{-1} when $s \geq 2|\lambda| - k$.

TABLE 2.- UNSTEADY-MOMENT FUNCTION $C_m(s)$ FOR INCOMPRESSIBLE TWO-DIMENSIONAL FLOW

[Moment is taken about quarter-chord point]

Gust condition	Range of s for -	
	$0 < s \leq 2 \lambda $	$s \geq 2 \lambda $
Gust approaching wing or receding from wing at speeds less than that of wing ($\lambda > 0$)	$-\frac{s}{2\lambda^3} (1 - \lambda) \sqrt{s(2\lambda - s)}$	0
Gust overtaking wing ($\lambda < 0$)	$-\frac{(1 - \lambda)(2\lambda + s)}{2\lambda^3} \sqrt{ s(2\lambda + s) }$	0

TABLE 3.- PRESSURE COEFFICIENT C_p FOR SUPERSONIC TWO-DIMENSIONAL FLOW AND LOADING

COEFFICIENT $1/q$ FOR DRUM WINGS WITH SUPERSONIC LEADING EDGES

(a) Gusts approaching wing or receding from wing at speeds less than that of wing ($M_g > -M$)

Coefficient	Region in x, t plane for -		
	$t = 0;$ $x = t;$ $x = c - Mt$	$x = t; x = -t; x = c - Mt$	$x = -t;$ $x = -Mt;$ $x = c - Mt$
C_p	(a) 0	(b) $\frac{kM}{xVM} \left(\frac{M}{\sqrt{M^2 - 1}} \cos^{-1} \frac{Mx + t}{x + Mt} + \frac{M_g}{\sqrt{M_g^2 - 1}} \cos^{-1} \frac{t - M_g x}{ M_g t - x } \right)$	(c) $\frac{kM}{V\sqrt{M^2 - 1}}$
$1/q$	(d) 0	(b) $\frac{\partial \ln}{xVM} \left[\frac{M_g(M_g + M)}{M_g^2 - 1} \sqrt{t^2 - x^2} + \frac{M(x + Mt)}{\sqrt{M^2 - 1}} \cos^{-1} \frac{Mx + t}{x + Mt} + \frac{1}{(M_g^2 - 1)\sqrt{ M_g^2 - 1 }} \left[x(M_g^3 + M) + M_g t(M_g^2 M - M_g - 2M) \right] \cos^{-1} \frac{t - M_g x}{ M_g t - x } \right]$	(c) $\frac{\partial \ln(x + Mt)}{V\sqrt{M^2 - 1}}$

(a) $C_p = \frac{kM M_g}{MV\sqrt{M_g^2 - 1}} \quad (x < M_g t; M_g > 1)$

(b) In the last term the \cos^{-1} is replaced by \cosh^{-1} for $|M_g| < 1$.

(c) $C_p = \frac{kM}{VM} \left(\frac{M}{\sqrt{M^2 - 1}} + \frac{M_g}{\sqrt{M_g^2 - 1}} \right) \quad (x > M_g t; -M < M_g < -1)$

(d) $\frac{1}{q} = \frac{\partial \ln}{VM(M_g^2 - 1)^{3/2}} \left[x(M_g^3 + M) + M_g t(M_g^2 M - M_g - 2M) \right] \quad (x < M_g t; M_g > 1)$

(e) $\frac{1}{q} = \frac{\partial \ln}{VM} \left[\frac{M(x + Mt)}{\sqrt{M^2 - 1}} + \frac{x(M_g^3 + M) + M_g t(M_g^2 M - M_g - 2M)}{(M_g^2 - 1)^{3/2}} \right] \quad (x > M_g t; -M < M_g < -1)$

**TABLE 3.- PRESSURE COEFFICIENT C_p FOR SUPERSONIC TWO-DIMENSIONAL FLOW AND LOADING
 COEFFICIENT l/q FOR DELTA WINGS WITH SUPERSONIC LEADING EDGES - Concluded**

(b) Gusts overtaking wing ($M_g < -M$)

Coefficient	Region in x,t plane between the lines for -			
	$t = 0;$ $x = c + M_g t;$ $x = -Mt$	$x = c + M_g t; x = t + c \frac{M+1}{M_g+M};$ $x = c - Mt$	$x = t + c \frac{M+1}{M_g+M}; x = -t + c \frac{M-1}{M_g+M}; x = c - Mt$	$x = -t + c \frac{M-1}{M_g+M};$ $x = -Mt; x = c - Mt$
C_p	0	$\frac{-VM_g}{VM(M_g^2 - 1)}$	$\frac{hW}{xVM} \left[\frac{M}{M_g^2 - 1} \cos^{-1} \frac{(Mx+t)(M_g+M) - (M^2-1)c}{(M_g+M)(x+Mt)} - \frac{M_g}{\sqrt{M_g^2-1}} \cos^{-1} \frac{(M_g+1)c + (t-M_gx)(M_g+M)}{(M_g+M)(c-x+M_g t)} \right]$	$\frac{hW}{V(M^2-1)}$
l/q	0	$\frac{\theta Ma}{VM(M_g^2-1)^{3/2}} \left[c(M_g+M) - x(M_g^3+M) - M_g t (M_g^2 M - M_g - 2M) \right]$	$\frac{\theta Ma}{xVM} \left\{ -\frac{M_g}{M_g^2-1} \sqrt{[t(M_g+M)+c]^2 - [x(M_g+M)-Mc]^2} + \frac{M(x+Mt)}{\sqrt{M^2-1}} \cos^{-1} \frac{(M_g+M)(t+Mx) - c(M^2-1)}{(M_g+M)(x+Mt)} - \frac{x(M_g^3+M) - c(M_g+M) + M_g t (M_g^2 M - M_g - 2M)}{(M_g^2-1)^{3/2}} x \cos^{-1} \frac{(M_g+M)(t-M_gx) + c(M_g M + 1)}{(M_g+M)(c-x+M_g t)} \right\}$	$\frac{\theta Ma(x+Mt)}{V(M^2-1)}$

TABLE 4.- UNSTEADY-LIFT FUNCTION $h(s)$ FOR SUPERSONIC FLOW

(a) Gusts approaching wing or receding from wing at speeds less than that of wing ($M_g > -M$)

Wing plan form	Function given	Range of M_g for -	Range of s for -		
			$0 \leq s \leq \frac{M}{M+1}$	$\frac{M+1}{M+2} \leq s \leq \frac{M}{M-1}$	$s > \frac{M}{M-1}$
Two dimensional	$\frac{hk(s)}{V_0^2 - 1}$	$M_g > -M$	(a) $\frac{2(M+M_g)s}{V_0^2}$	(b) $\frac{1}{2M} \left[\frac{M+M_g}{M} s \cos^{-1} \frac{M(s-2)}{s} + \frac{M}{\sqrt{M^2-1}} \cos^{-1} \frac{2M^2 - M^2s + s}{2M} + \frac{M_g}{\sqrt{M_g^2-1}} \left(1 - \frac{M+M_g}{M} s \right) \cos^{-1} \frac{s(1+M_g) - 2M}{s(M+M_g) - 2M} \right]$	(c) $\frac{h}{V_0^2 - 1}$
		$M_g = -M$	(a) $\frac{2(M+1)s}{V_0^2}$	(b) $\frac{1}{2M} \left[\frac{M+1}{M} s \cos^{-1} \frac{M(s-2)}{s} + \frac{M}{\sqrt{M^2-1}} \cos^{-1} \frac{2M^2 - M^2s + s}{2M} - \sqrt{\left(\frac{M}{2}\right)^2 - \left(1 - \frac{s}{2}\right)^2} \right]$	(c) $\frac{h}{V_0^2 - 1}$
Wide delta	$\frac{hk(s)}{V_0^2 - 1}$	$M_g > -M$	(a) $\frac{(M+M_g)^2 s^2}{V_0^2}$	(b) $\frac{h}{2M} \left[\frac{M+M_g}{M} s \cos^{-1} \frac{M(s-2)}{s} + \frac{M}{\sqrt{M^2-1}} \cos^{-1} \frac{2M^2 - M^2s + s}{2M} + \frac{M_g(M+M_g)}{M_g^2-1} \left(1 - \frac{M+M_g}{M} s \right) \sqrt{\left(\frac{s}{M}\right)^2 - \left(1 - \frac{s}{2}\right)^2} + \frac{1}{M_g^2(M_g^2-1)\sqrt{M_g^2-1}} \left[s^2(M+M_g)^2(M_g+M-M_g^2) - 4Ms(M+M_g)^2 + 4M^2(M+M_g^2) \right] \cos^{-1} \frac{s(1+M_g) - 2M}{s(M+M_g) - 2M} \right]$	(c) $\frac{h}{V_0^2 - 1}$
		$M_g = -M$	(a) $\frac{(M+1)^2 s^2}{V_0^2}$	(b) $\frac{h}{2M} \left[\frac{M+1}{M} s \cos^{-1} \frac{M(s-2)}{s} + \frac{M}{\sqrt{M^2-1}} \cos^{-1} \frac{2M^2 - M^2s + s}{2M} - \frac{s(M+1)(s+M) + M(1+2M)\sqrt{\left(\frac{s}{M}\right)^2 - \left(1 - \frac{s}{2}\right)^2}}{2M} \right]$	(c) $\frac{h}{V_0^2 - 1}$
Rectangular	$\frac{2 \Delta h(s)}{A(M^2 - 1)}$	$M_g \geq -1$	(a) $\frac{M+M_g}{2M^2} s^2$	(b) $\frac{1}{2M(M+1)(M_g+1)} \left[M_g - M + \frac{(M+1)(M+M_g)}{M} s - \frac{(M^2-1)(M+M_g)}{M^2} s^2 \right]$	(c) $\frac{2}{A(M^2 - 1)}$
		$-M < M_g < -1$	(a) $\frac{M+M_g}{2M^2} s^2$	(b) $\frac{M+M_g}{2M(M+1)(1-M_g)} \left[1 + \frac{M+1}{M} s - \frac{(M+1)(2M_g+M-1)}{M^2} s^2 \right]$	(c) $\frac{2}{A(M^2 - 1)}$

(a) $\frac{hk(s)}{V_0^2 - 1} = \frac{h}{2M} \left[1 - \left(1 - \frac{M_g}{\sqrt{M_g^2 - 1}} \right) \left(1 - \frac{M+M_g}{M} s \right) \right] \quad \left(s > \frac{M}{M+M_g}, M_g > 1 \right)$

(b) In the last term the \cos^{-1} is replaced by \cosh^{-1} for values of $-1 < M_g < 1$.

(c) $\frac{hk(s)}{V_0^2 - 1} = \frac{h}{2M} \left[1 + \frac{M_g}{M} \left(1 - \frac{M+M_g}{M} s \right) \sqrt{\frac{M^2 - 1}{M_g^2 - 1}} \right] \quad \left(s < \frac{M}{M+M_g}, -M < M_g < -1 \right)$

(a) $\frac{hk(s)}{V_0^2 - 1} = \frac{h}{2M} \left[\frac{(M+M_g)^2}{M} s \left(1 - \frac{M_g^2 - M - 2M_g}{(M_g^2 - 1)^{3/2}} \right) - \frac{(M+M_g)^2 s}{M(M_g^2 - 1)^{3/2}} + \frac{M_g^2 + M}{(M_g^2 - 1)^{3/2}} \right] \quad \left(s > \frac{M}{M+M_g}, M_g > 1 \right)$

(a) $\frac{hk(s)}{V_0^2 - 1} = \frac{h}{2M} \left[\frac{M}{\sqrt{M^2 - 1}} + \frac{s^2(M+M_g)^2(M_g+M-M_g^2) - 4Ms(M+M_g)^2 + 4M^2(M+M_g^2)}{M_g^2(M_g^2 - 1)^{3/2}} \right] \quad \left(s < \frac{M}{M+M_g}, -M < M_g < -1 \right)$

(c) $\frac{2 \Delta h(s)}{A(M^2 - 1)} = \frac{2}{A(M_g^2 - 1)} \left[M_g + \frac{M}{M} (M+M_g) s - \frac{M+M_g}{M^2} (1+M_g) s^2 \right] \quad \left(s > \frac{M}{M+M_g}, M_g > 1 \right)$

(c) $\frac{2 \Delta h(s)}{A(M^2 - 1)} = \frac{M+M_g}{A(M+1)(1-M_g)} \left[1 + \frac{M+1}{M} s - \frac{(M+1)(2M_g+M-1)}{M^2} s^2 \right] \quad \left(s < \frac{M}{M+M_g}, -1 < M_g < -1 \right)$

(b) $\frac{2 \Delta h(s)}{A(M^2 - 1)} = \frac{2(M+M_g)}{A(M^2 - 1)(M_g^2 - 1)} \left[(M_g - 1) - \frac{M_g(M^2 - 1)}{M} s + \frac{M_g(M^2 - 1)(M+M_g)}{M^2} s^2 \right] \quad \left(s < \frac{M}{M+M_g} \right)$

TABLE 4.- UNDERBODY-LIFT FUNCTION $k(s)$ FOR SUPERSONIC FLOW - Concluded

(b) Curves overtaking wing ($M_0 < -M$)

Wing plan form	Function given	Range of s for -			
		$0 \leq s \leq \frac{-2M}{M + M_0}$	$\frac{-2M}{M + M_0} \leq s \leq \frac{2M(M_0 - 1)}{(M + M_0)(M + 1)}$	$\frac{2M(M_0 - 1)}{(M_0 + M)(M + 1)} \leq s \leq \frac{2M(M_0 + 1)}{(M_0 + M)(M - 1)}$	$s \geq \frac{2M(M_0 + 1)}{(M_0 + M)(M - 1)}$
Two dimensional	$\frac{k(s)}{\sqrt{M^2 - 1}}$	$\frac{2M_0(M + M_0)}{M^2 M_0^2 - 1} s$	$\frac{k M_0}{M \sqrt{M_0^2 - 1}} \left[\frac{M + M_0}{2M} \left(1 + \frac{\sqrt{M_0^2 - 1}}{M_0} s \right) - \frac{\sqrt{M_0^2 - 1}}{M_0} \right]$	$\frac{k}{2M} \left[\frac{M}{\sqrt{M^2 - 1}} \cos^{-1} \frac{2M(1 + M_0) - s(M^2 - 1)(M + M_0)}{2M(M + M_0)} + \left(1 + \frac{M + M_0}{2M} s \right) \cos^{-1} \frac{M(M + M_0)s - 2M M_0}{s(M + M_0) + 2M} + \frac{M_0(M + M_0)}{2M \sqrt{M_0^2 - 1}} \cos^{-1} \frac{(1 + M_0)(M + M_0)s - 2M(M_0^2 - 1)}{s(M + M_0)^2} \right]$	$\frac{k}{\sqrt{M^2 - 1}}$
Wide delta	$\frac{k(s)}{\sqrt{M^2 - 1}}$	$\frac{(M + M_0)s}{M^2 (M_0^2 - 1)^{3/2}} \left[2M M_0 (M_0^2 - 1) + (M + M_0)(M_0^2 - 2M_0 - M)s \right]$	$\frac{k}{M} \left[\frac{s(M + M_0)}{\sqrt{M^2 (M_0^2 - 1)^{3/2}}} \left[s(M + M_0)(M_0^2 - 2M_0 - M) + 2M M_0 (M_0^2 - 1) \right] + \left(1 + \frac{M + M_0}{2M} s \right)^2 \right]$	$\frac{k}{2M} \left[\frac{M}{\sqrt{M^2 - 1}} \cos^{-1} \frac{2M(1 + M_0) - s(M^2 - 1)(M + M_0)}{2M(M + M_0)} + \left(1 + \frac{M + M_0}{2M} s \right)^2 \cos^{-1} \frac{M(M + M_0)s - 2M M_0}{s(M + M_0) + 2M} + \frac{s(M + M_0)}{k M^2 (M_0^2 - 1)^{3/2}} \left[s(M + M_0)(M_0^2 - 2M_0 - M) + 2M M_0 (M_0^2 - 1) \right] \cos^{-1} \frac{s(1 + M_0)(M + M_0) - 2M(M_0^2 - 1)}{s(M + M_0)^2} + \frac{M_0(M + M_0)}{2M \sqrt{M_0^2 - 1}} \cos^{-1} \left[\sqrt{\left(1 + \frac{M + M_0}{2M} s \right)^2 - \left(M_0 - \frac{M + M_0}{2} s \right)^2} \right] \right]$	$\frac{k}{\sqrt{M^2 - 1}}$
Rectangular	$\frac{R \Delta k(s)}{A(M^2 - 1)}$	$\frac{-M_0(M + M_0)^2}{2M^2 (M_0^2 - 1)} s^2$	$\frac{R}{2M(M + M_0)(M_0^2 - 1)} \left[M_0^2 - 1 + \frac{(M + M_0)(M_0^2 - 2)}{M} s - \frac{(M + M_0)^2(1 + M_0)}{k M^2} s^2 \right]$	$\frac{1}{2M(M_0 + 1)(M + 1)(M_0 + M)} \left[(M_0 + 1)(1 + 2M + M_0) + \frac{(M + 1)(M_0 + 1)(M + M_0)}{M} s - \frac{(M^2 - 1)(M + M_0)^2}{k M^2} s^2 \right]$	$\frac{R}{A(M^2 - 1)}$

TABLE 5.- UNSTEADY PITCHING MOMENT ABOUT LEADING EDGE FOR SPHEROIDIC FLOW

(a) Curves approaching wing or receding from wing
 at speeds less than that of wing $M_\infty > 1$

[Moments are taken about leading edge]

Wing plan form	Function given	Range of M_∞ for -	Range of s for -			
			$s \leq \frac{2M}{M+M_\infty}$	$\frac{2M}{M+M_\infty} \leq s \leq \frac{2M}{M+1}$	$\frac{2M}{M+1} \leq s \leq \frac{2M}{M-1}$	$s > \frac{2M}{M-1}$
Two dimensional	C_m	$M_\infty > 1$	$\frac{(M+M_\infty)^2 s^2}{2s^3}$	$\frac{(M+M_\infty)^2 s^2}{2s^3} - \frac{M_\infty}{M^2 \sqrt{M_\infty^2 - 1}} [s^2 (M+M_\infty)^2 - M_\infty^2]$	$\frac{2}{M+1} \left[\frac{M_\infty}{\sqrt{M_\infty^2 - 1}} \left[1 - \frac{(M+M_\infty)^2}{M^2} \right] \cos^{-1} \frac{s(1+M_\infty) - 2M}{s(M+M_\infty) - 2M} + \frac{M}{\sqrt{M^2 - 1}} \cos^{-1} \frac{2M^2 - M^2 + s}{2M} + \frac{(M+M_\infty)^2}{M^2} s^2 \cos^{-1} \frac{M(s-2)}{s} \right] - \frac{(M+M_\infty)}{2M} \left[\sqrt{\left(\frac{s}{2M}\right)^2 - \left(1 - \frac{s}{2}\right)^2} \right]$	$\frac{2}{\sqrt{M^2 - 1}}$
		$M_\infty = 1$	$\frac{(M+1)^2 s^2}{2s^3}$	(a)	$\frac{2}{M+1} \left[\frac{M}{\sqrt{M^2 - 1}} \cos^{-1} \frac{2M^2 - M^2 + s}{2M} + \frac{(1+M)^2 s^2}{M^2} \cos^{-1} \frac{M(s-2)}{s} \right] - \left(1 + \frac{M+1}{M}\right) \sqrt{\left(\frac{s}{2M}\right)^2 - \left(1 - \frac{s}{2}\right)^2}$	$\frac{2}{\sqrt{M^2 - 1}}$
Wide delta	C_m	$M_\infty > 1$	$\frac{(M+M_\infty)^3 s^3}{3s^4}$	$\frac{1}{6M^2 (M_\infty^2 - 1)^{3/2}} \left[\frac{1}{2} (M_\infty^2 - 1)^{3/2} + (M+3M_\infty - 2M_\infty^2) (M+M_\infty)^3 s^3 - 12M^2 s (M+M_\infty)^2 + 12s^2 (M+M_\infty) \right]$	$\frac{2}{3(M+1)} \left[\frac{(M+M_\infty)^3 s^3}{2s^3} \cos^{-1} \frac{M(s-2)}{s} + \frac{M}{\sqrt{M^2 - 1}} \cos^{-1} \frac{2M^2 - M^2 + s}{2M} + \frac{1}{2(M_\infty^2 - 1)^{3/2}} \left[\frac{(M+M_\infty)^3 (M+3M_\infty - 2M_\infty^2) s^3}{2s^3} - \frac{2M^2 (M+M_\infty)^2 + 2(M+M_\infty)}{M^2} \right] \cos^{-1} \frac{s(1+M_\infty) - 2M}{s(M+M_\infty) - 2M} + \frac{(M+M_\infty)}{2(M_\infty^2 - 1)} \left[\frac{(M+M_\infty)(1 - M_\infty - 2M_\infty^2) s^2}{M^2} - \frac{M_\infty^2 (M+M_\infty) + M_\infty}{2M} \sqrt{\left(\frac{s}{2M}\right)^2 - \left(1 - \frac{s}{2}\right)^2} \right] \right]$	$\frac{6}{3\sqrt{M^2 - 1}}$
		$M_\infty = 1$	$\frac{(M+1)^3 s^3}{3s^4}$	(a)	$\frac{2}{3(M+1)} \left[\frac{(M+1)^3 s^3}{2s^3} \cos^{-1} \frac{M(s-2)}{s} + \frac{M}{\sqrt{M^2 - 1}} \cos^{-1} \frac{2M^2 - M^2 + s}{2M} + \frac{1}{3} \left[\frac{(1+M)^2 (M+3) s^2}{M^2} + \frac{(M+3)(M+1)s}{2M} - M + 1 \right] \sqrt{\left(\frac{s}{2M}\right)^2 - \left(1 - \frac{s}{2}\right)^2} \right]$	$\frac{6}{3\sqrt{M^2 - 1}}$
Rectangular	$\rho^2 \Delta C_m$	$M_\infty > 1$	$\frac{(M^2 - 1)(2M+M_\infty)(M+M_\infty)s^3}{12M^4}$	$\frac{(M^2 - 1)(2M+M_\infty)(M+M_\infty + M^2 M_\infty)s^3}{12M^4 (M_\infty^2 - 1)} - \frac{M_\infty (M+M_\infty)s^2}{2M} + M_\infty$	$\frac{-(M-1)}{2(M+1)} \left[\frac{(M^2 - 1)(M-1)(M+M_\infty)s^3}{2s^3} - \frac{3(M+1)(M+M_\infty)s}{2M} + 2(M-M_\infty) \right]$	$\frac{4M}{3}$

^(a)This region does not exist for $M_\infty = 1$.

TABLE 5.- UNDERWING PITCHING MOMENT ABOUT LEADING EDGE FOR SUPERSONIC FLOW - Continued

(b) Delta overhanging wing ($M_\infty < -M$)

Wing plan form	Function given	Range of β for -			
		$\beta < \frac{-M}{M_\infty + M}$	$\frac{-M}{M_\infty + M} < \beta < \frac{\sin(M_\infty - 1)}{(M+1)(M_\infty + M)}$	$\frac{\sin(M_\infty - 1)}{(M+1)(M_\infty + M)} < \beta < \frac{\sin(M_\infty + 1)}{(M-1)(M_\infty + M)}$	$\beta > \frac{\sin(M_\infty + 1)}{(M-1)(M_\infty + M)}$
Two dimensional	C_m	$\frac{M_\infty(M_\infty + M)}{2\beta^2 \sqrt{M_\infty^2 - 1}} \left[\frac{2\beta}{M_\infty + M} + (M_\infty + M)\beta^2 \right]$	$2 \left(\frac{\beta}{M_\infty} + \frac{1}{M + M_\infty} \right)^2 \left[\frac{(M + M_\infty)^2}{M} + \frac{M_\infty(M_\infty + M)\beta^2}{M \sqrt{M_\infty^2 - 1}} \right] - \frac{M_\infty(M_\infty + M)\beta^2}{M \sqrt{M_\infty^2 - 1}}$	$\frac{\beta \sqrt{M_\infty + M}}{\sin \left(\frac{\beta}{M_\infty} \beta + 1 \right)} \cos^{-1} \frac{M(M_\infty + M)\beta - \sin M_\infty}{(M_\infty + M)\beta + \sin M_\infty} + \frac{\beta}{\beta \sqrt{M_\infty^2 - 1}} \cos^{-1} \frac{\sin(M_\infty + 1) - (M^2 - 1)(M + M_\infty)\beta}{\sin(M + M_\infty)} + \frac{M_\infty(M_\infty + M)}{2\beta \sqrt{M_\infty^2 - 1}} \left[\frac{2\beta}{M_\infty} + (M + M_\infty)\beta^2 \right] \times \cos^{-1} \frac{M(M + M_\infty)(M_\infty + 1) - \sin(M_\infty^2 - 1)}{M(M + M_\infty)^2} + \frac{\left[\frac{M(M + M_\infty) + \sin M}{\sin(M + M_\infty)} \left(\frac{M + M_\infty}{M} \beta + 1 \right)^2 - \left(\frac{M + M_\infty}{M} \beta - M_\infty \right)^2 \right]}{2\beta \sqrt{M_\infty^2 - 1}}$	$\frac{\beta}{\sqrt{M_\infty^2 - 1}}$
Wide delta	C_m	$\frac{(M + M_\infty)}{\cos^2(M_\infty - 1)^{3/2}} \left\{ \frac{2\beta \sqrt{M_\infty}}{M} (M_\infty^2 - 1) - (M + M_\infty)(2M_\infty + M - \sin M_\infty^2) \left[(M + M_\infty)\beta^2 + \cos M_\infty^2 \right] \right\}$	$\frac{\beta \sqrt{M_\infty + M}}{\sin \left(\frac{\beta}{M_\infty} \beta + 1 \right)^3} + \frac{(M + M_\infty)}{\cos^2(M_\infty - 1)^{3/2}} \left\{ \frac{2\beta \sqrt{M_\infty}}{M} (M_\infty^2 - 1) - (M + M_\infty)(2M_\infty + M - \sin M_\infty^2) \left[(M + M_\infty)\beta^2 + \cos M_\infty^2 \right] \right\}$	$\frac{\beta \sqrt{M_\infty + M}}{\sin \left(\frac{\beta}{M_\infty} \beta + 1 \right)^3} \cos^{-1} \frac{M(M + M_\infty)\beta - \sin M_\infty}{(M + M_\infty)\beta + \sin M_\infty} + \frac{\beta}{\beta \sqrt{M_\infty^2 - 1}} \cos^{-1} \frac{\sin(M_\infty + 1) - (M^2 - 1)(M + M_\infty)\beta}{\sin(M + M_\infty)} + \frac{M + M_\infty}{\cos^2(M_\infty - 1)^{3/2}} \left\{ \frac{2\beta \sqrt{M_\infty}}{M} (M_\infty^2 - 1) - (M + M_\infty)(2M_\infty + M - \sin M_\infty^2) \left[(M + M_\infty)\beta^2 + \cos M_\infty^2 \right] \right\} \cos^{-1} \frac{M(M + M_\infty)(M_\infty + 1) - (M_\infty^2 - 1)\sin M_\infty}{(M + M_\infty)^2} + \frac{\frac{2\beta \sqrt{M_\infty}}{M} (M + M_\infty)(M_\infty^2 - 1) \left[(M + M_\infty)\beta^2 + \cos M_\infty^2 \right] + \sin(M + M_\infty)(2M_\infty^2 + 2M_\infty - 2) + \cos^2(M_\infty^2 - 1) \left[\left(\frac{M + M_\infty}{M} \beta + 1 \right)^2 - \left(\frac{M + M_\infty}{M} \beta - M_\infty \right)^2 \right]}{2\beta \sqrt{M_\infty^2 - 1}}$	$\frac{\beta}{2\sqrt{M_\infty^2 - 1}}$
Rectangular	$\frac{2\beta C_m}{\beta \sqrt{M_\infty^2 - 1}}$	$\frac{-M_\infty(M_\infty^2 - 1)(M_\infty + M)\beta}{2\beta \sqrt{M_\infty^2 - 1}} \left[\cos M_\infty^2 + (M + M_\infty)\beta^2 \right]$	$\frac{-(M^2 - 1)(M_\infty^2 + \sin M_\infty + M_\infty)}{2\beta \sqrt{M_\infty^2 - 1}} \left[\cos M_\infty^2 + (M + M_\infty)\beta^2 \right] + \frac{(M^2 - 1)(M + M_\infty)}{\cos^2(M + M_\infty)^2} \left[\frac{2\beta}{M} + 3(M + M_\infty)\beta^2 \right]$	$\frac{-(M^2 - 1)(M - 1) \left[\cos M_\infty^2 + (M + M_\infty)\beta^2 \right] + (M^2 - 1)(M_\infty - 1 + \sin M_\infty)}{2\beta \sqrt{M_\infty^2 - 1}} + \frac{(M - 1) \left[\cos M_\infty^2 + M_\infty(2M + 1) + \cos^2 M_\infty + M - 1 \right]}{\cos^2(M_\infty + M)^2}$	β

**TABLE 6.- DIMENSIONLESS PRESSURE γ FOR WIDE RECTANGULAR WINGS
 IN SUPERSONIC FLOW^(a)**

(a) Gusts approaching wing or receding from wing at speeds below that of wing ($M_g > -M$)

Range of Mt for -	Range of M_g for -	
	$M_g > -1$	$-1 < M_g < -1$
$0 \leq Mt \leq \frac{x}{M_1}$	(b) 0	0
$\frac{x}{M_1} < Mt < \frac{x}{M_1}$	(c) $\frac{xM_1(2M - M_0)}{2(MM_1 - M_0)} + \frac{m_1 n_1 M M_0 t}{2(MM_1 - 2M + M_0)}$	$\frac{xM_1 M_0}{2(MM_1 - 2M + M_0)} + \frac{m_1 n_1 M M_0 t}{2(MM_1 - M_0)}$
$Mt \geq \frac{x}{M_1}$	x	(d) x

(a) The primes have been dropped from the x' ordinate.

$$(b) \gamma(x,t) = (M_0 t - x) \left[\frac{M_0 (m_1 - 2)}{2(MM_1 - M_0)} - \frac{M_0 m_1}{2(MM_1 - M_0)} - 1 \right] \quad \left(Mt > \frac{Mx}{M_0}; M_g > 1 \right)$$

$$(c) \gamma(x,t) = \frac{xM_1 M_0}{2(MM_1 - 2M + M_0)} + \frac{m_1 n_1 M M_0 t}{2(MM_1 - M_0)} \quad \left(Mt < \frac{Mx}{M_0}; -1 < M_g < 1 \right)$$

$$(d) \gamma(x,t) = x \left[1 - \frac{m_1(2M - M_0)}{2(MM_1 - M_0)} + \frac{m_1 M_0}{2(MM_1 - 2M + M_0)} \right] + t \left[\frac{m_1 n_1 M M_0}{2(MM_1 - M_0)} - \frac{m_1 M M_0 (m_1 - 2)}{2(MM_1 - M_0)} \right] \quad \left(Mt < \frac{Mx}{M_0} \right)$$

(b) Gusts overtaking wing

Range of Mt for -	$M_g < -M$
$0 \leq Mt \leq \frac{M(x-1)}{M_0}$	0
$\frac{M(x-1)}{M_0} \leq Mt \leq \frac{x}{M_1} - \frac{M}{M_0}$	$\frac{1}{2} \left(x - M_0 t - 1 \right) \left[\frac{M_0 (2 - m_1)}{MM_1 - M_0} + \frac{M_0 m_1}{MM_1 - M_0} + 1 \right]$
$\frac{x}{M_1} - \frac{M}{M_0} \leq Mt \leq \frac{x}{M_1} - \frac{M}{M_0}$	$\frac{xM_1(2M - M_0)}{2(MM_1 - M_0)} - \frac{m_1 M (M_0 t + 1)(2 - m_1)}{2(MM_1 - M_0)}$
$Mt \geq \frac{x}{M_1} - \frac{M}{M_0}$	x

TABLE 7.-- UNSTEADY-LIFT FUNCTION $k(s)$ FOR A NARROW-DELTA WING IN COMPRESSIBLE FLOW

(a) Gusts approaching wing or receding from wing at speeds less than that of wing

Range of s for -	$M_g > -M$
$0 \leq s \leq \frac{2M}{M_e}$	$\frac{M_e^3 s^2}{xM^3} \left[\frac{1}{2mM_e + 1} + \frac{\pi}{4} \int_2^\infty \frac{f(\eta) d\eta}{(mM_e \eta + 1)^3} \right]$
$\frac{2M}{M_e} \leq s \leq 2M \left(2m + \frac{1}{M_e} \right)$	$s^2 \left[k(1) - \frac{2mM_e^2 - M_e + M}{4xm^2M^3} \right] + \frac{s(2mM_e - M_e + M)}{xm^2M^2M_e} + \frac{1}{xm^2M_e^2M} \left[2mM_e(M_e - 2M) + M_e - M \right]$
$s \geq 2M \left(2m + \frac{1}{M_e} \right)$	$\int_0^{\frac{M_e s - 2M}{2mM_e M}} f(\eta) d\eta + \frac{s^2 M_e^3}{4M^3} \int_{\frac{M_e s - 2M}{2mM_e M}}^\infty \frac{f(\eta)}{(mM_e \eta + 1)^3} d\eta$

(b) Gusts overtaking wing ($M_g < -M$)

Range of s for -	$M_g < -M$
(a) $0 \leq s \leq \frac{2M}{ M_e }$	$\frac{s}{xmM} \left\{ \frac{M_e - M}{2mM} \left[\frac{s}{2M} (1 - 2mM_e) - 4m \right] - \frac{M_e}{2M} s \right\}$
(b) $s \geq \frac{2M}{ M_e }$	$\int_0^{\frac{s}{2mM}} f(\eta) d\eta + \frac{(M_e s + 2M)^2}{4M^3} M_e \int_{\frac{s}{2mM}}^\infty \frac{f(\eta) d\eta}{(mM_e \eta + 1)^3}$

(a)

$$k(s) = \frac{-M_e(2M + M_e s)^2}{xM^3(1 + 2mM_e)} + \int_0^{s/2mM} f(\eta) d\eta + \left(\frac{2M + M_e s}{2M} \right)^2 \frac{M_e}{M} \int_2^{s/2mM} \frac{f(\eta) d\eta}{(1 + mM_e \eta)^3}$$

($s > 4mM$; $2m|M_e| < 1$)

(b)

$$k(s) = \frac{-1}{4xm^2M^3(1 + 2mM_e)} \left[(M - M_e + 2mM_e)(s^2 - 8mMs) - 16m^2M_e^2M \right] + \frac{(M_e s + 2M)^2 M_e}{4M^3} \int_2^{s/2mM} \frac{f(\eta) d\eta}{(mM_e \eta + 1)^3}$$

($s < 4mM$; $2m|M_e| > 1$)

TABLE 8.- UNSTEADY PITCHING MOMENT C_m ABOUT THE LEADING EDGE FOR A NARROW DELTA WING IN COMPRESSIBLE FLOW

(a) Gusts approaching wing or receding from wing at speeds less than that of wing

Range of s for -	$M_g > -M$
$s < \frac{2M}{M_e}$	$\frac{M_e^3 s^3}{6\alpha M^4 (2\alpha M_e + 1)^2} [M_e(3 + 4\alpha M_e) - M(1 + 2\alpha M_e)] - \frac{M_e^3 s^3}{2\alpha M^3} \int_2^\infty \frac{f(\eta) d\eta}{(1 + \alpha M_e \eta)^3} +$ $\frac{M_e^4 s^3}{8\alpha M^4} \int_2^\infty \frac{f(\eta) d\eta}{(1 + \alpha M_e \eta)^4}$
$\frac{2M}{M_e} < s < 2M \left(2\alpha + \frac{1}{M_e} \right)$	$\frac{M_e - M(1 + 2\alpha M_e)}{24\alpha M^4 M_e^2} \left[\frac{M_e^3 s^3}{(2\alpha M_e + 1)^2} - 12M_e M^2 s + 16M^3 \right] + \frac{4(M_e - M)}{3\alpha M M_e} -$ $\frac{M_e^3 s^3}{2\alpha M^3} \int_2^\infty \frac{f(\eta) d\eta}{(1 + \alpha M_e \eta)^3} + \frac{M_e^4 s^3}{8\alpha M^4} \int_2^\infty \frac{f(\eta) d\eta}{(1 + \alpha M_e \eta)^4}$
$s > 2M \left(2\alpha + \frac{1}{M_e} \right)$	$\frac{2}{3} \int_0^{\frac{M_e s - 2M}{2\alpha M_e M}} f(\eta) d\eta - \frac{M_e^3 s^3}{2\alpha M^3} \int_{\frac{M_e s - 2M}{2\alpha M_e M}}^\infty \frac{f(\eta) d\eta}{(\alpha M_e \eta + 1)^3} + \frac{M_e^4 s^3}{8\alpha M^4} \int_{\frac{M_e s - 2M}{2\alpha M_e M}}^\infty \frac{f(\eta) d\eta}{(\alpha M_e \eta + 1)^4}$

TABLE 8.-- UNSTEADY PITCHING MOMENT C_m ABOUT THE LEADING EDGE FOR A NARROW

DELTA WING IN COMPRESSIBLE FLOW - Concluded

(b) Gusts overtaking wing

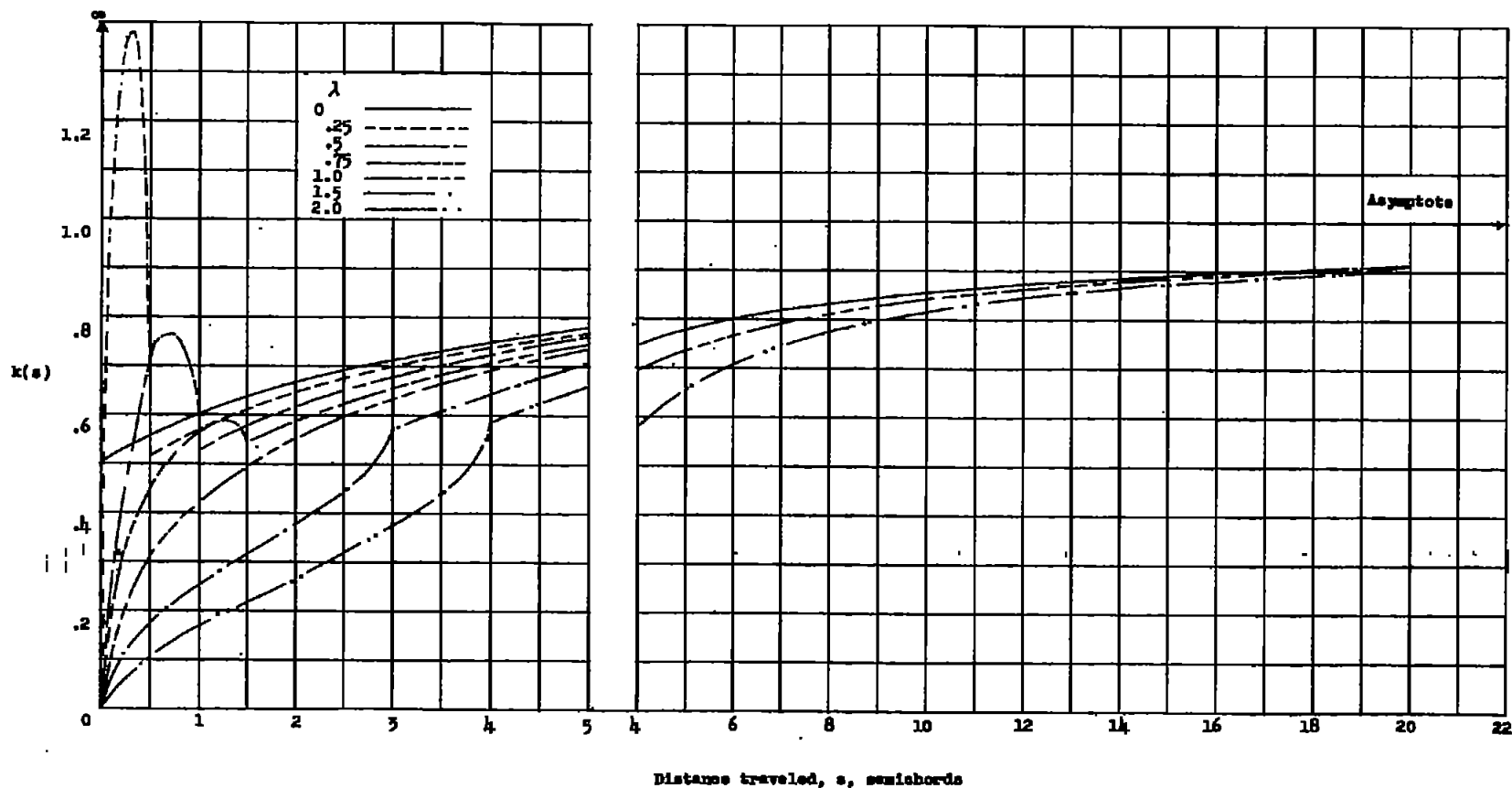
Range of s for -	$M_g < -M$
$s \leq \frac{2M}{ M_0 }$	(a) $\frac{s}{24\alpha M^2 M^4} \left\{ 4\alpha M^2 (M - M_0) - (s^2 M_0 + 6\alpha s) [2\alpha M_0^2 + (M - M_0)(1 - 2\alpha M_0)] \right\}$
$s > \frac{2M}{ M_0 }$	(b) $\frac{2}{3} \int_0^{s/2\alpha M} f(\eta) d\eta - \frac{(M_0 s + 2M)^3}{24\alpha^3} \int_{s/2\alpha M}^{\infty} \frac{f(\eta) d\eta}{(\alpha M_0 \eta + 1)^3} + \frac{(M_0 s + 2M)^3 M_0}{8\alpha^4} \int_{s/2\alpha M}^{\infty} \frac{f(\eta) d\eta}{(1 + \alpha M_0 \eta)^4}$

$$(a) \quad C_m = \frac{-(M_0 s + 2M)^3 [(2\alpha M_0 + 1)(4\alpha M_0 - 2\alpha M + 1) - 1]}{12\alpha M^4 (2\alpha M_0 + 1)^2} + \frac{2}{3} \int_0^{s/2\alpha M} f(\eta) d\eta + \frac{(M_0 s + 2M)^3}{24\alpha^3} \int_2^{s/2\alpha M} \frac{f(\eta) d\eta}{(1 + \alpha M_0 \eta)^3} -$$

$$\frac{(M_0 s + 2M)^3 M_0}{8\alpha^4} \int_2^{s/2\alpha M} \frac{f(\eta) d\eta}{(\alpha M_0 \eta + 1)^4} \quad (s > 4\alpha M; 2\alpha |M_0| < 1)$$

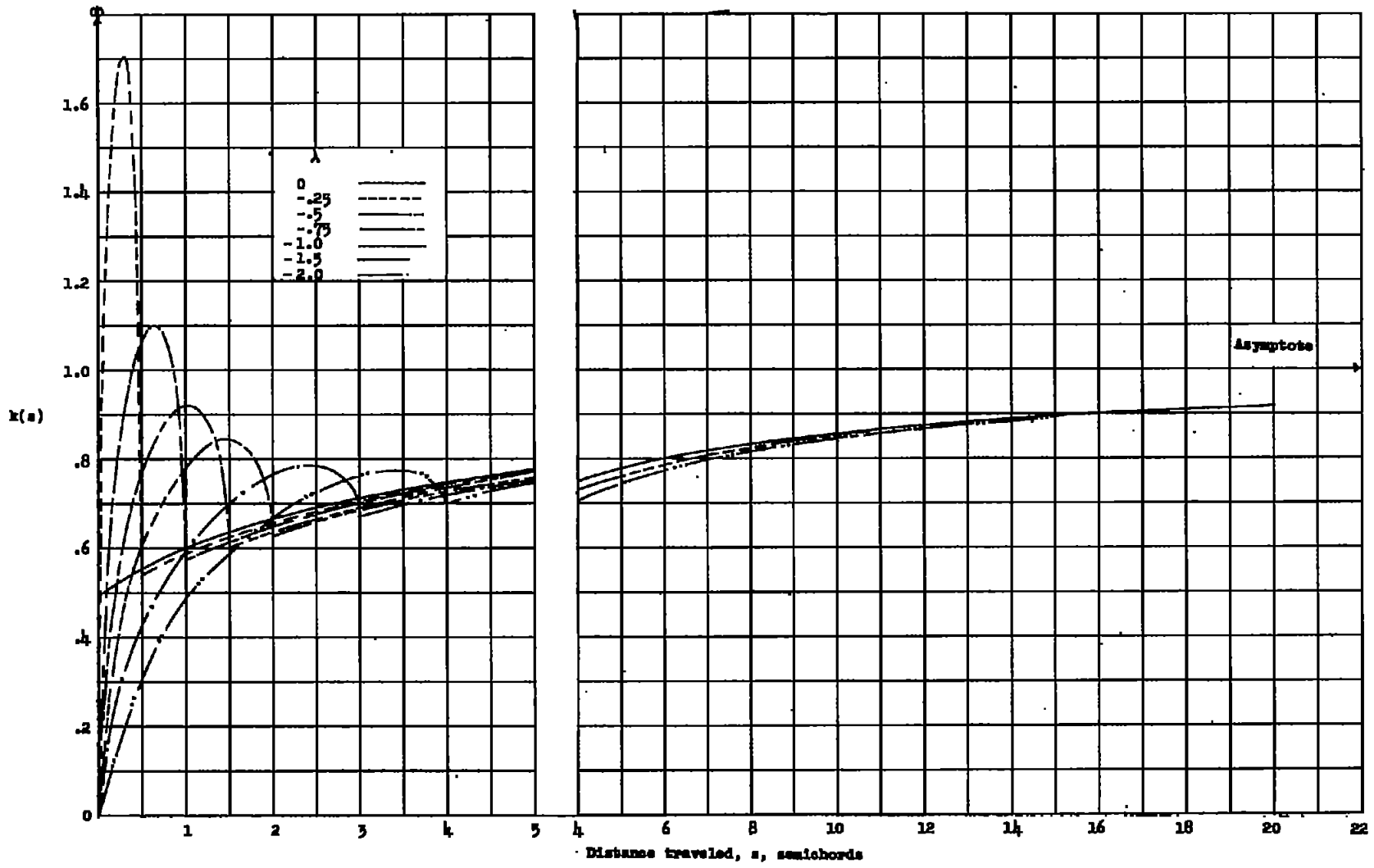
$$(b) \quad C_m = \frac{(M_0 s + 2M)^3 [M_0 - M(1 + 2\alpha M_0)]}{24\alpha M^2 M_0^2 (2\alpha M_0 + 1)^2} - \frac{1}{6\alpha M^2 M_0^2} \left\{ (2M + 3M_0 s) [M_0 - M(1 + 2\alpha M_0)] + 8\alpha M_0 (M - M_0) \right\} - \frac{(M_0 s + 2M)^3}{24\alpha^3} \int_2^{\infty} \frac{f(\eta) d\eta}{(1 + \alpha M_0 \eta)^3} +$$

$$\frac{(M_0 s + 2M)^3 M_0}{8\alpha^4} \int_2^{\infty} \frac{f(\eta) d\eta}{(\alpha M_0 \eta + 1)^4} \quad (s < 4\alpha M; 2\alpha |M_0| > 1)$$



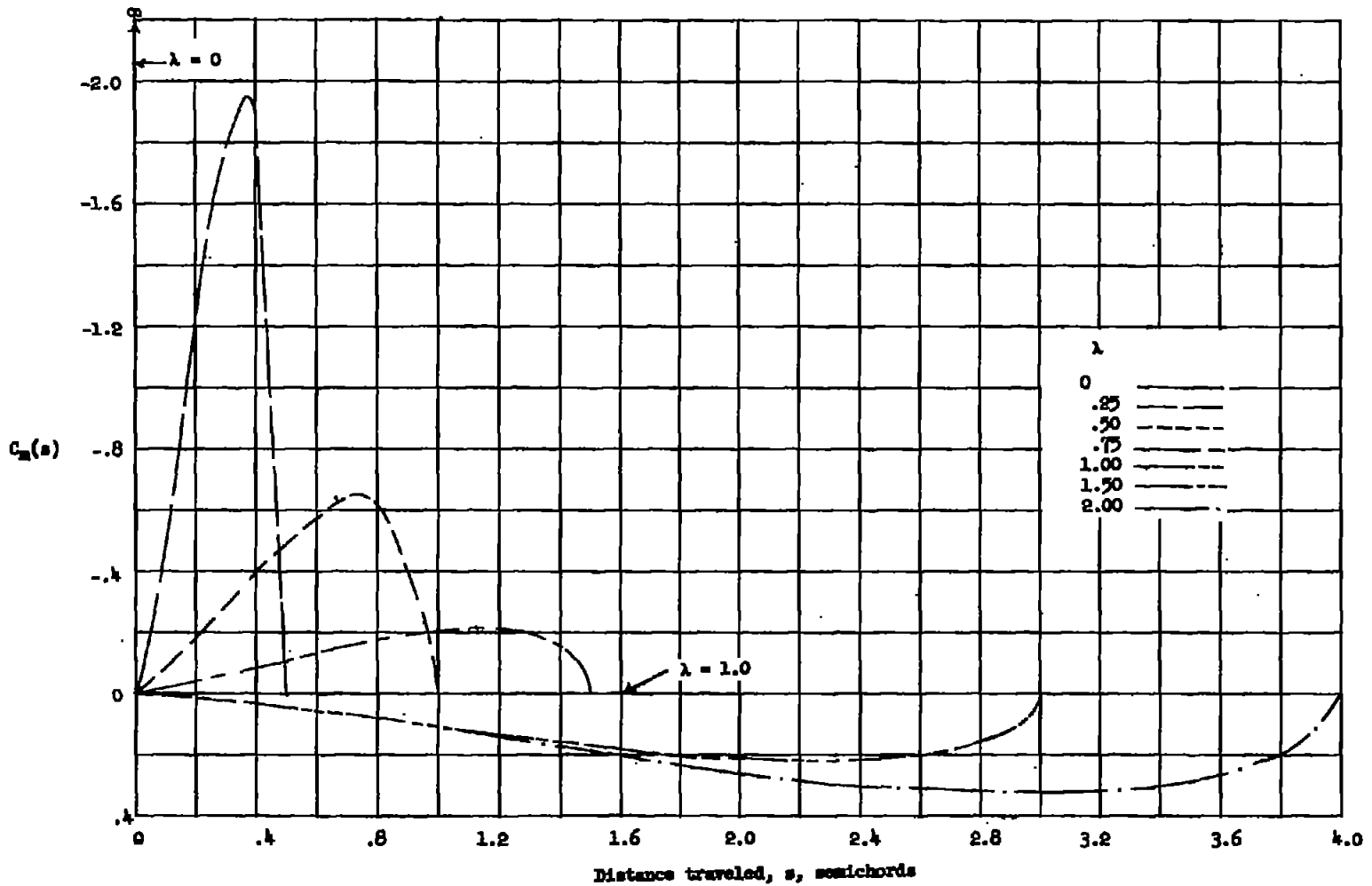
(a) Gusts approaching from leading edge.

Figure 1.-- Indicial-lift functions for a wing in incompressible two-dimensional flow when penetrating traveling sharp-edged gusts for several values of the parameter λ .



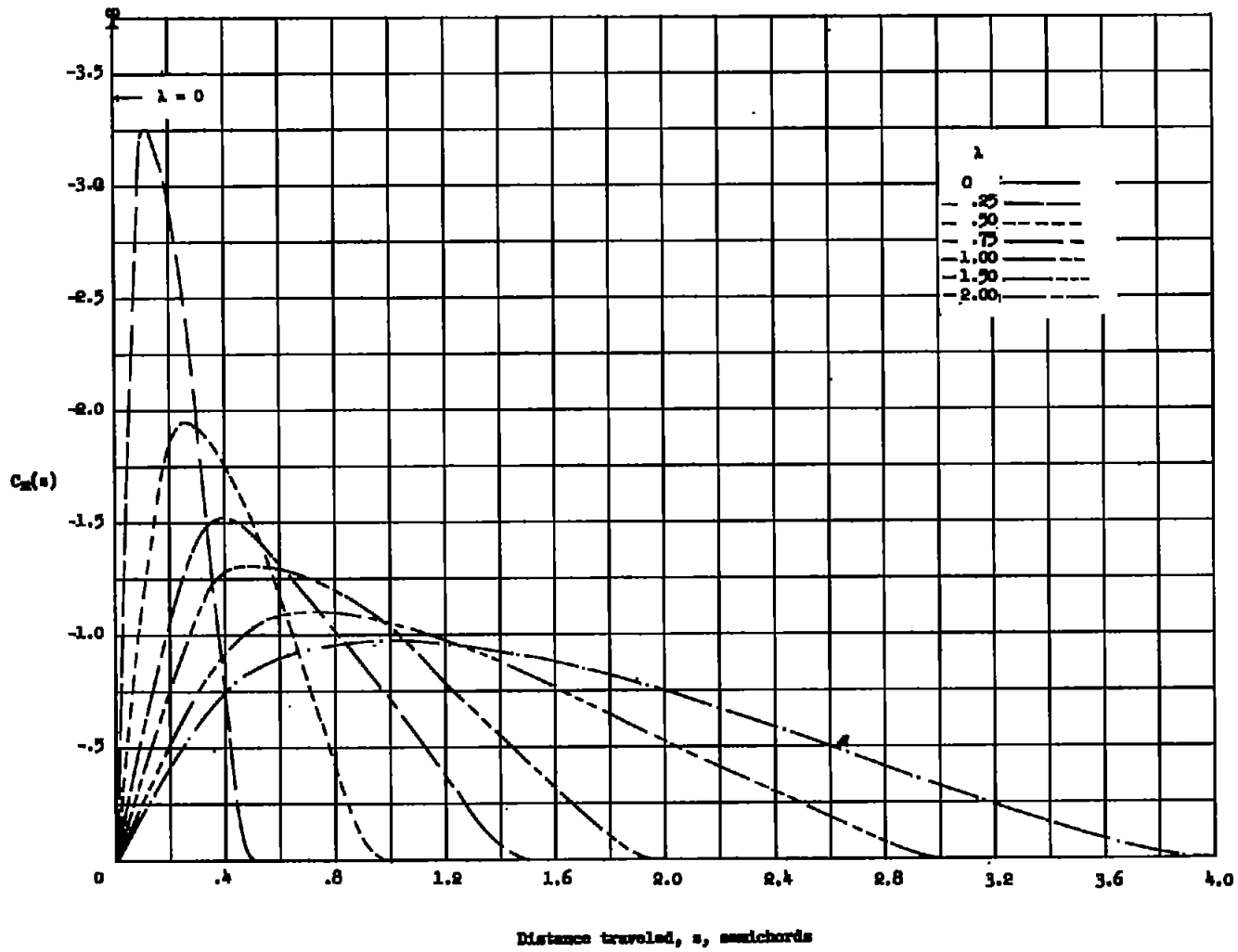
(b) Gusts approaching from trailing edge.

Figure 1.- Concluded.



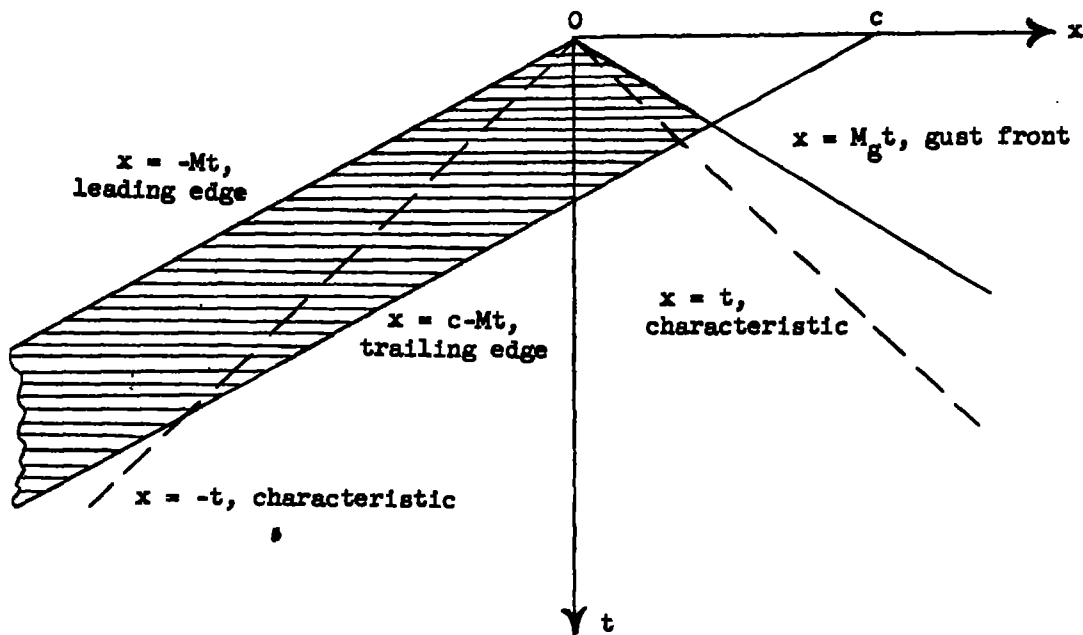
(a) Gusts approaching from leading edge.

Figure 2.- Indicial-moment functions for a wing in incompressible two-dimensional flow when penetrating traveling sharp-edged gusts (moment about quarter chord).

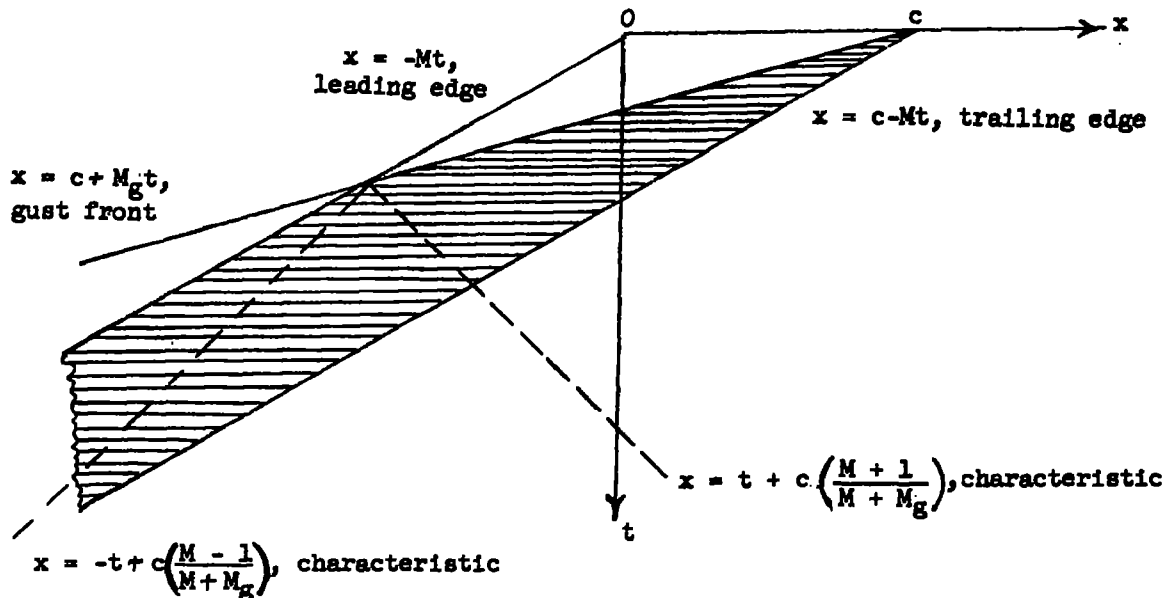


(b) Gusts approaching from trailing edge.

Figure 2.- Concluded.

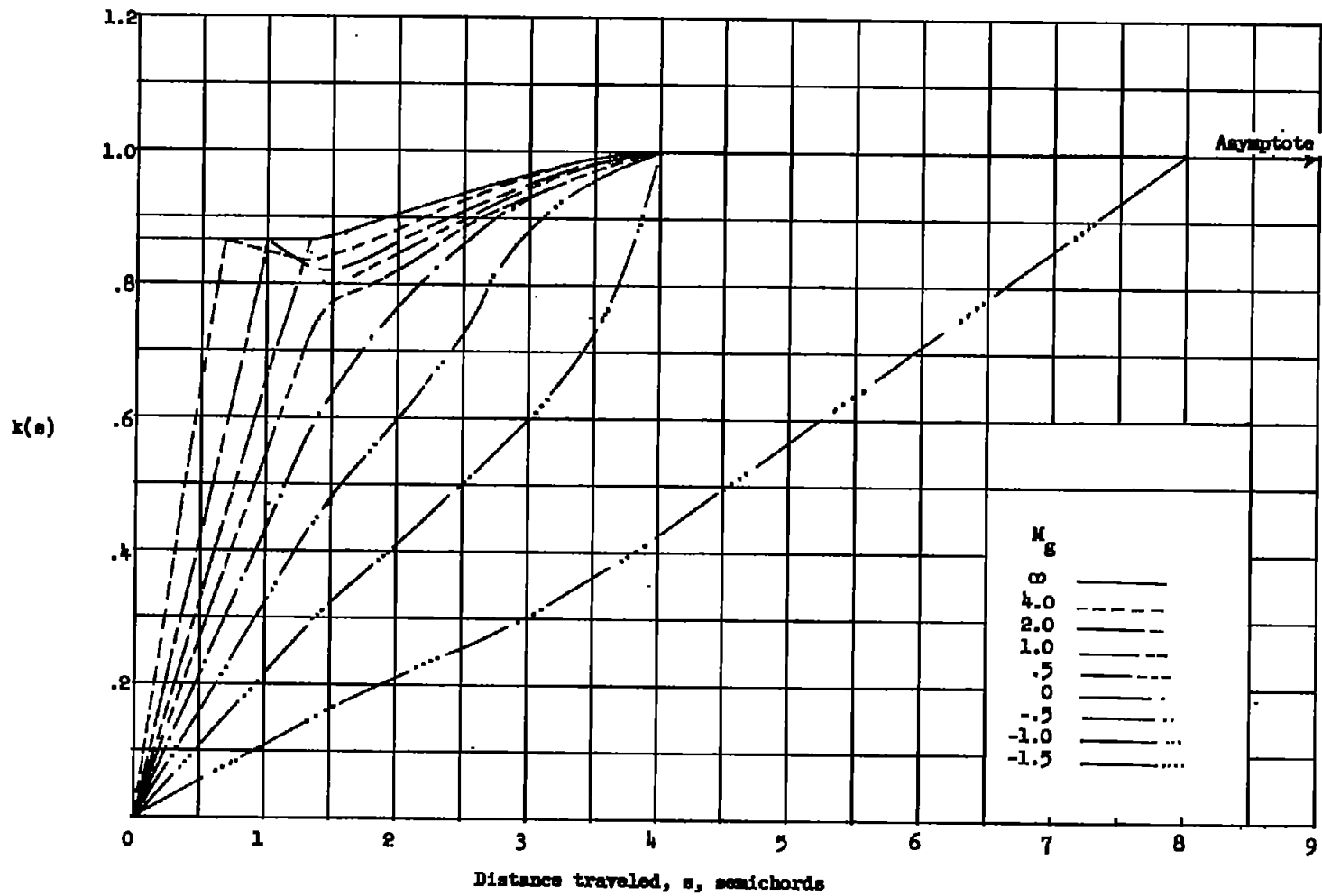


(a) Gusts approaching wing or receding from wing at speeds less than that of wing. $M_g > -M$.



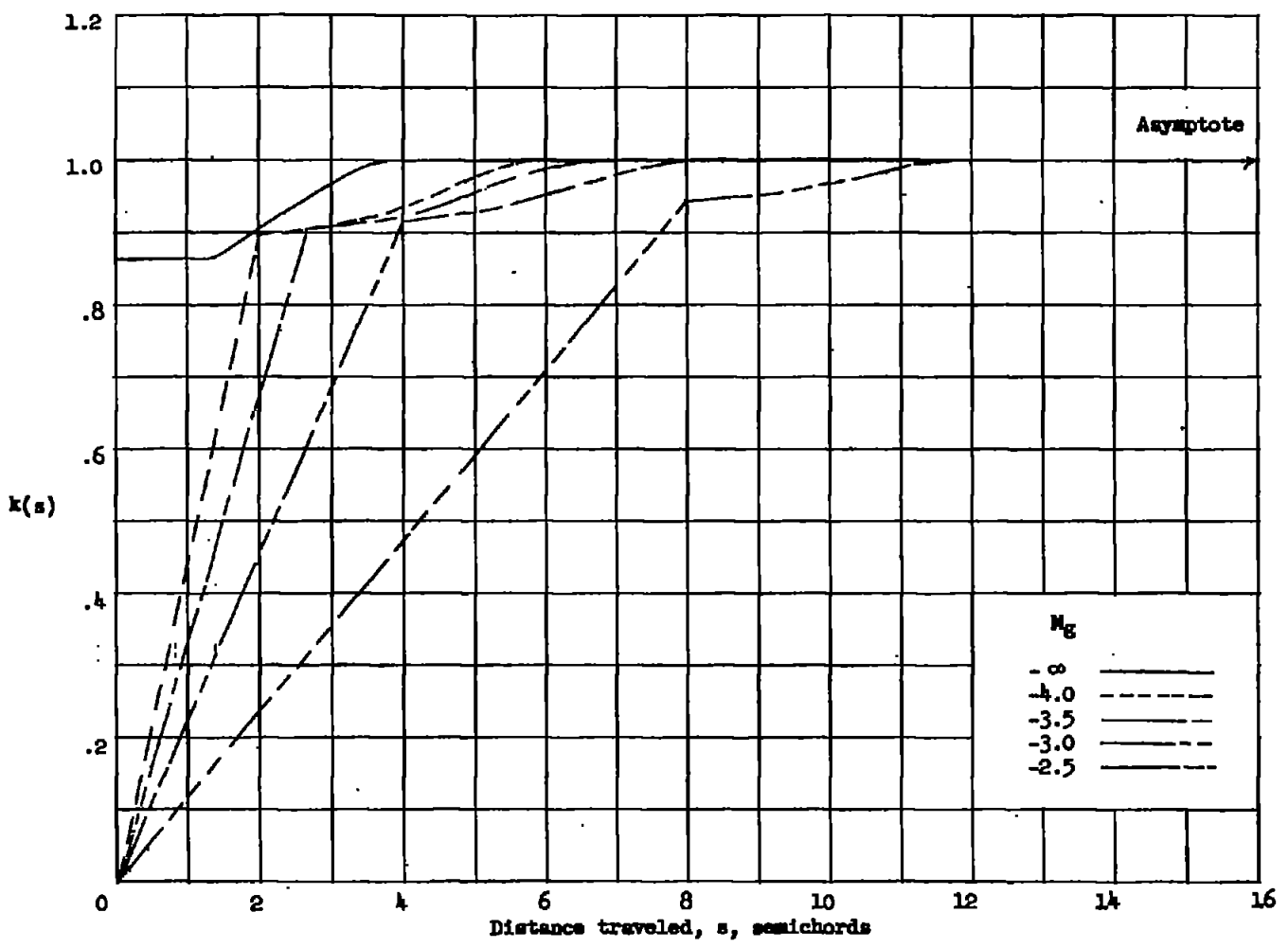
(b) Gusts overtaking wing. $M_g < -M$.

Figure 3.- Sketches of geometric characteristics for wings in two-dimensional supersonic flow and for delta wings with supersonic leading edges.



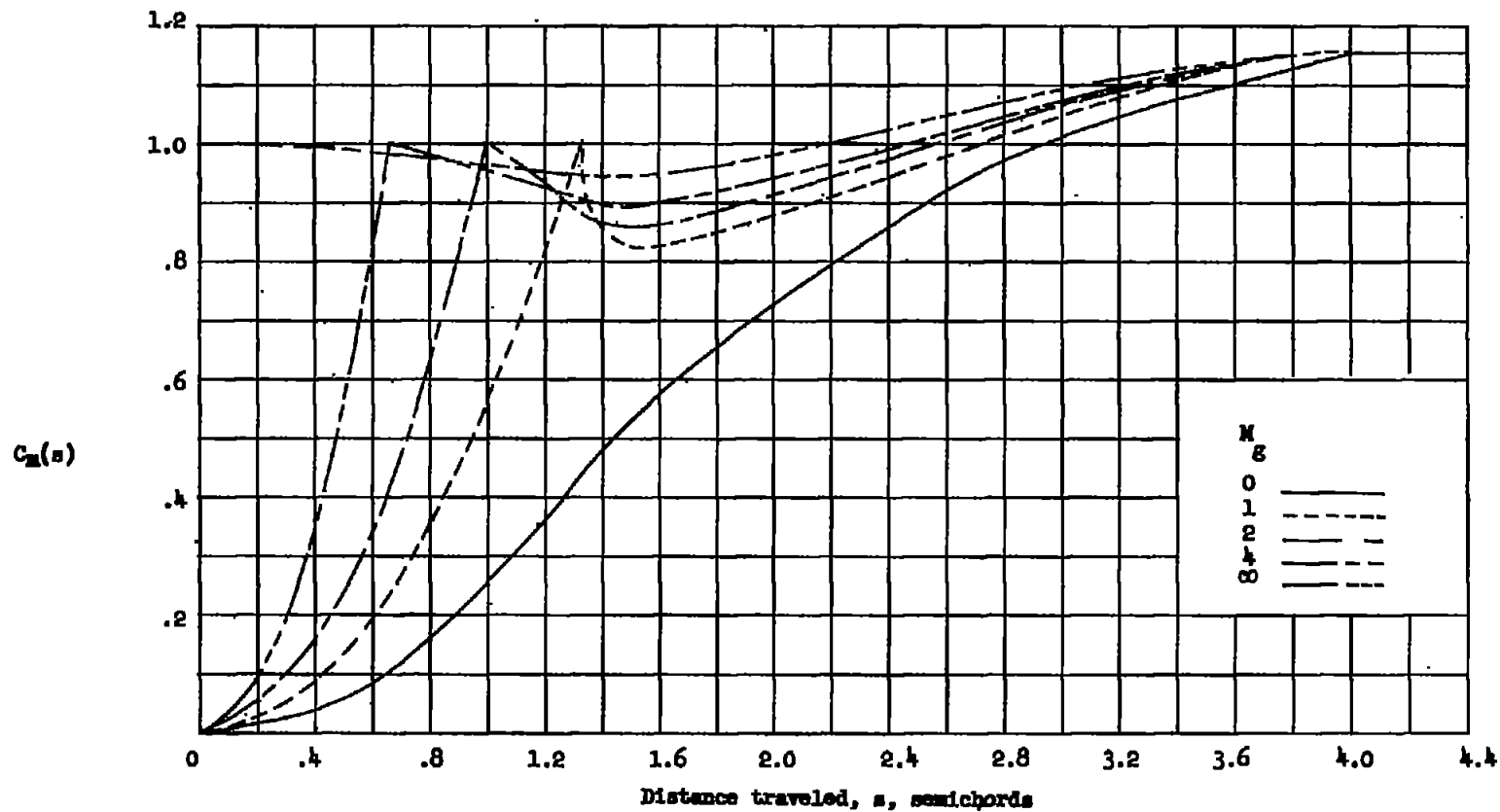
(a) Gusts approaching from leading edge.

Figure 4.- Indicial-lift functions for a two-dimensional wing flying at $M = 2$ when penetrating traveling sharp-edged gusts.



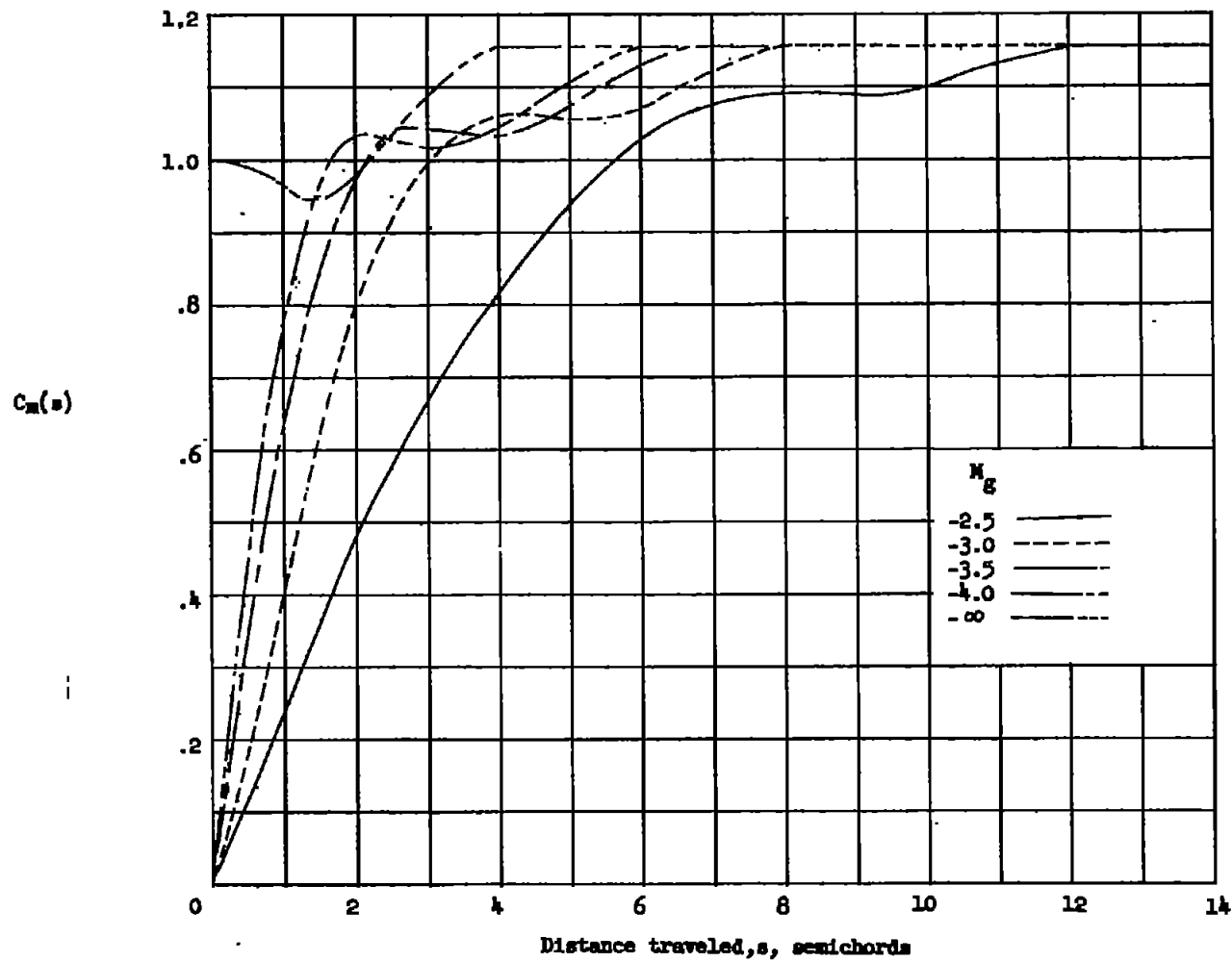
(b) Gusts approaching from trailing edge.

Figure 4.- Concluded.



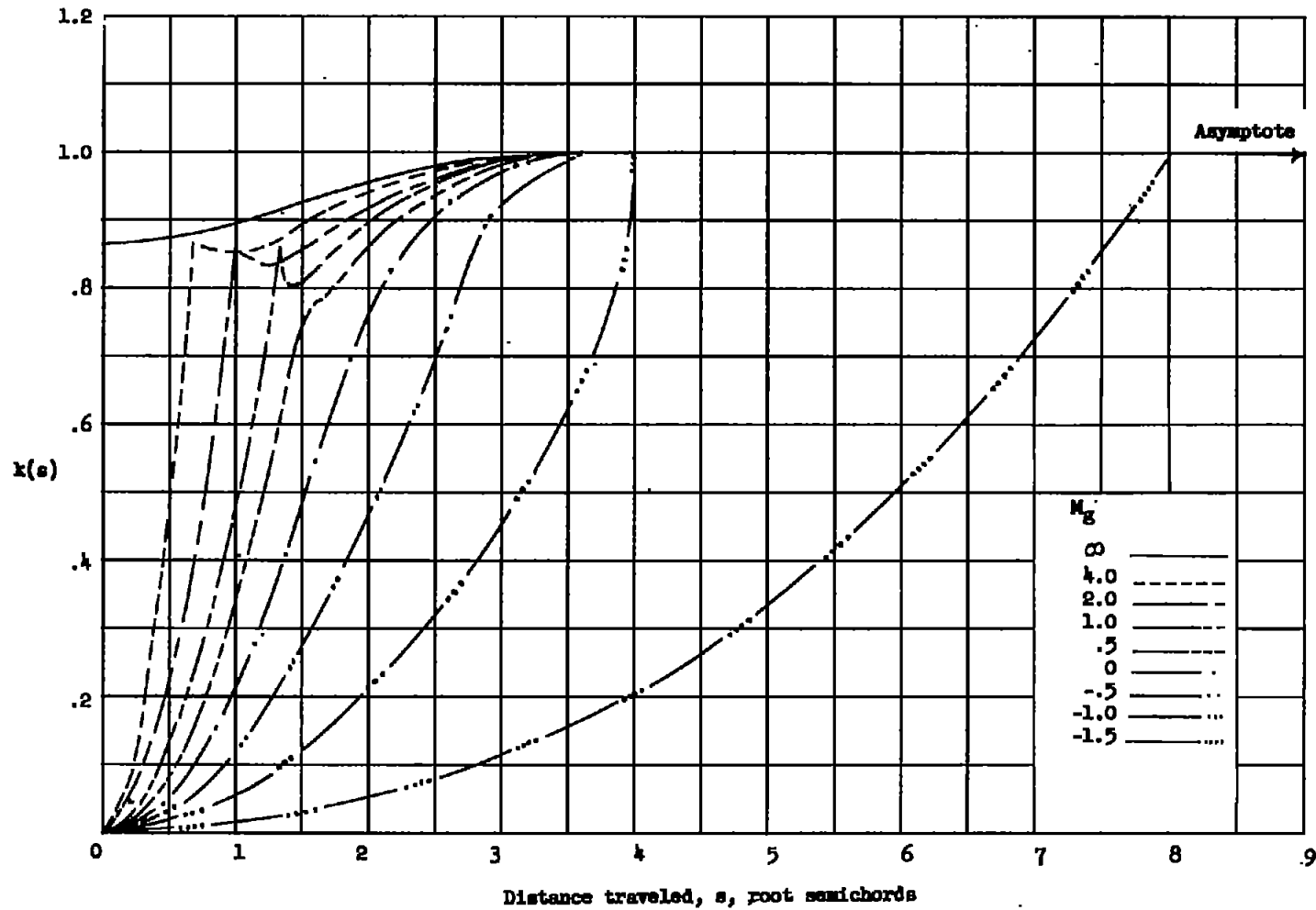
(a) Gust approaching from leading edge.

Figure 5.- Indicial-lift function for a two-dimensional wing flying at $M = 2$ when penetrating a traveling sharp-edged gust (moment about leading edge).



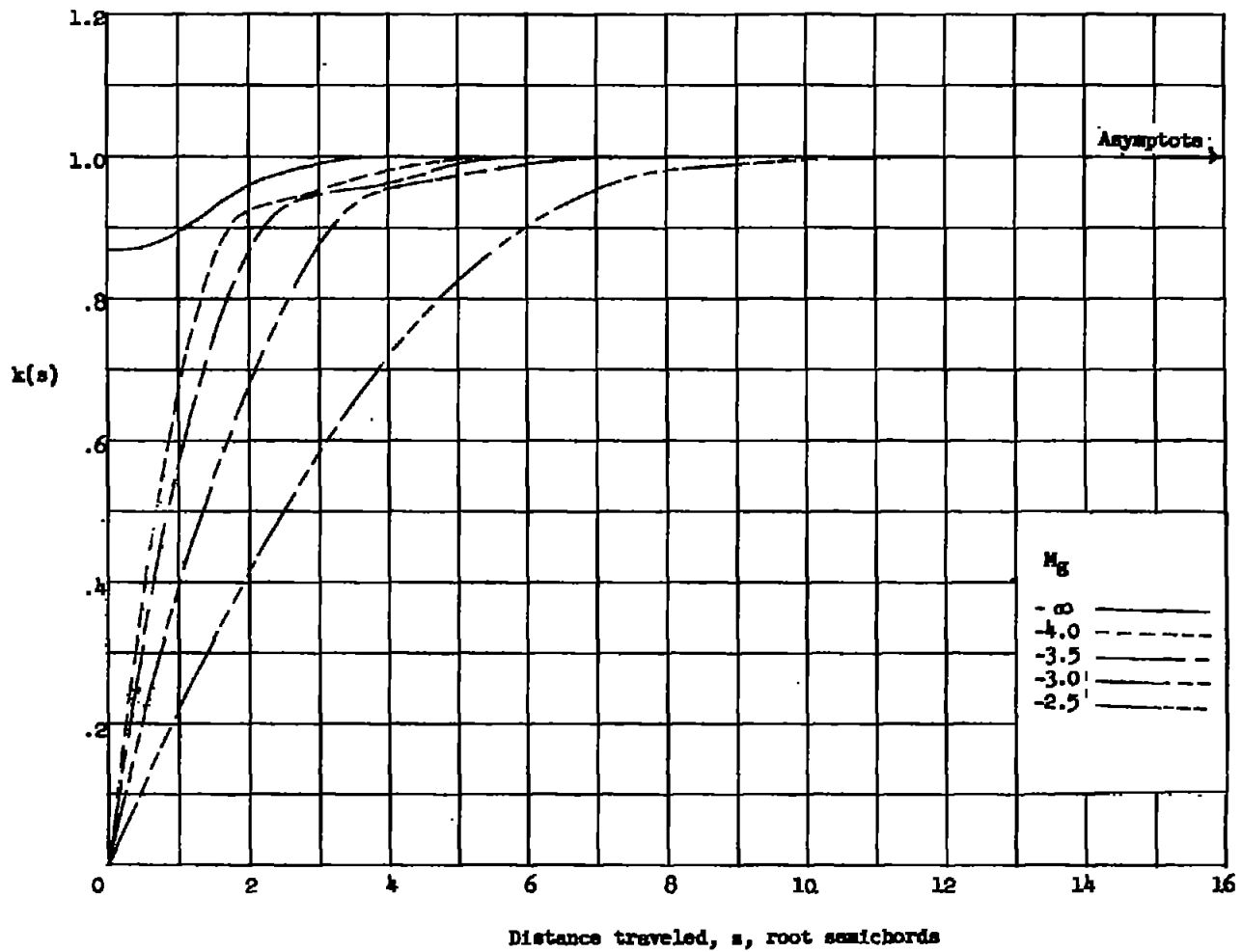
(b) Gust approaching from trailing edge.

Figure 5.- Concluded.



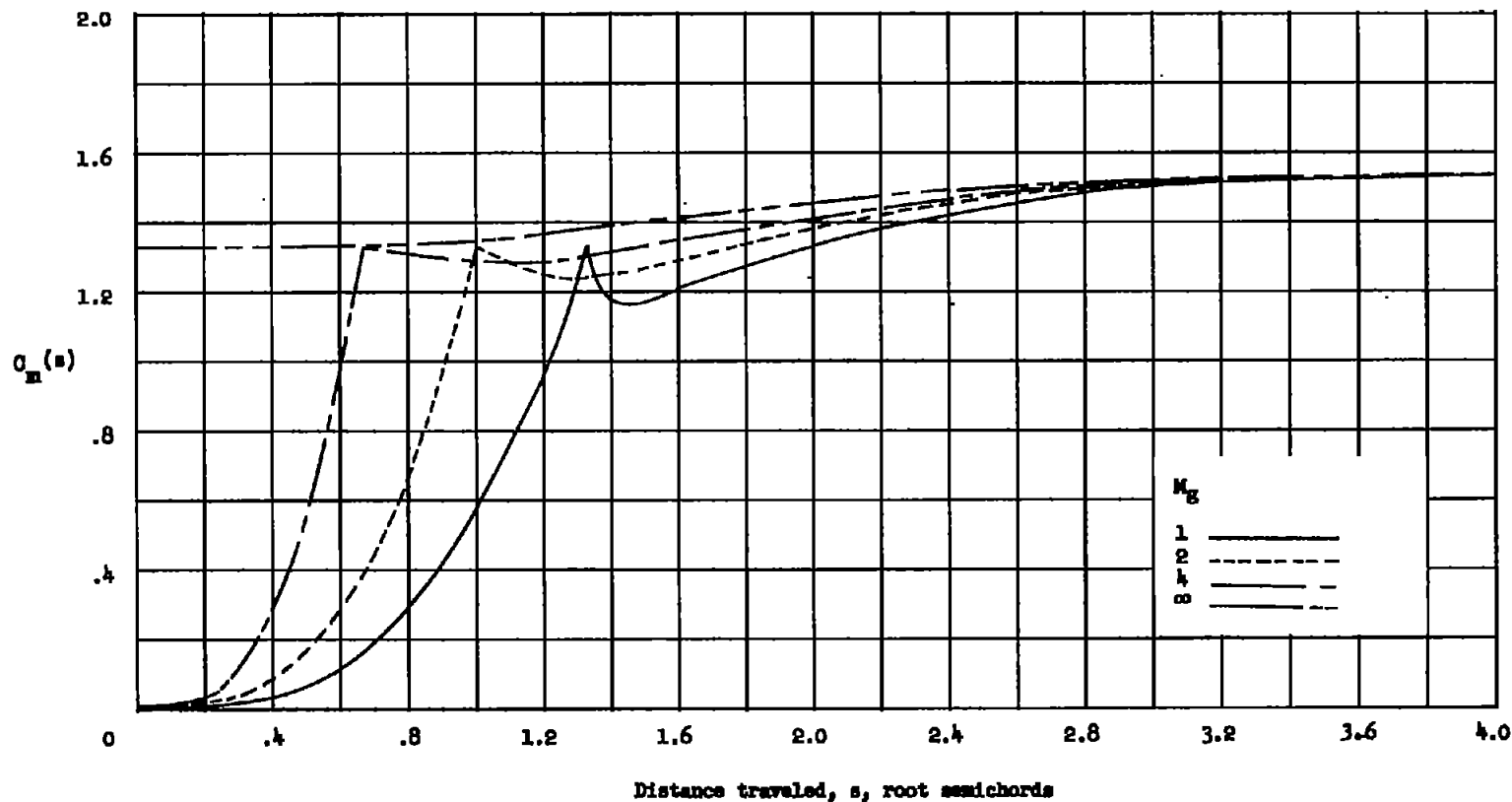
(a) Gust approaching from leading edge.

Figure 6.- Indicial-lift functions for a wide delta wing flying at $M = 2$ when penetrating traveling sharp-edged gusts.



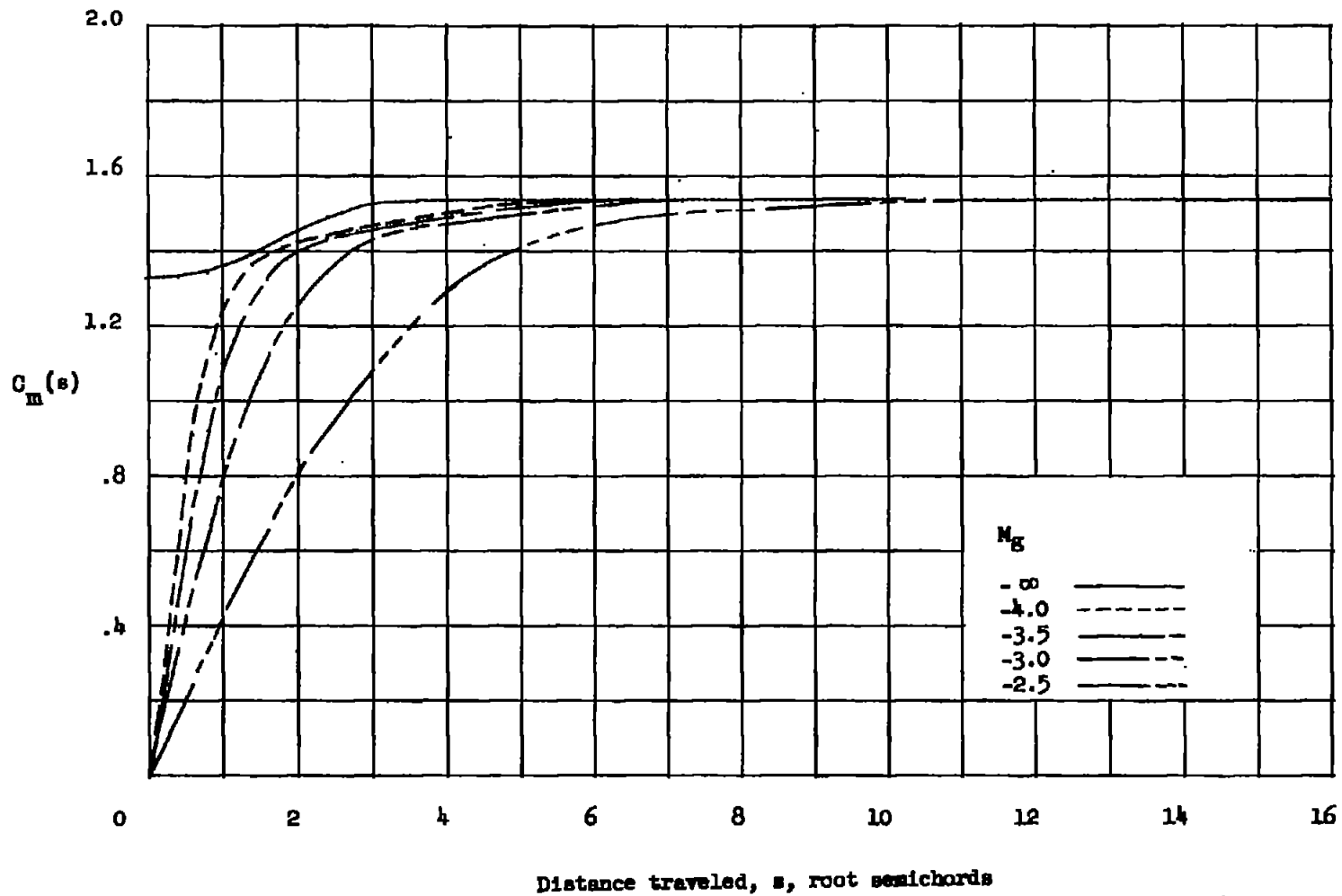
(b) Gust approaching from trailing edge.

Figure 6.- Concluded.



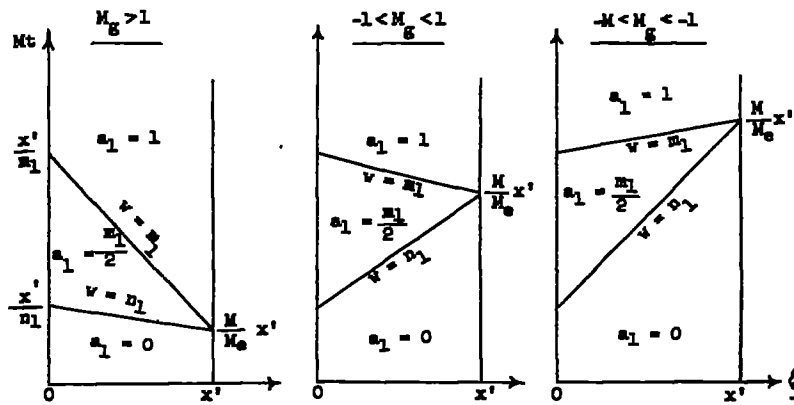
(a) Gust approaching from leading edge.

Figure 7.- Indicial-moment functions for a wide delta wing flying at $M = 2$ when penetrating traveling sharp-edged gusts (moment about leading edge).

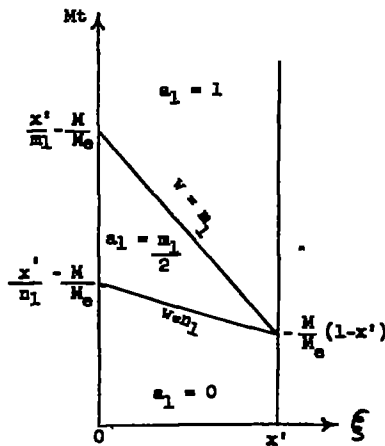


(b) Gusts approaching from trailing edge.

Figure 7.- Concluded.

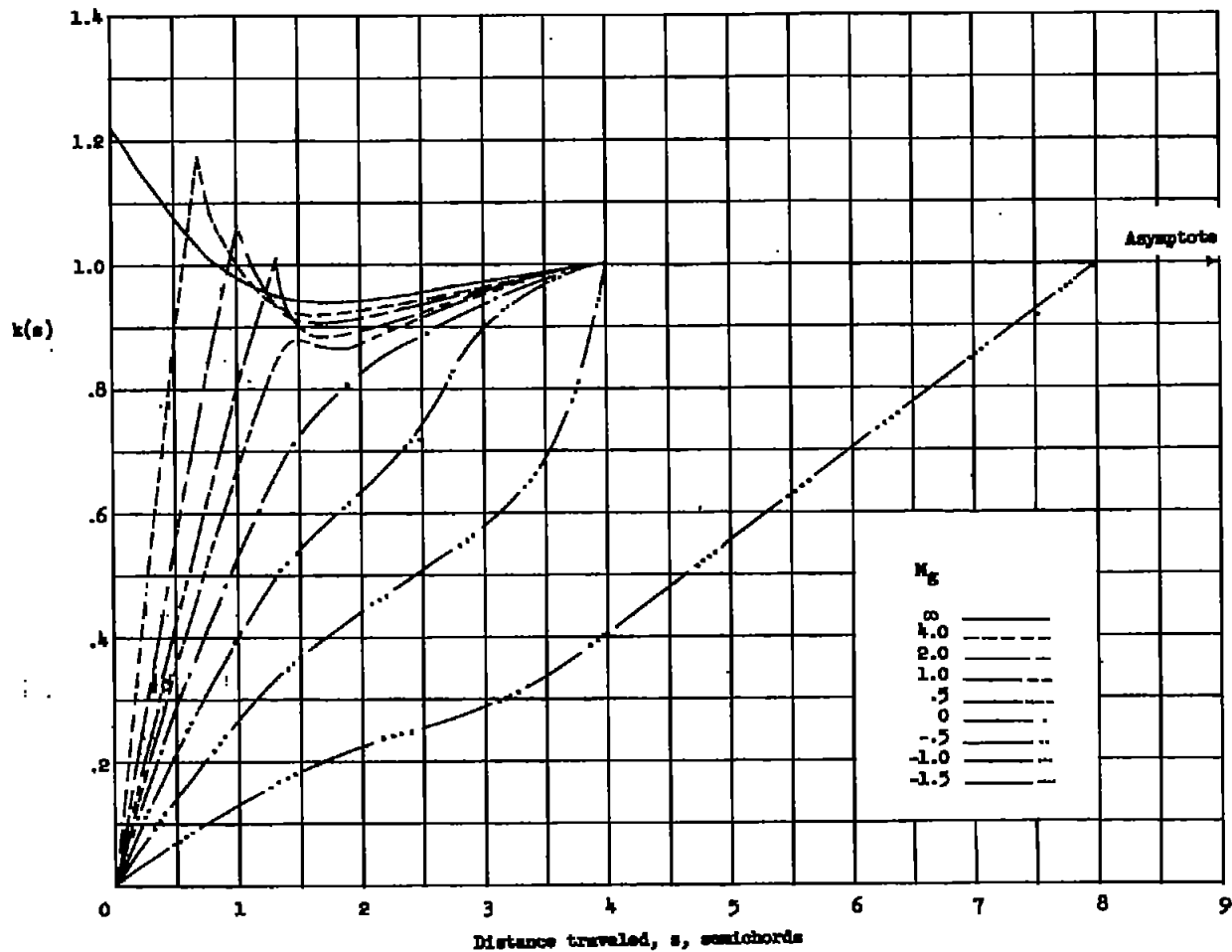


(a) Gusts approaching wing or receding from wing at speeds less than that of wing. $M_g > -M$.



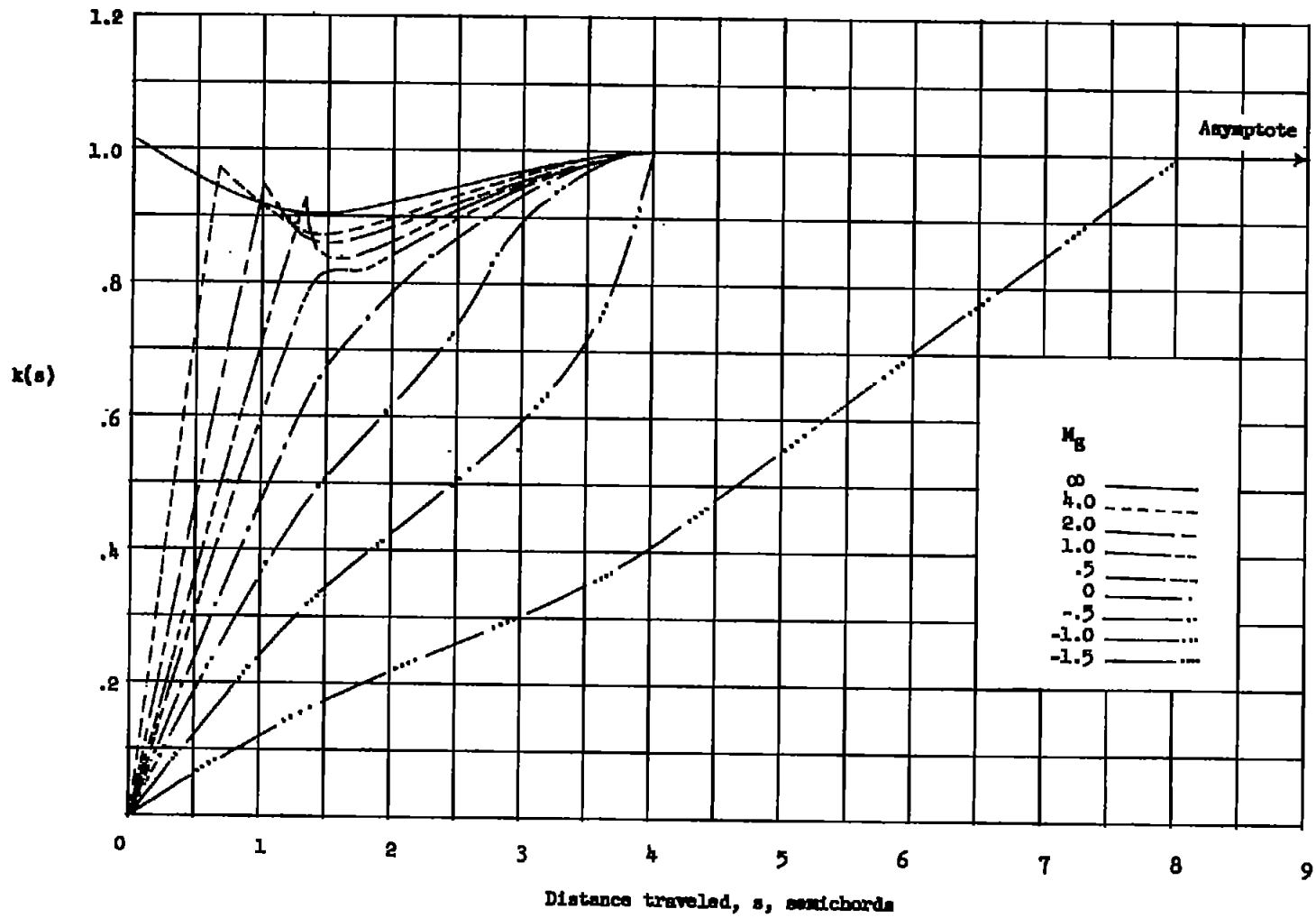
(b) Gusts overtaking wing. $M_g < -M$.

Figure 8.- Sketches of geometric characteristics for rectangular wing in supersonic flow.



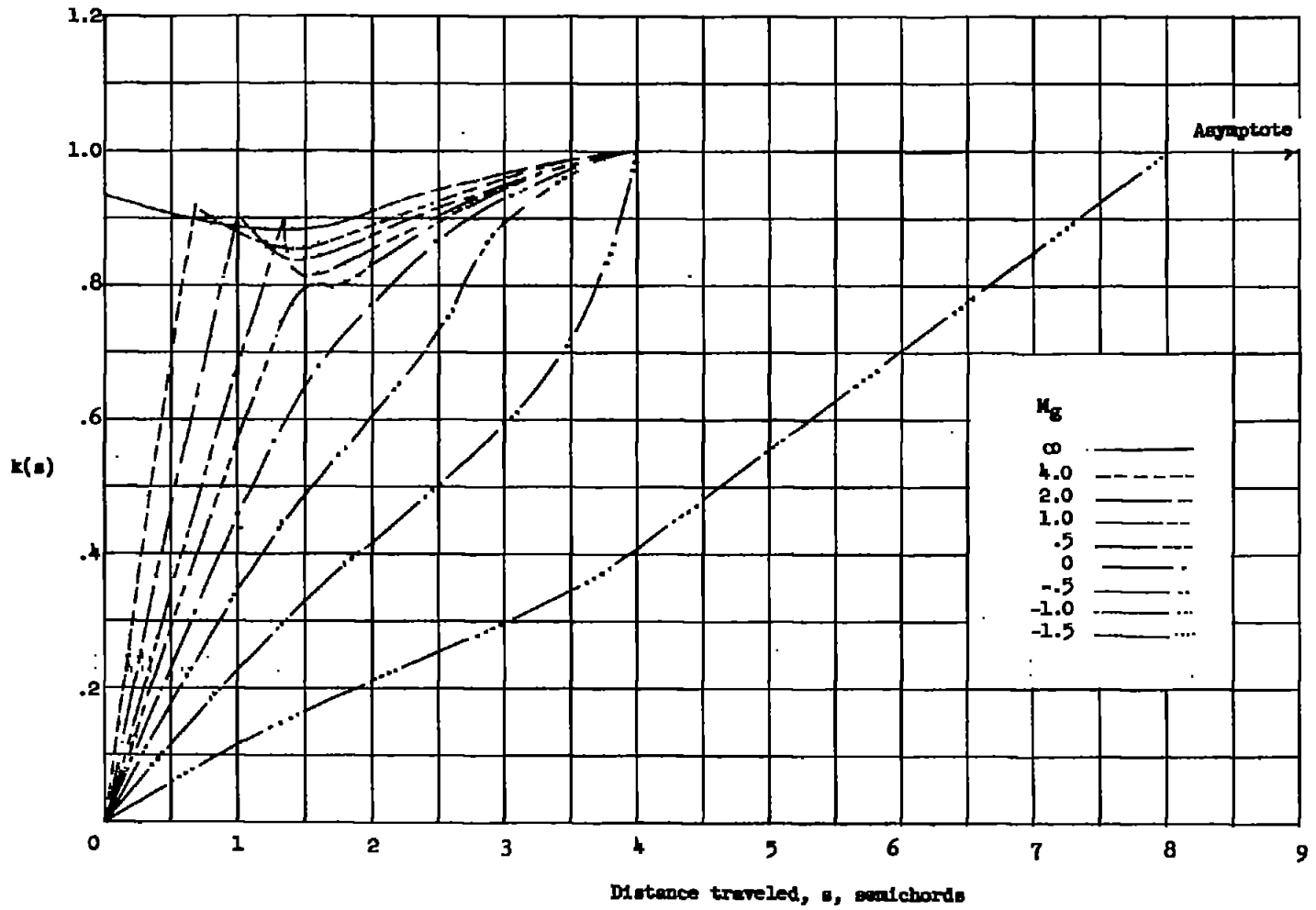
(a) $A = 1$.

Figure 9.- Indicial-lift functions for wide rectangular wings of various aspect ratios when flying at $M = 2$ and penetrating traveling sharp-edged gusts approaching from leading edge.



(b) $A = 2.$

Figure 9.- Continued.



(c) $A = 4.$

Figure 9.- Concluded.

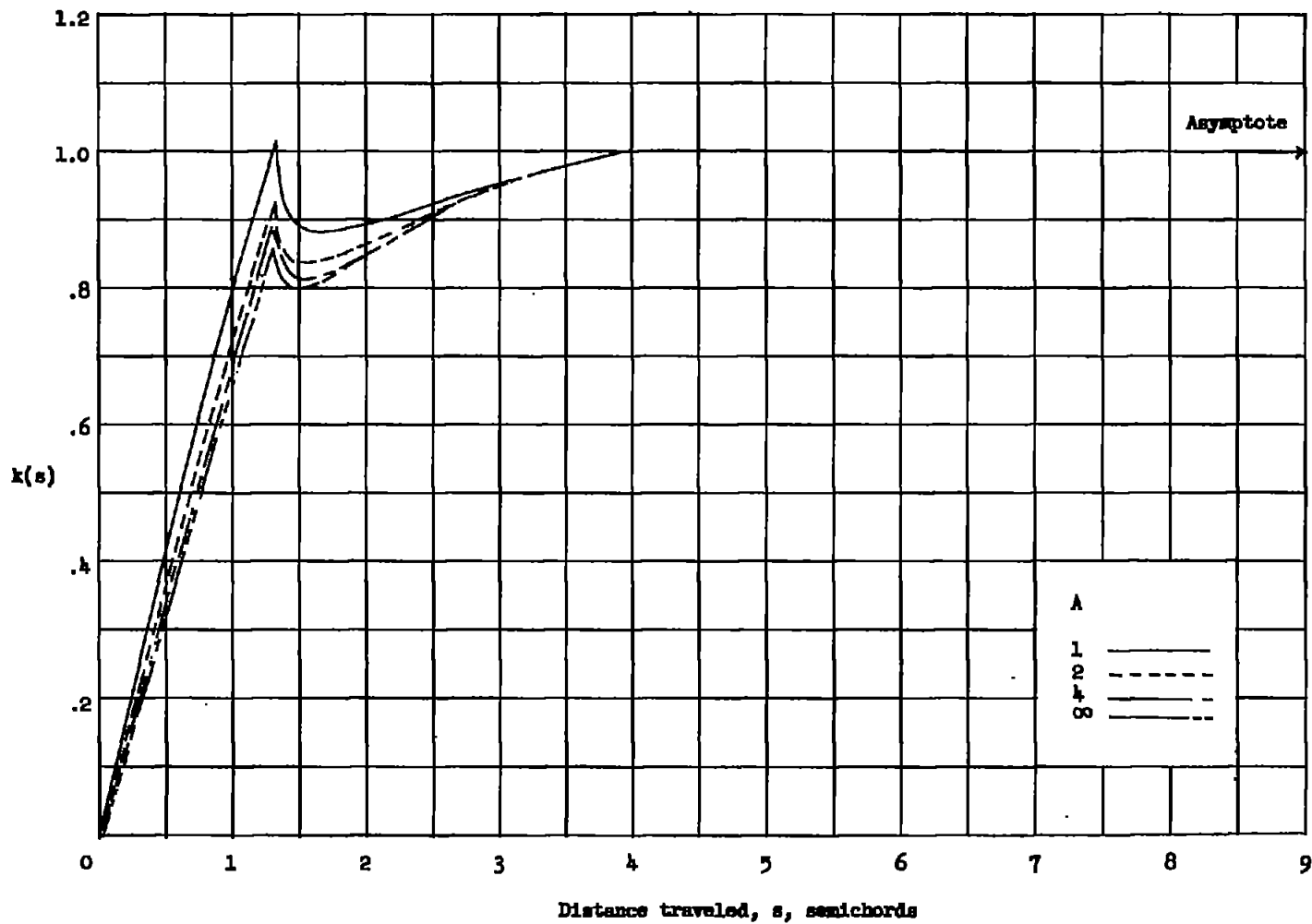
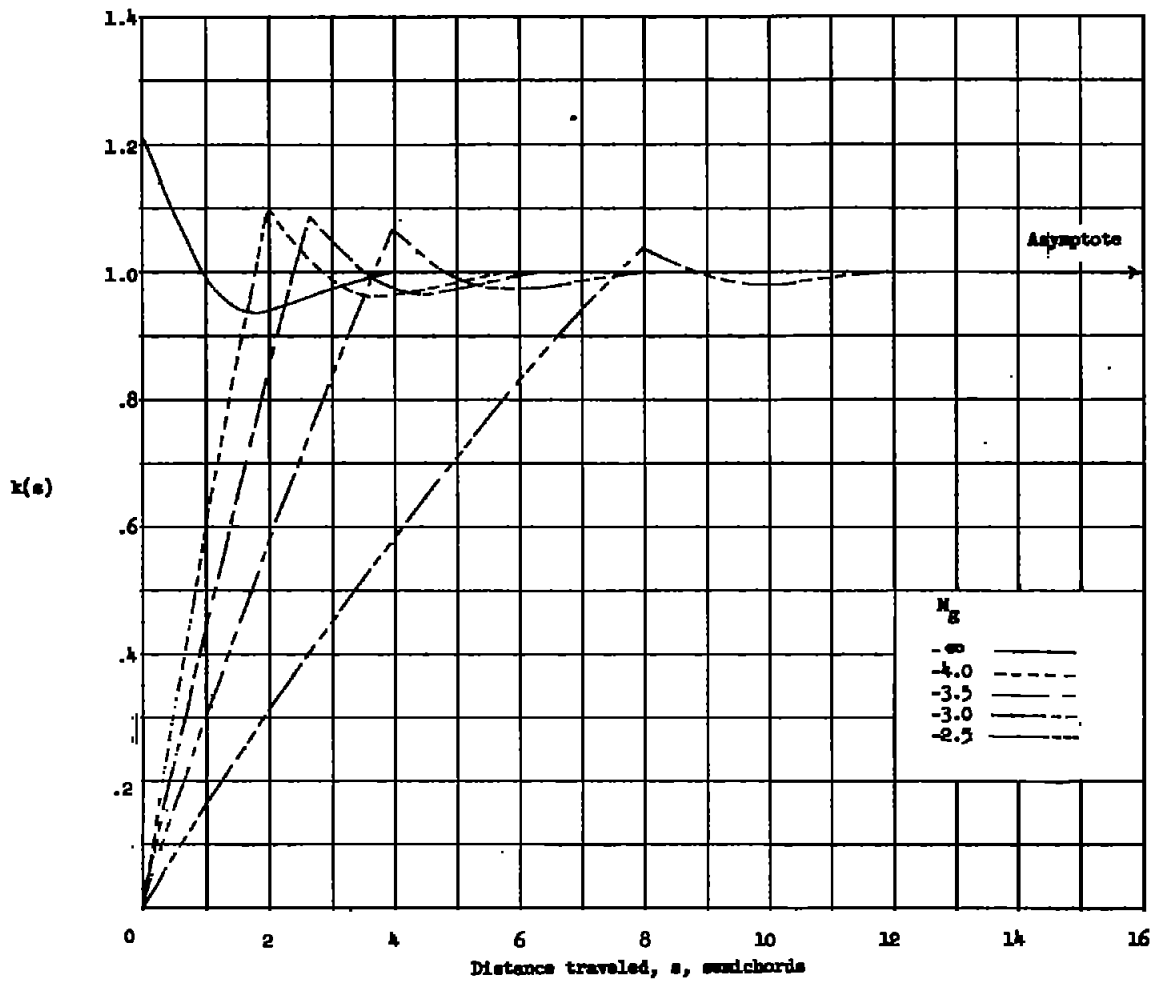
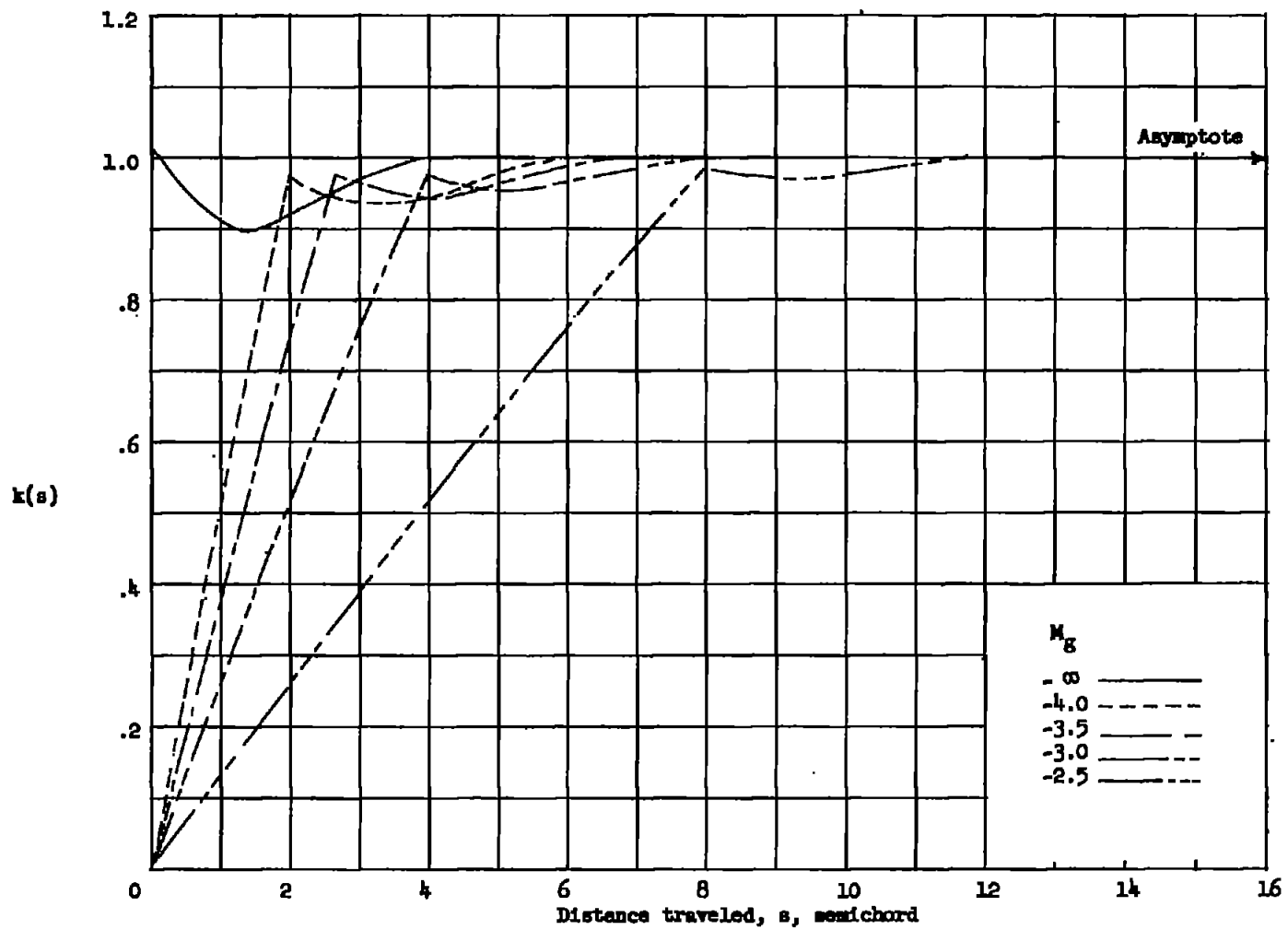


Figure 10.- Indicial-lift functions for wide rectangular wings of various aspect ratios when flying at $M = 2$ and penetrating traveling sharp-edged gusts approaching from leading edge at $M_g = 1.0$.



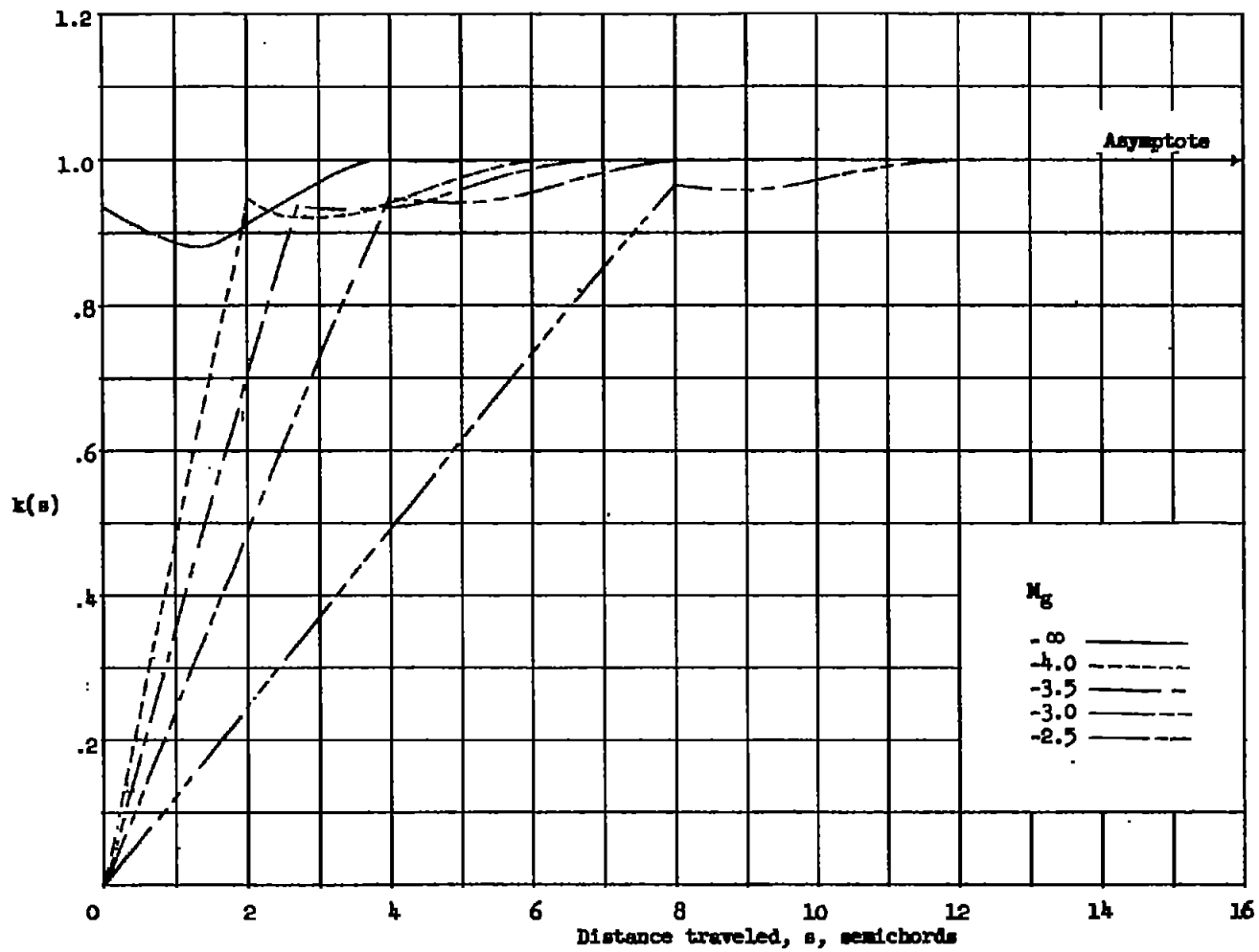
(a) $A = 1.$

Figure 11.- Indicial-lift functions for wide rectangular wings of various aspect ratios when flying at $M = 2$ and penetrating traveling sharp-edged gusts approaching from trailing edge.



(b) $A = 2.$

Figure 11.- Continued.



(c) $A = 4.$

Figure 11.- Concluded.

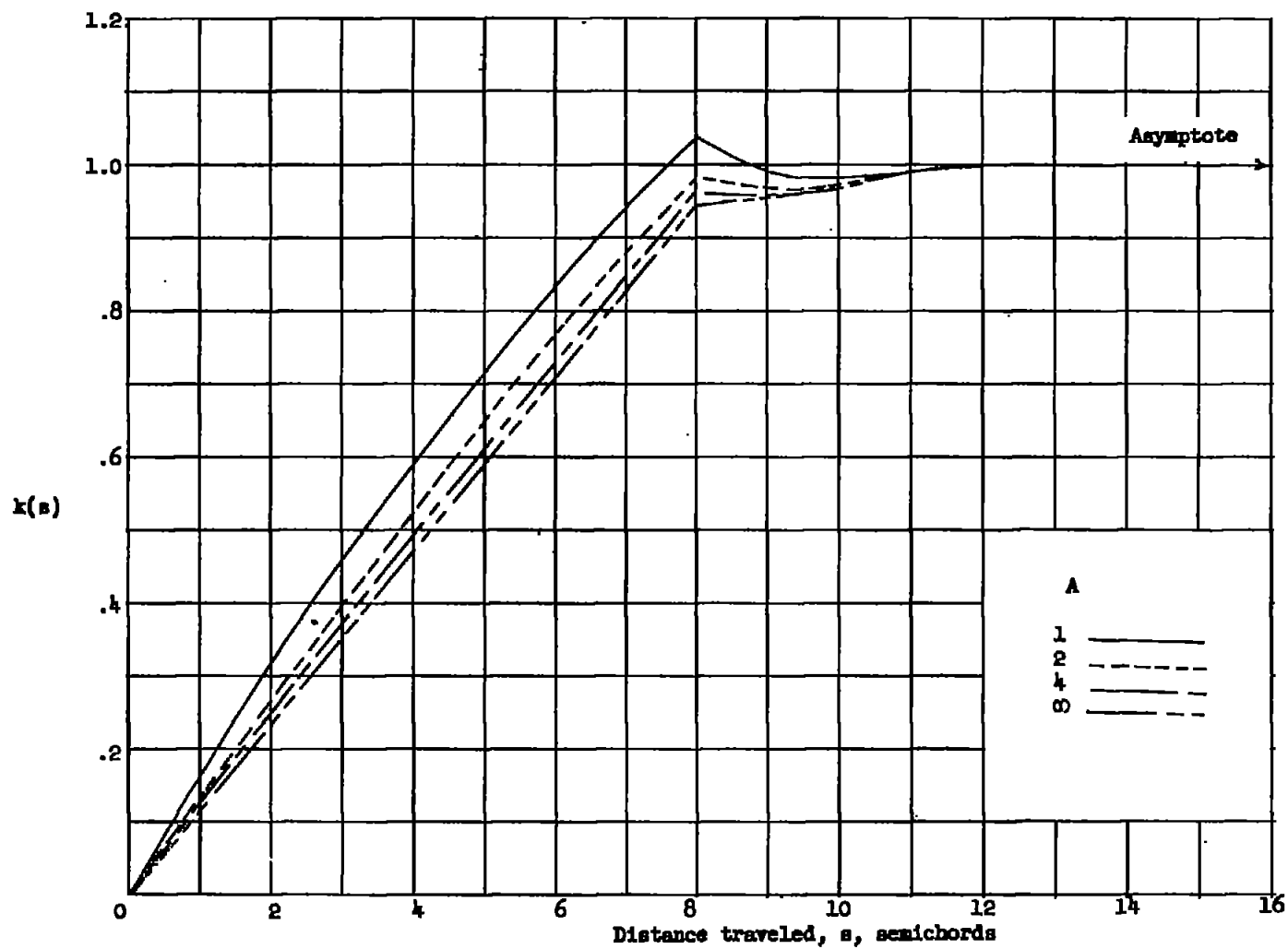
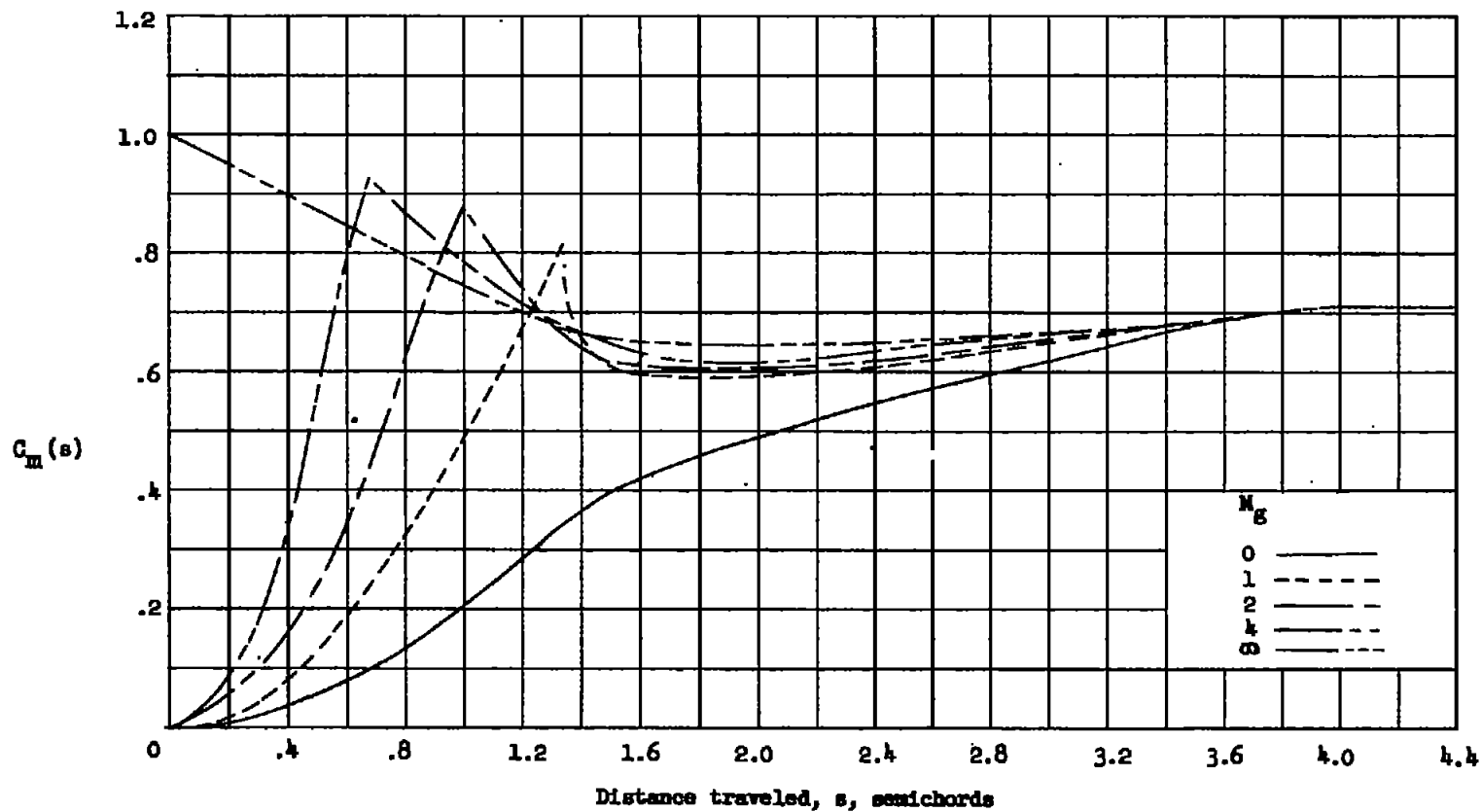
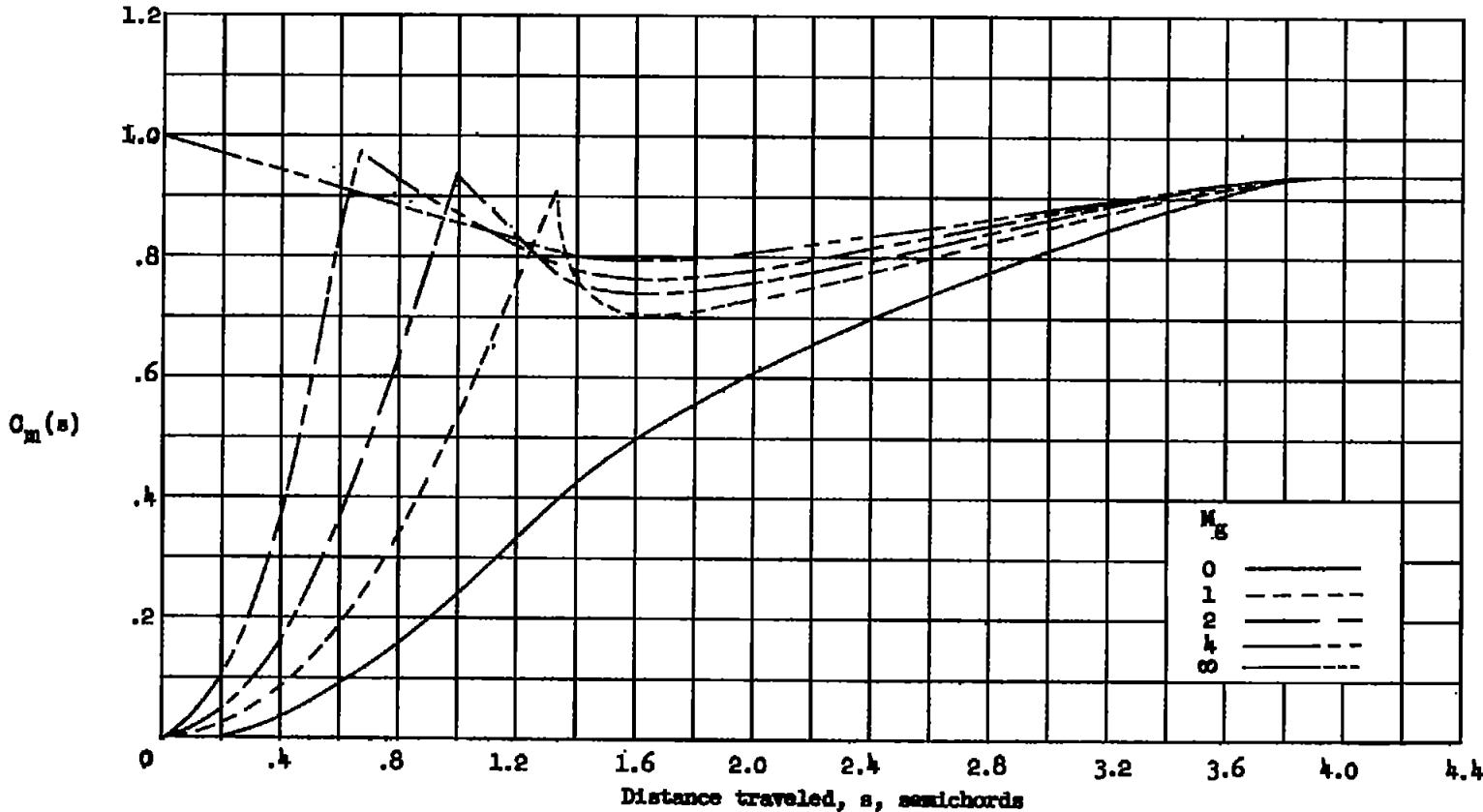


Figure 12.- Indicial-lift functions for wide rectangular wings flying at $M = 2$ when penetrating traveling sharp-edged gusts approaching from trailing edge at $M_g = -2.5$.



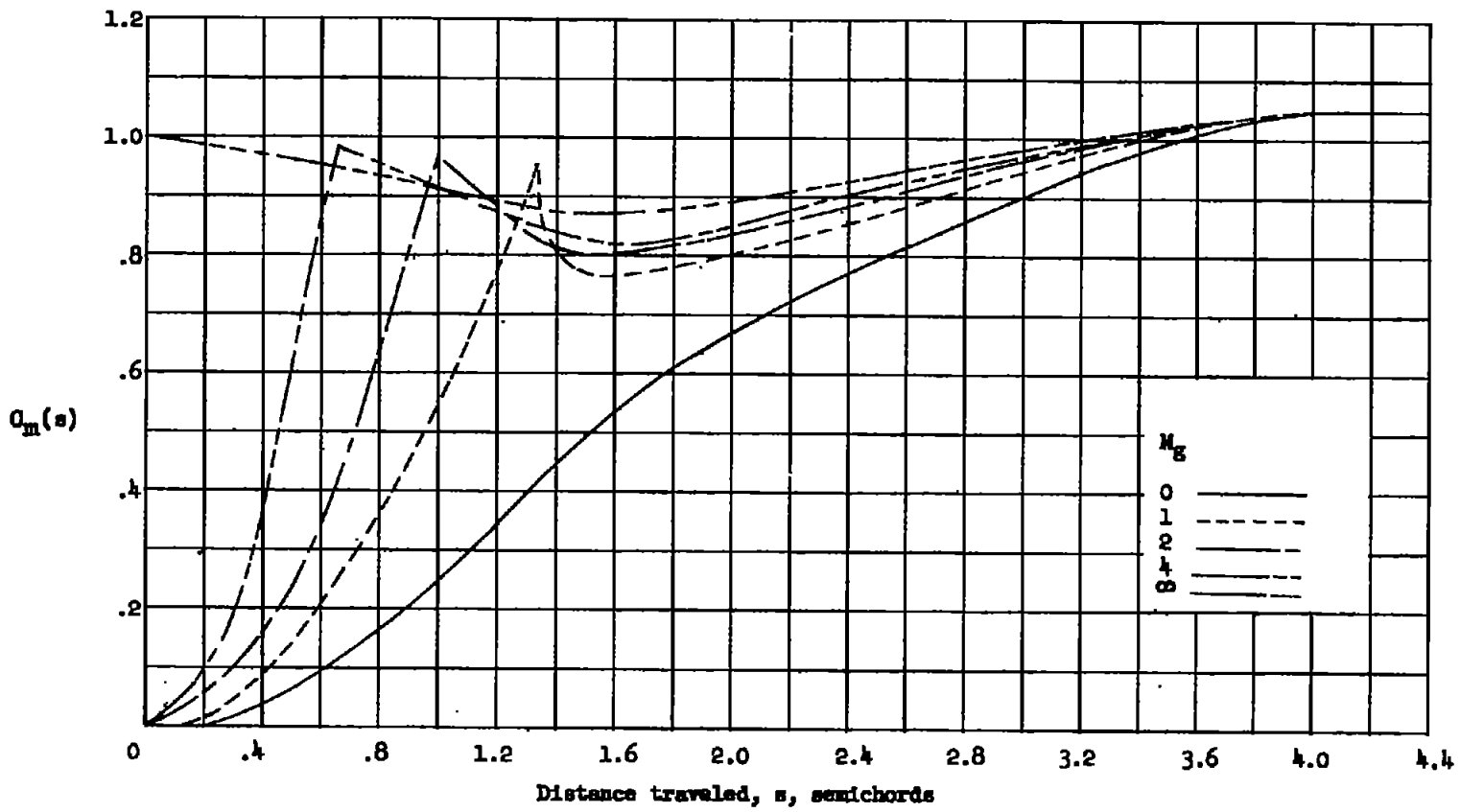
(a) $A = 1$.

Figure 13.- Indicial-moment functions for wide rectangular wings of various aspect ratios when flying at $M = 2$ and penetrating traveling sharp-edged gusts approaching from leading edge (moment about leading edge).



(b) $A = 2$.

Figure 13.- Continued.



(c) $A = 4.$

Figure 13.- Concluded.

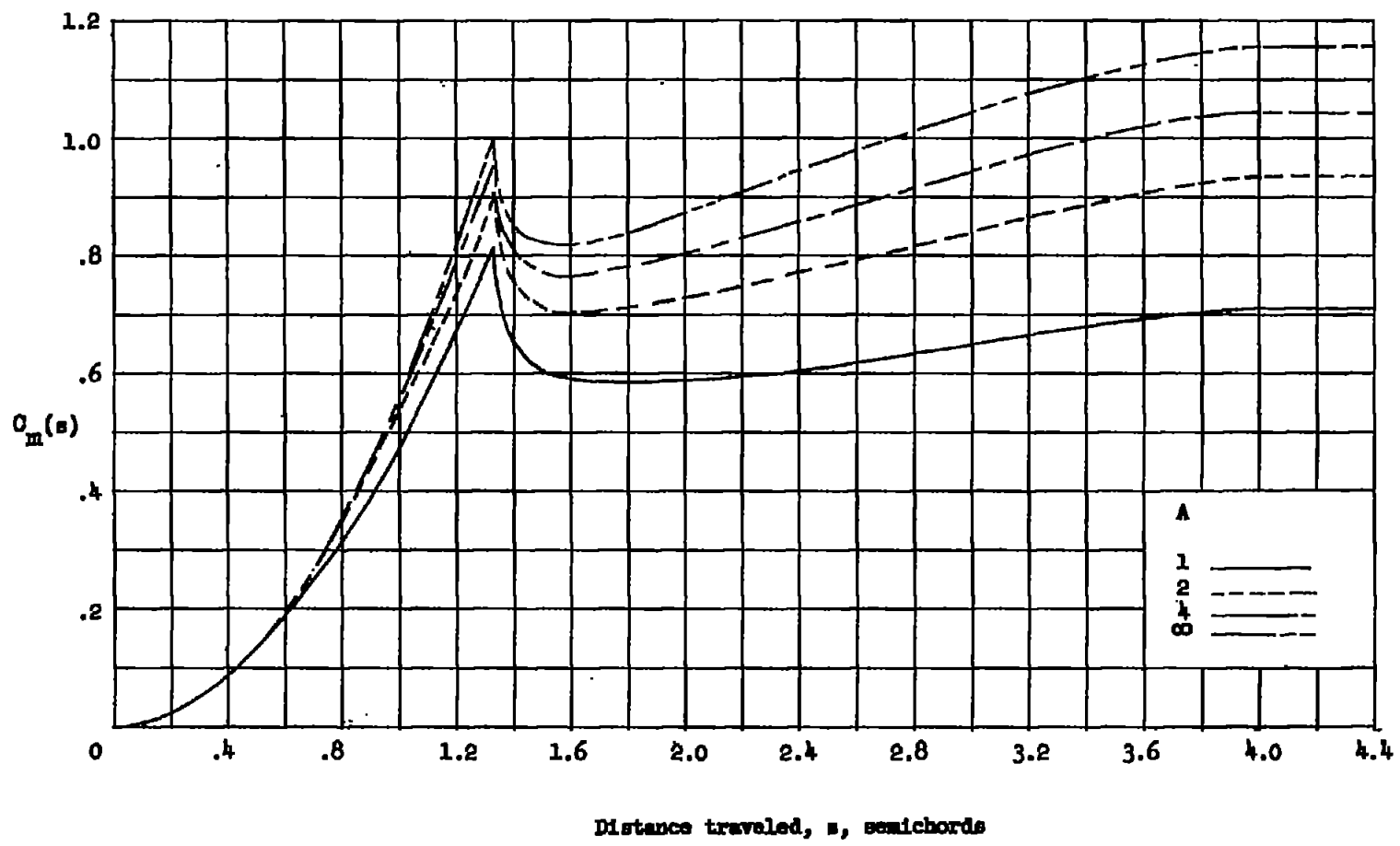
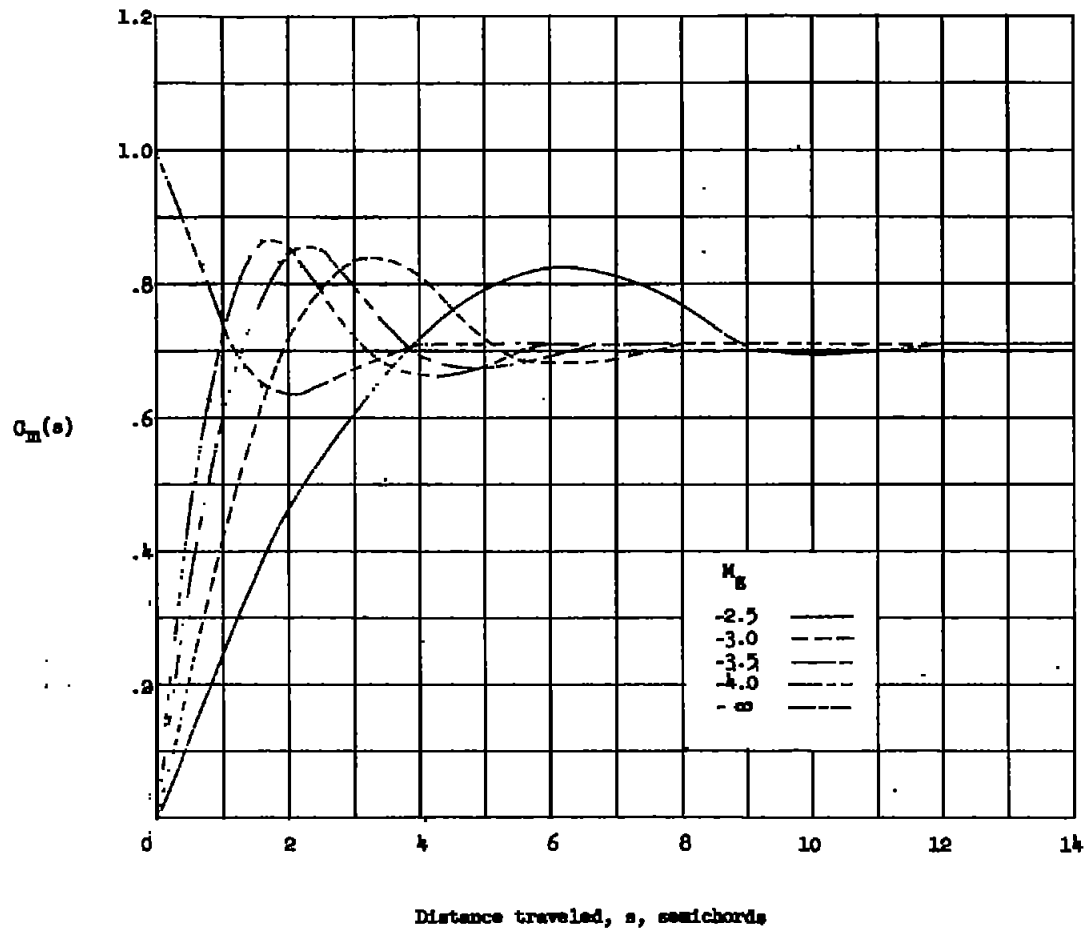
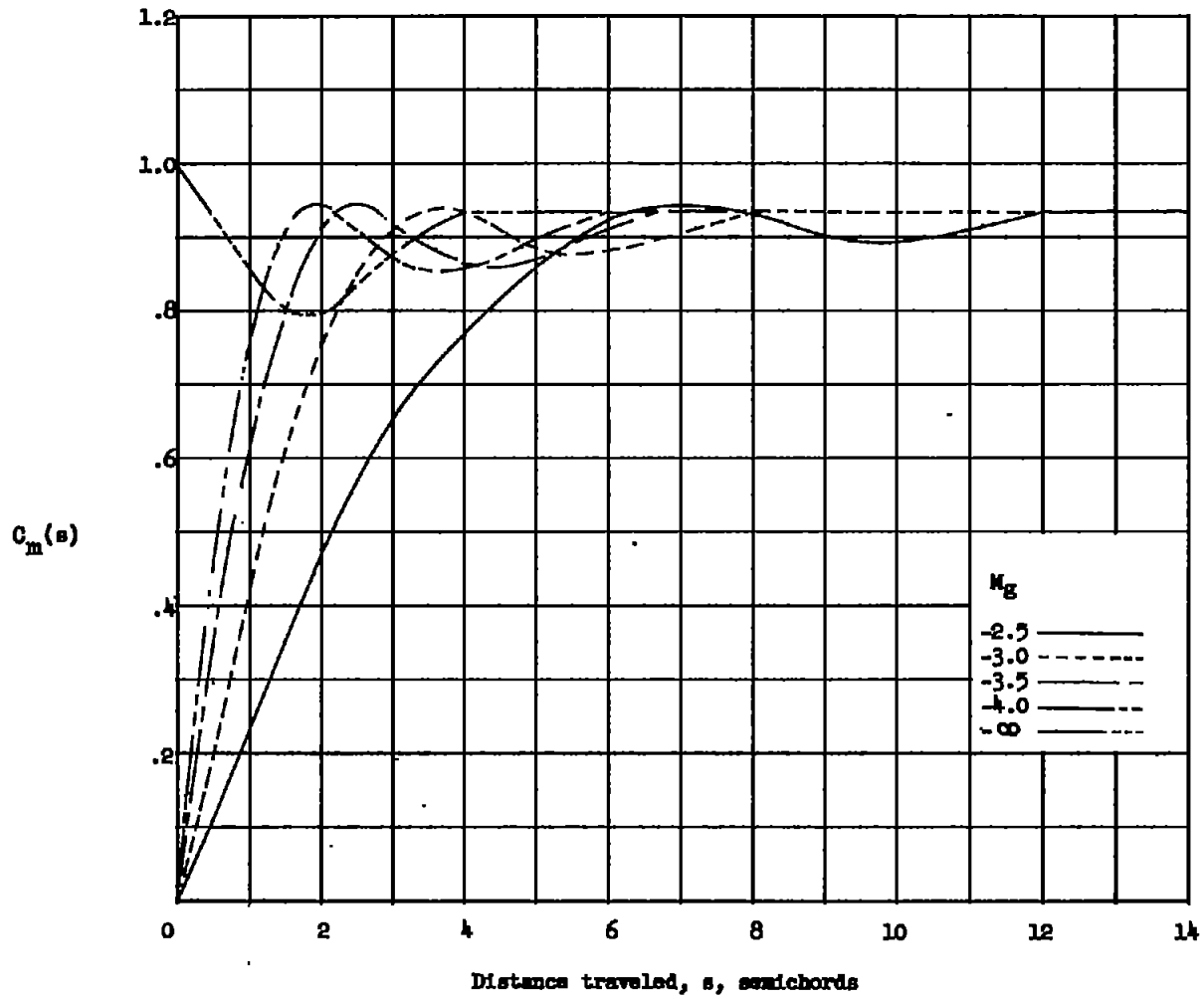


Figure 14.- Indicial-moment functions for wide rectangular wings flying at $M = 2$ when penetrating traveling sharp-edged gusts approaching from leading edge at $M_g = 1.0$ (moment about leading edge).



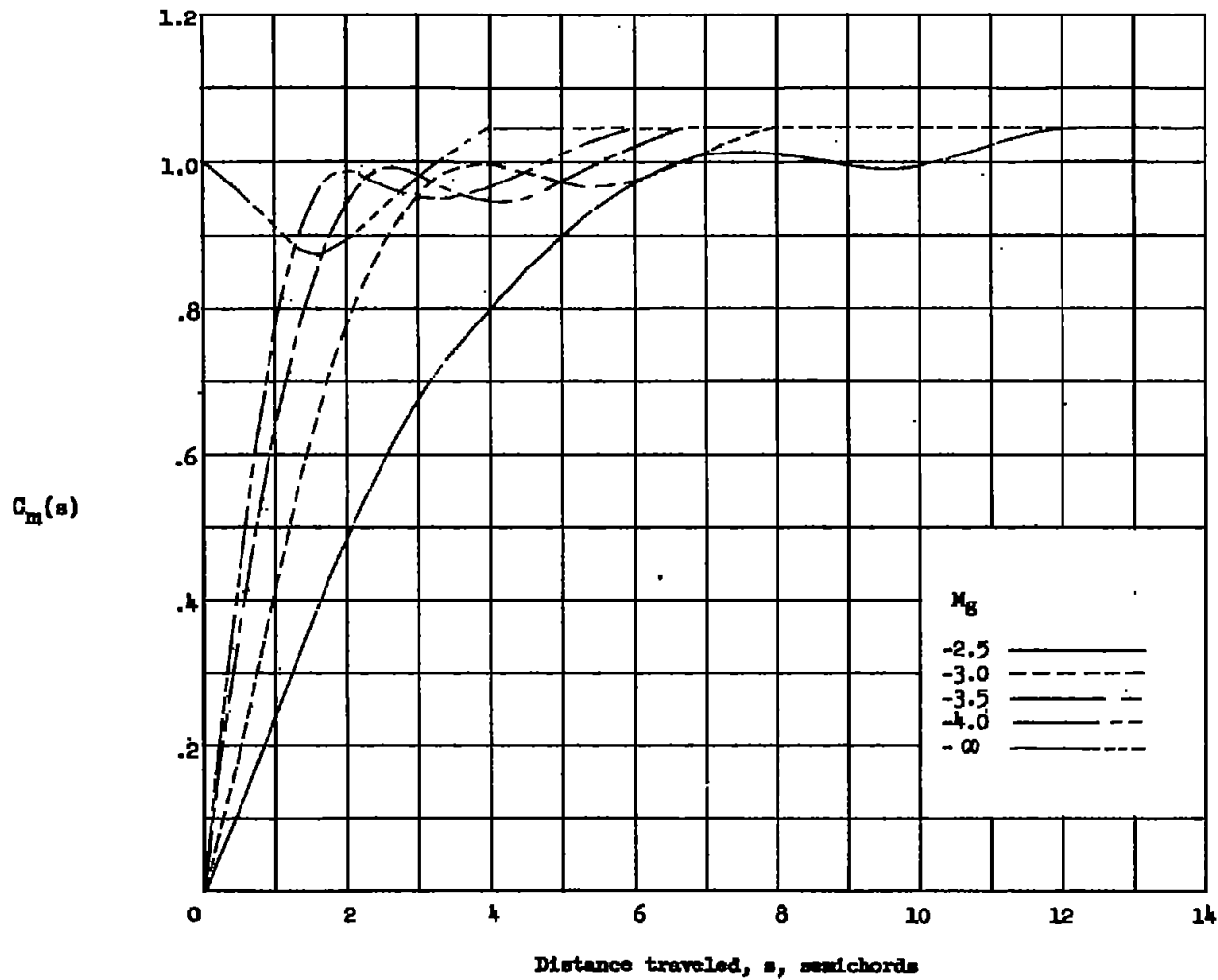
(a) $A = 1$.

Figure 15.- Indicial-moment functions for wide rectangular wings of various aspect ratios when flying at $M = 2$ and penetrating traveling sharp-edged gusts approaching from trailing edge (moment about leading edge).



(b) $A = 2.$

Figure 15.- Continued.



(c) $A = 4$.

Figure 15.- Concluded.

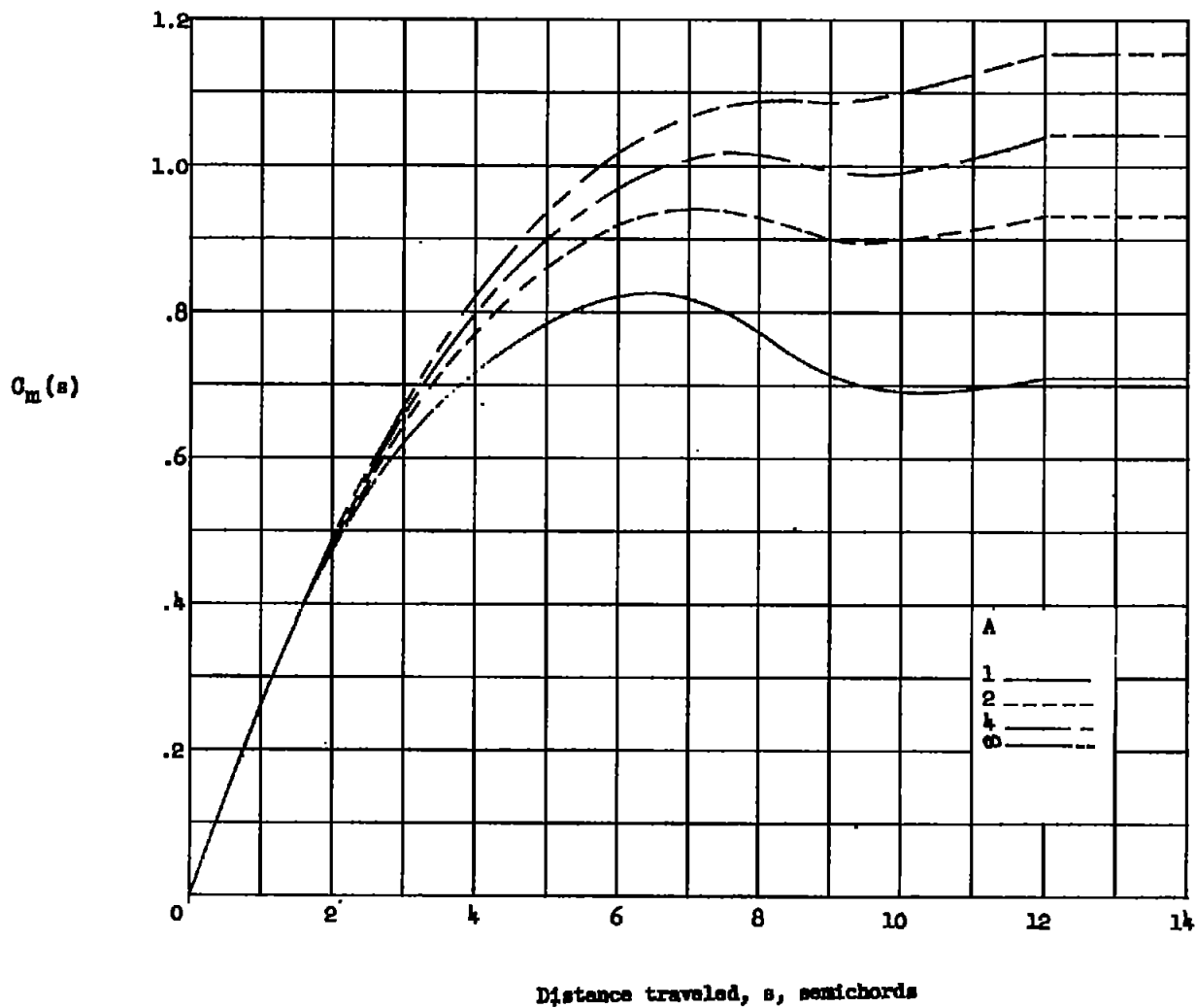
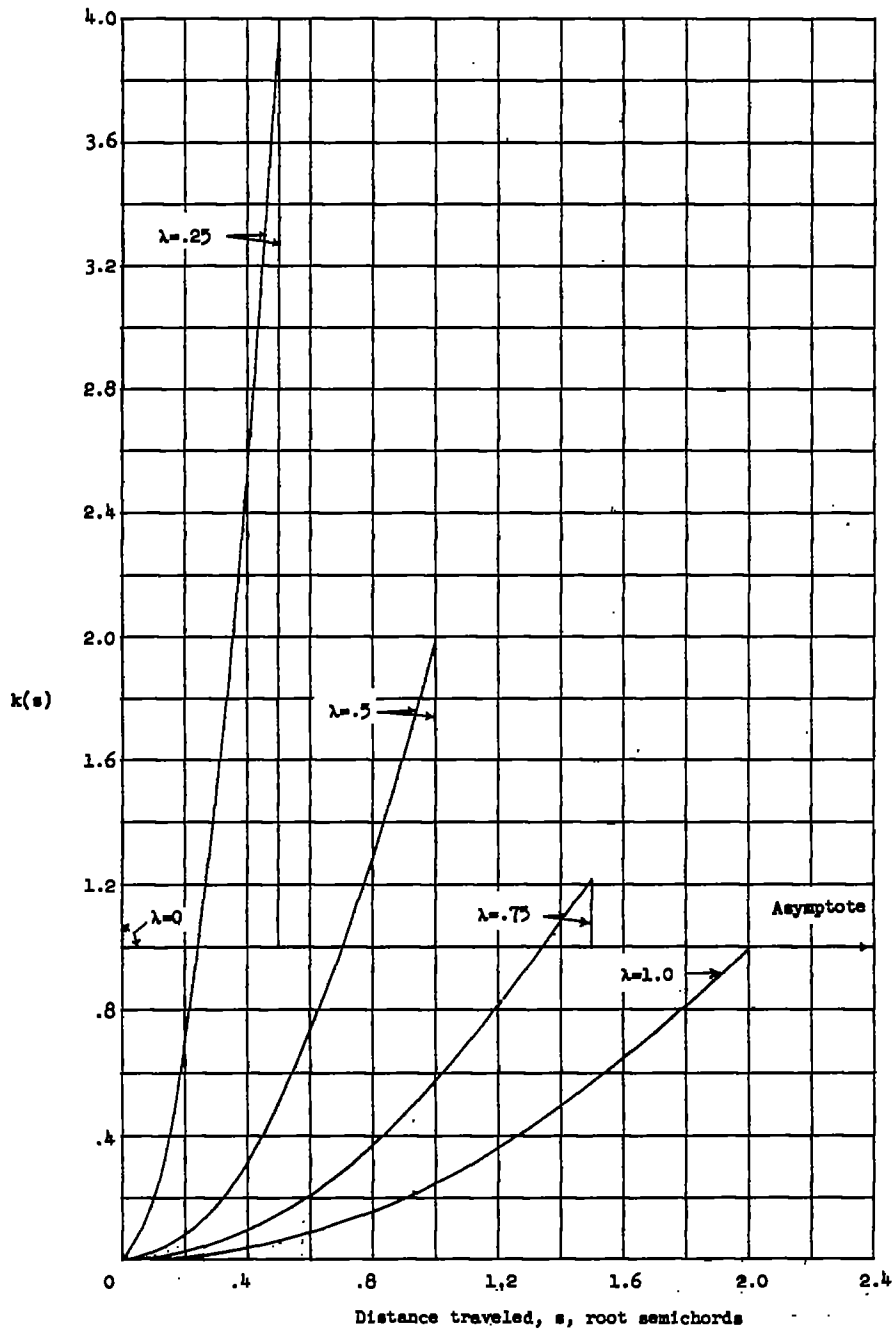
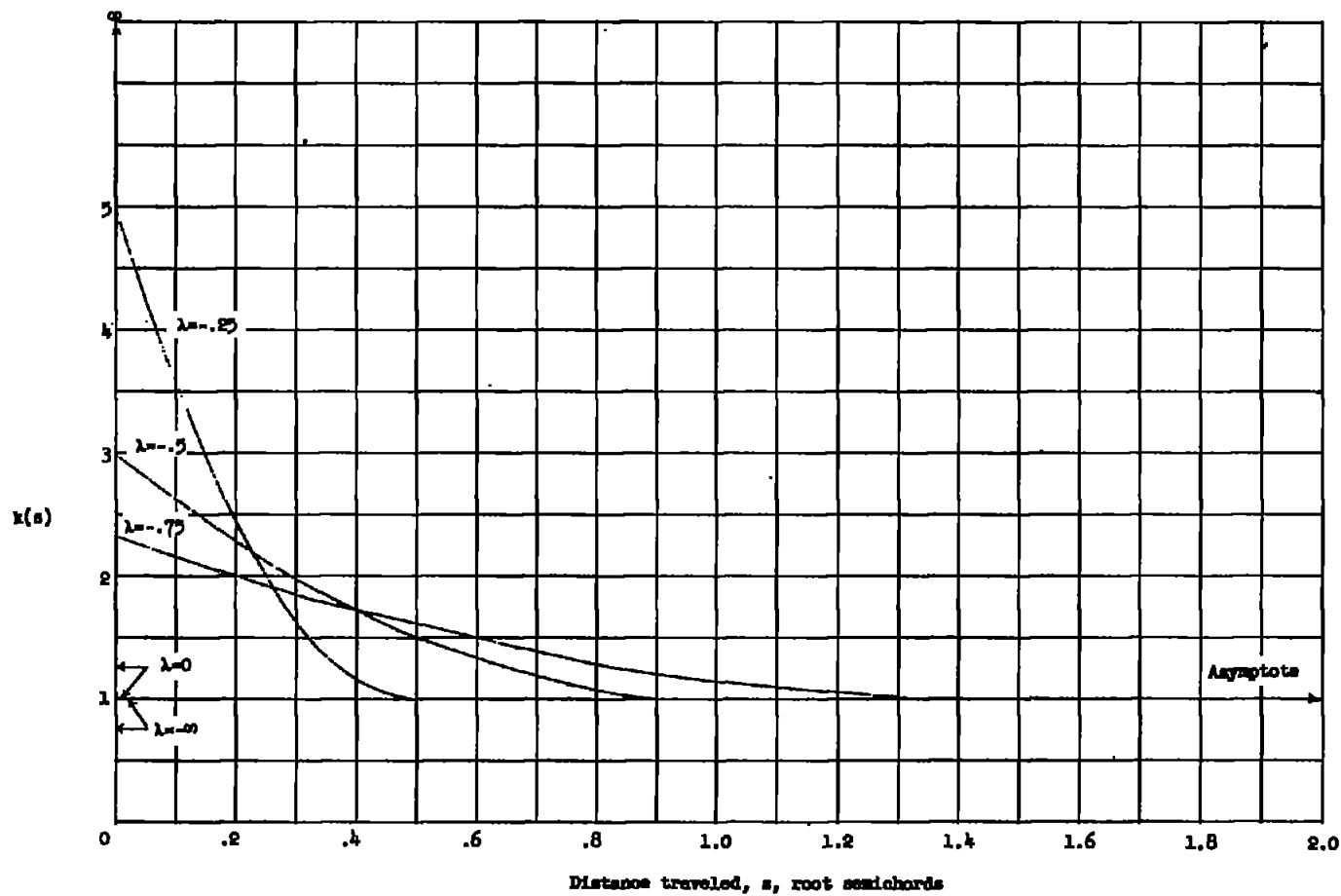


Figure 16.- Indicial-moment functions for wide rectangular wings flying at $M = 2$ when penetrating traveling sharp-edged gusts approaching from trailing edge at $M_g = -2.5$.



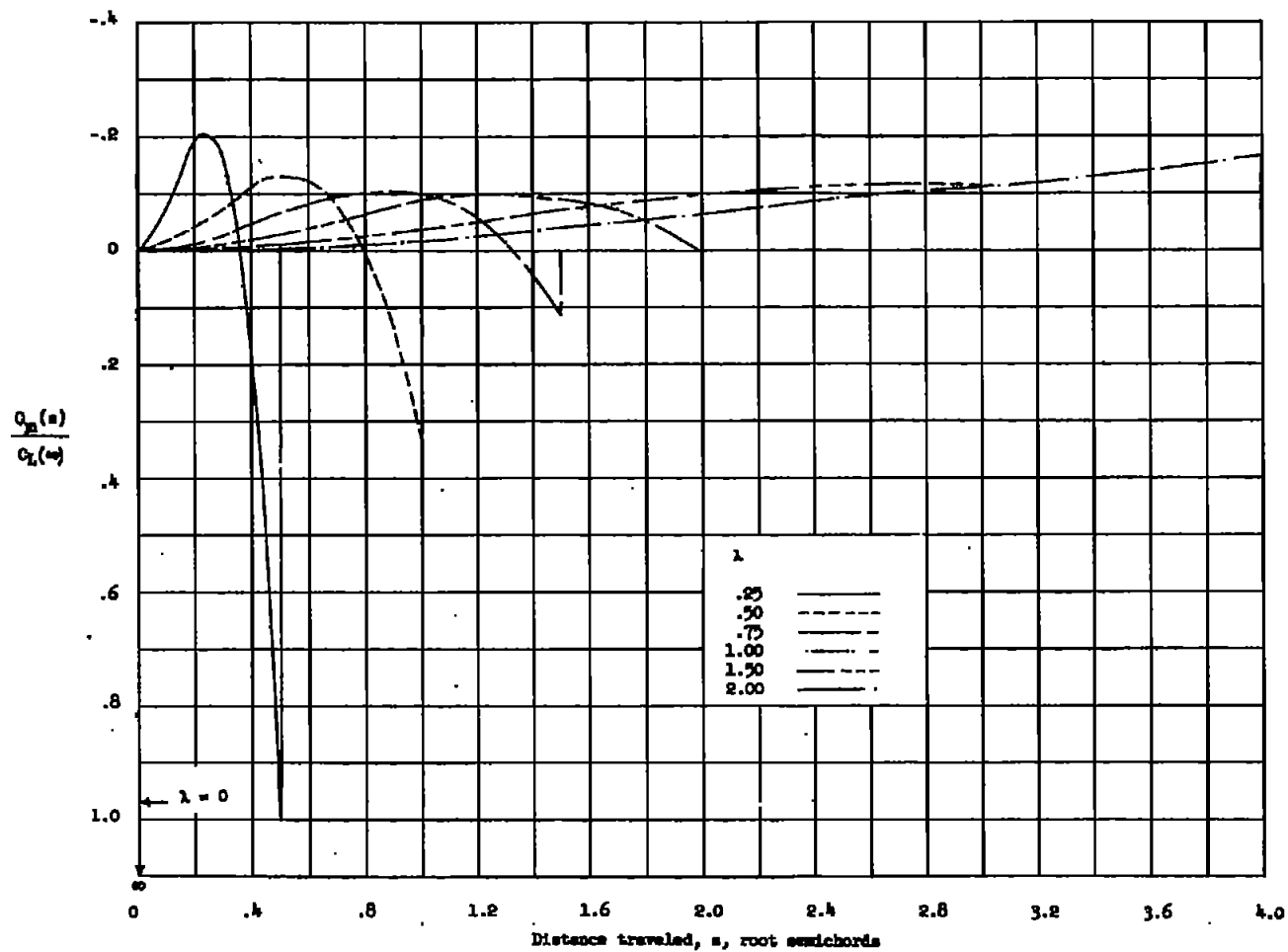
(a) Gusts approaching from leading edge.

Figure 17.- Indicial-lift functions for very narrow delta wing in incompressible flow when penetrating traveling sharp-edged gusts.



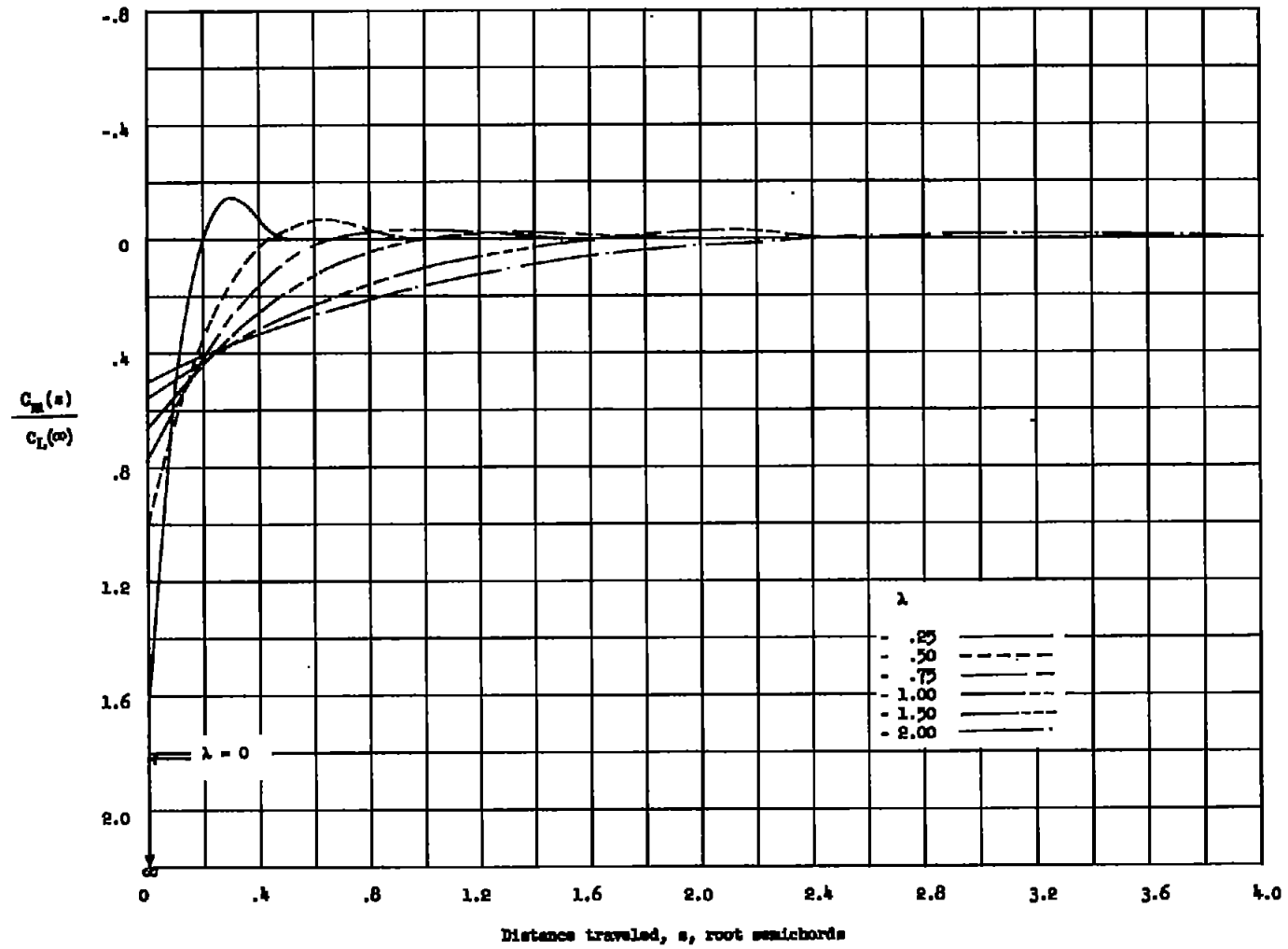
(b) Gusts approaching from trailing edge.

Figure 17.- Concluded.



(a) Gusts approaching from leading edge.

Figure 18.- Indicial-moment functions for very narrow delta wing in incompressible flow when penetrating traveling sharp-edged gusts (moment about two-thirds chord).



(b) Gusts approaching from trailing edge.

Figure 18.- Concluded.

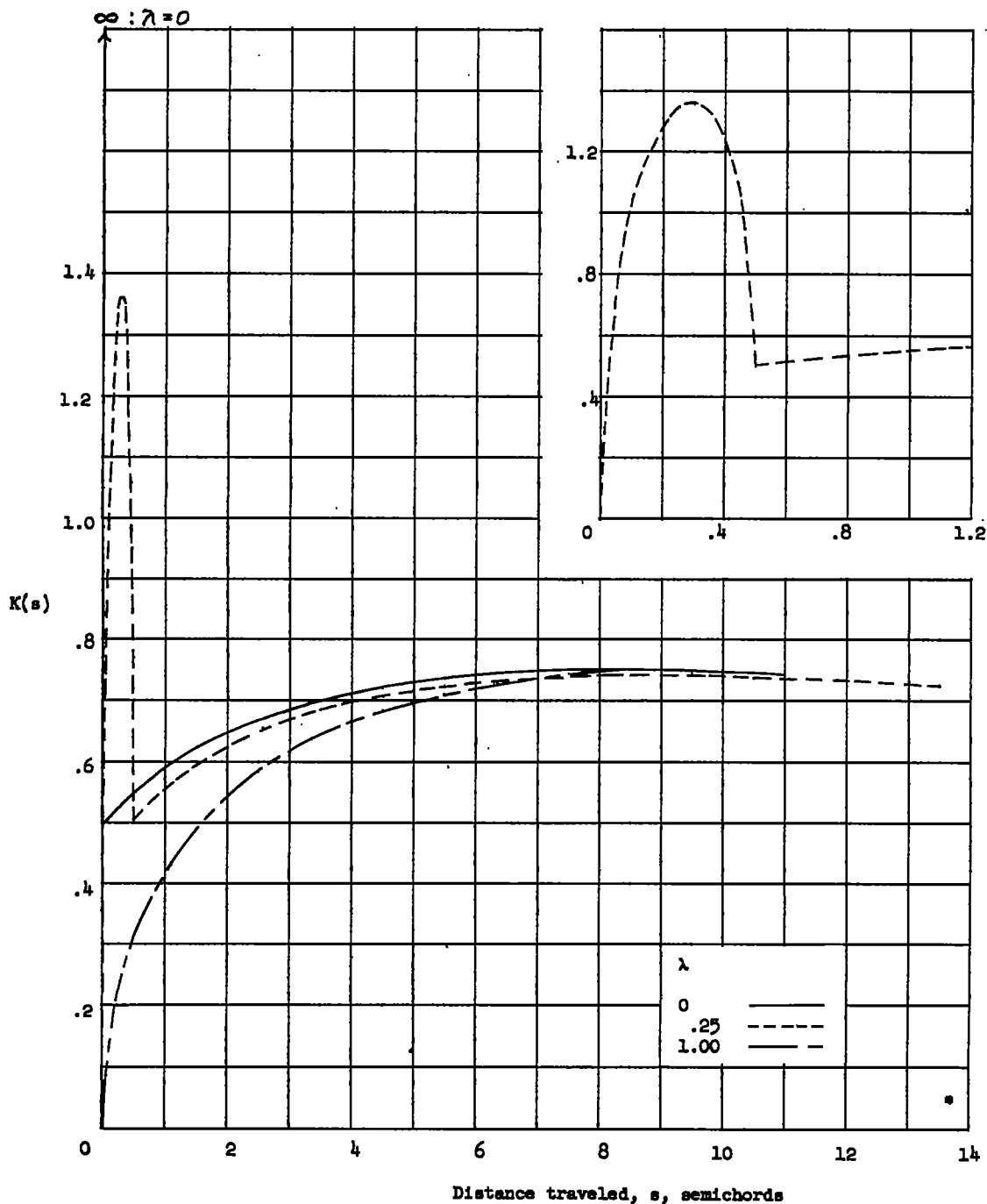


Figure 19.- Alleviation factor for a wing with mass-density ratio of $\mu = 50$ in incompressible two-dimensional flow when penetrating traveling sharp-edged gusts approaching from leading edge.

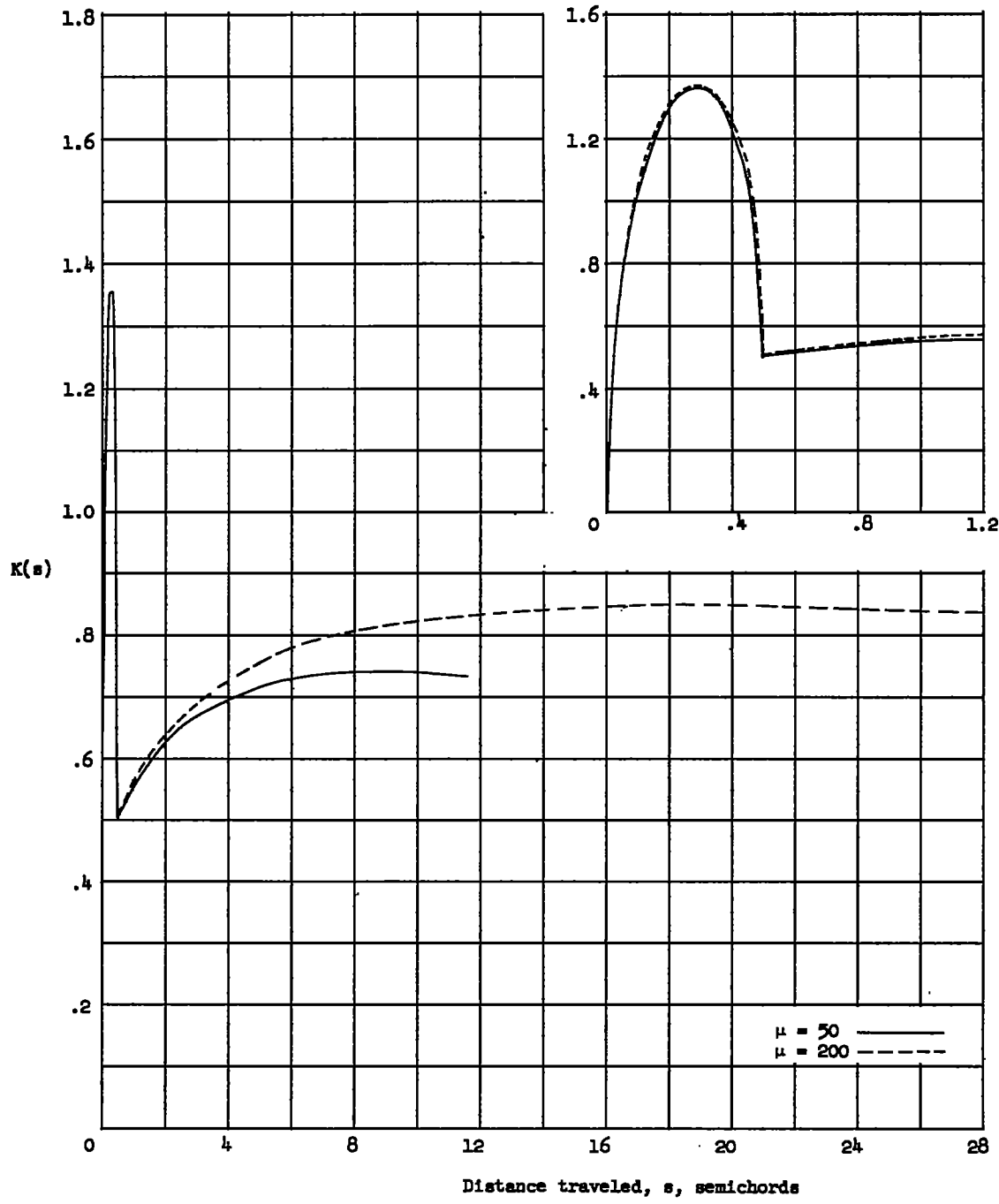


Figure 20.- Alleviation factors for a wing with mass-density ratios of $\mu = 50$ and 200 in incompressible two-dimensional flow when penetrating a traveling sharp-edged gust approaching from leading edge at $\lambda = 0.25$.

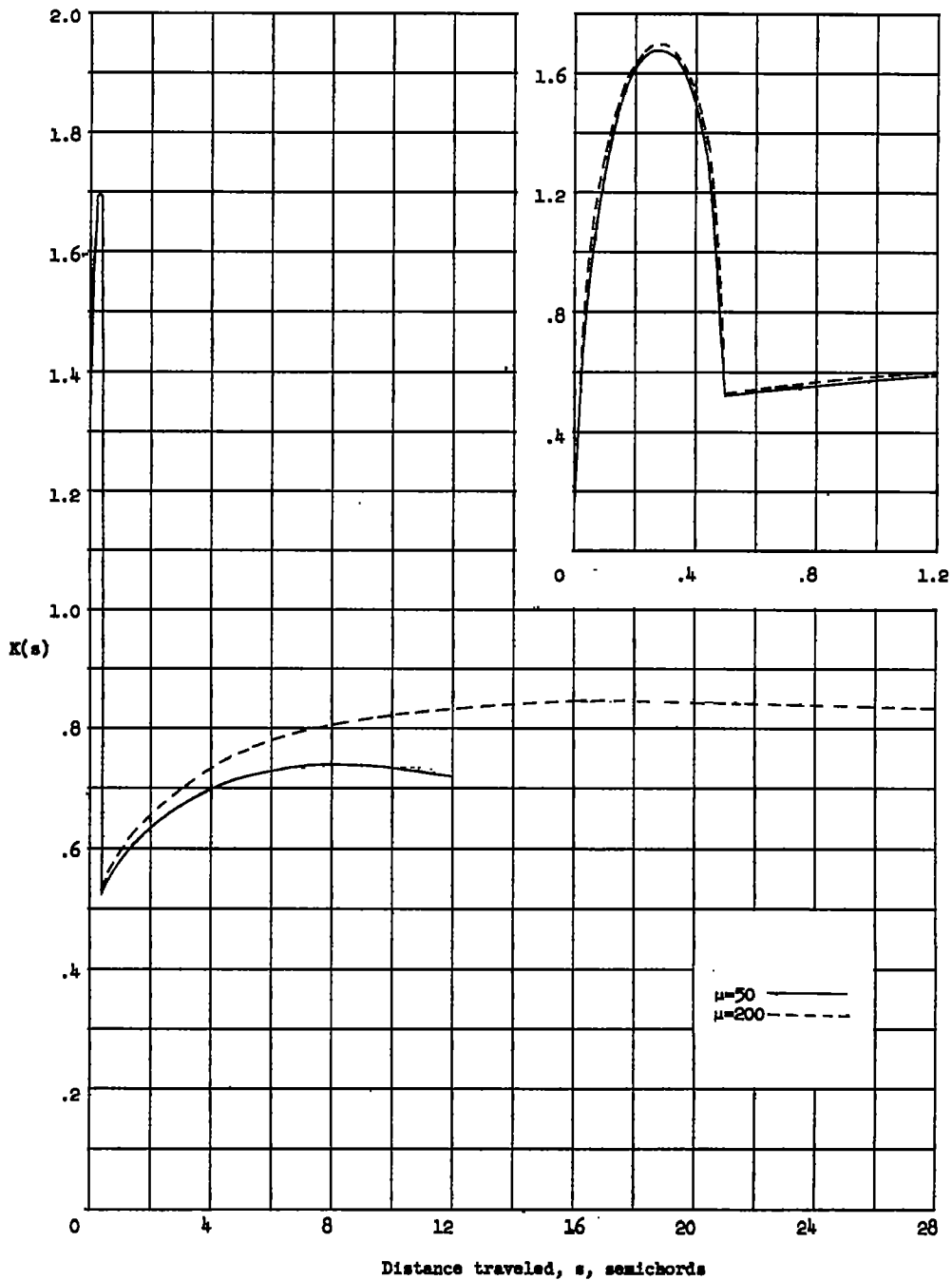


Figure 21.- Alleviation factors for a wing with mass-density ratios of $\mu = 50$ and 200 in incompressible two-dimensional flow when penetrating a traveling sharp-edged gust approaching from trailing edge at $\lambda = -0.25$.

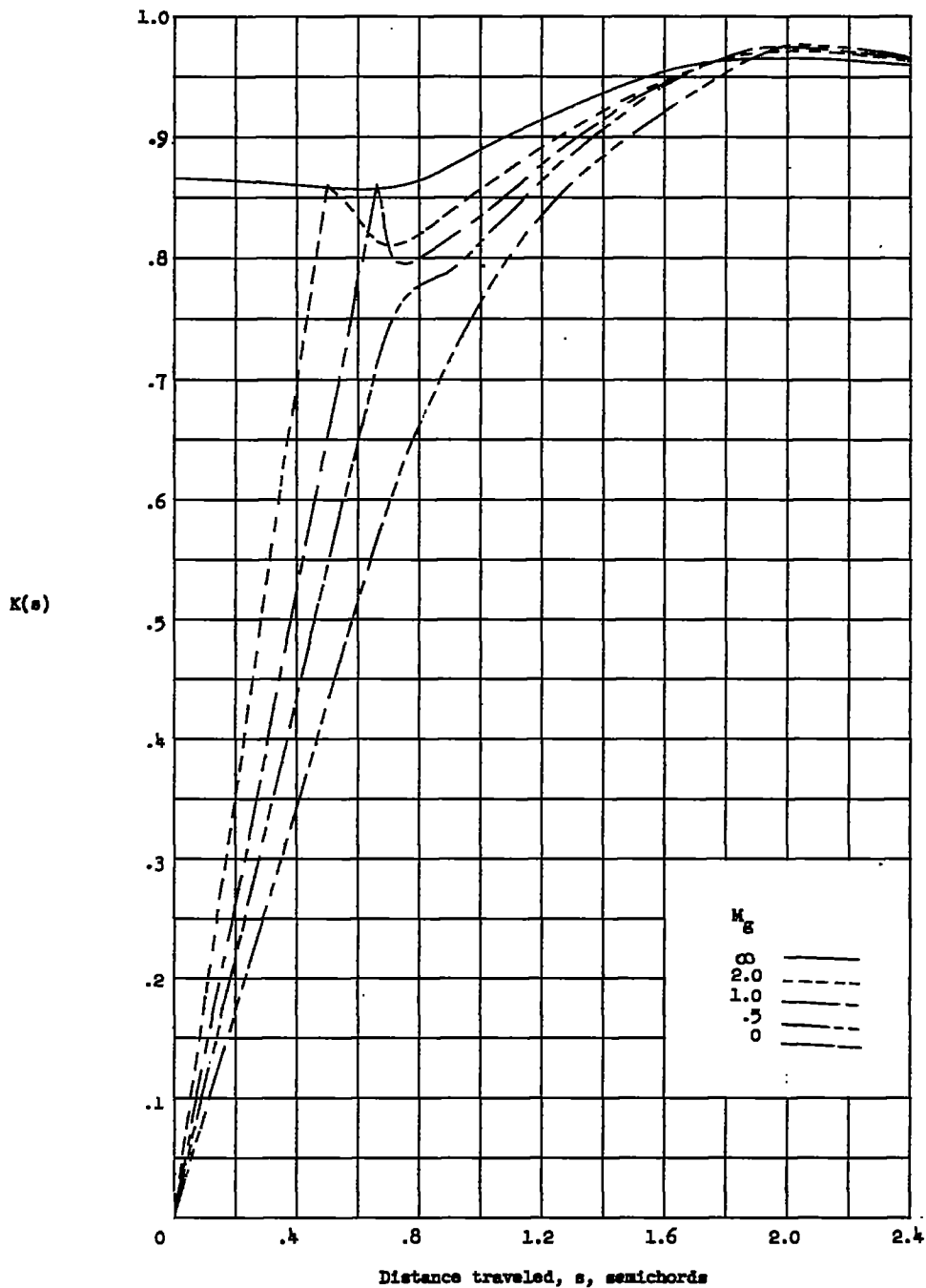


Figure 22.- Alleviation factor for two-dimensional wing flying at $M = 2$ with a mass-density ratio of $\mu = 50$ when penetrating traveling sharp-edged gusts approaching from leading edge.